PREPARATION OF PENTABLOCK NANOMICELLAR FORMULATIONS FOR PROSTATE CANCER DRUG DELIVERY SYSTEMS

DISSERTATION IN
Pharmaceutical Sciences
and
Pharmacology

Presented to the faculty of the University
of Missouri-Kansas City in partial fulfilment
of the requirement for the degree of

DOCTOR OF PHILOSOPHY

BY

ALEX OSELU OWITI

B. Pharm, M. Pharm, Federal University of Para, Brazil, 2011

Kansas City Missouri, USA

2018

PREPARATION OF PENTABLOCK NANOMICELLAR FORMULATIONS FOR PROSTATE CANCER DRUG DELIVERY SYSTEMS

Alex Oselu Owiti, Candidate for Doctor of Philosophy Degree

University of Missouri-Kansas City, 2018

ABSTRACT

This study is divided into three specific aims. Specific aim #1 focused on synthesis of pentablock co-polymer using monomers of L-lactide, ε-caprolactone and ethylene-glycol with varied molecular weights, (ii) characterization of the synthesized block co-polymers using X-ray diffraction crystallography (XRD), nuclear magnetic resonance (NMR), Fourier transform infra-red (FTIR) and critical micellar concentration (CMC).

Specific aim #2 focused on: (i) preparation of nanomicelles with polymers synthesized in specific aim 1, loading hydrophobic paclitaxel drug or hydrophobic ion pairing complex(HIP) of doxorubicin molecules, and characterizing them for shape, size and polydispersity indices, (ii) conjugation of a ligand(PSMA antibody) on the surfaces of nanomicelles to ensure selectivity and targeted delivery, (iii) Optimization of parameters such as drug-to-polymer ratio on experimental design using JMP software and, (iv) determination of pentablock stability at different temperatures, and *in vitro* drug release of the drug-loaded nanomicellar formulation.

Specific aim #3 was focused on: (i) assessing the safety of the synthesized pentablock copolymers by cytotoxicity studies on prostate cancer cell lines, (ii) determining cellular uptake and accumulation of the nanomicellar formulation from

specific aim 2 in prostate cancer cell lines (PC-3), and (iii) evaluating the targetability of PSMA antibody conjugated nanomicelles in prostate cancer cells.

Chapter # 1 outlines the overview of literature review on prostate cancer prevalence, available treatment options, as well as the current challenges faced by both the patients and the health practitioners during the treatment of prostate cancer.

Chapter #2 discusses the common nanoformulations used in drug delivery systems. There are many promising drug delivery strategies such as liposomes, polymeric nanoparticles, nanomicelles, and combination of techniques have been studied in order to develop a sustained tumor drug delivery system.

Nanomicelles (NM) enhance solubility and absorption of active pharmaceutical ingredients (APIs). Various polymers and non-polymers are being utilized to prepare nanomicellar formulations to achieve high absorption and delivery of drugs. In this study, we hypothesized that drug-loaded nanomicelles could be developed using pentablock copolymers for delivery of either paclitaxel or doxorubicin.

Chapter #3 discusses how monomers of lactide, ε-caprolactone and polyethylene-glycol were utilized to prepare pentablock copolymer by ring opening technique. The pentablock nanomicelles (PBNM) were formulated by evaporation-rehydration technique.

Chapter #4 elucidates how PSMA antibody conjugated drug-loaded nanomicelles were prepared using MPEG--PLA-PCL-PLA-PEG-NH2 Pentablock copolymer for targeted delivery of hydrophobic anticancer drug (paclitaxel) to prostate cancer cells. The resultant pentablock nanomicelles were conjugated with PSMA

antibody resulting in PTX-PBNM-Ab. XRD, FT-IR and the H-NMR analyses confirmed the structure of the pentablock copolymers.

Chapter #5 discusses the preparation of a hydrophobic ion-paring complex (HIP complex) of doxorubicin using hydrophobic retinoic acid. The resultant hydrophobic (DOX-RA) complex was utilized to prepare drug-loaded nanomicelles by co-precipitation method The average sizes for PTX-PBNM, PTX-PBNM-Ab and DOX-RA/PBNM were 20 nm ± 5.00nm, 45nm ± 2.5nm, 25.5nm ± 5.00nm, respectively, and ζ-potential for both PTX-PBNM and DOX-RA/PBNM was around zero, while PTX-PBNM-Ab had -28mV. *In vitro* release studies revealed that pentablock nanomicelles released PTX at a slow first order rate. The DOX-RA/PBNM released doxorubicin slowly in phosphate buffer solution (PBS) at pH 7.4 compared to pH 5.5 and pH 4.0.

Transmission electron microscopy analysis revealed well-defined spherical nanomicellar structure for all the types of pentablock nanomicelles. The *in vitro* cell uptake studies demonstrated that pentablock nanomicelles were well uptaken in the cells and a large amount of both PTX and doxorubicin were ferried into the cells.

APPROVAL PAGE

The faculty listed below, appointed by the Dean of the School of Graduate Studies, have examined the dissertation entitled “Preparation of Pentablock Nanomicellar Formulations for Prostate Cancer Drug Delivery Systems,” presented by Alex Oselu Owiti, candidate for the Doctor of Philosophy degree, and certify that in their opinion it is worthy of acceptance.

Supervisory committee

Ashim K. Mitra, PhD., Committee chair
Division of Pharmaceutical Sciences

Russell Melchert, PhD.
Division of Pharmacology and Toxicology

Kun Cheng, PhD.
Division of Pharmaceutical Sciences

Hari K Bhat, PhD.
Division of Pharmacology and Toxicology

Sullivan Read, PhD.
School of Biological Sciences

TABLE OF CONTENTS

LIST OF TABLES

LIST OF ILLUSTRATIONS

ACKNOWLEDGEMENTS

My immense appreciation and gratitude go to the Brazilian Government through CAPES Foundation, Ministry of Education of Brazil, Brasília - DF 70040-020, for funding through SwB scholarship. It is with magnificent pleasure that I acknowledge my advisor Dr. Ashim K. Mitra. His courage and compassion to accept me in his lab and his constant motivation were great factors in my academic career at UMKC during my graduate studies. I thank him for believing in me and helping me wade through the difficult times during my tough journey of graduate program.

I wish to express my most sincere gratitude to my great dissertation supervisory committee members, Dr. Read Sullivan, Dr. Russell Melchert, and Dr. Hari K. Bhat. I

feel privileged to have such extraordinary mentors in my supervisory committee. I am greatly thankful to Dr. Dhananjay Pal for teaching me cell culture techniques and for his relevant scientific advice which helped me immensely in my research project. I would like to extend my appreciation to Mrs. Ranjana Mitra for her constant support for the students including myself during my stay at UMKC. I am greatly thankful to my lab mates for standing with me during the tough times of graduate studies. I feel privileged to have such good friends.

I sincerely thank Joyce Johnson and Sharon Self for their constant support throughout my stay at UMKC. I appreciate support from Dr. Jenifer Friend from the School of Graduate Studies for encouragement and support. I am grateful to the School of Graduate Studies for constant support. I would also like to express my sincere thanks to Dr. James B. Murowchick (School of Geological Sciences) for helping me in XRD, Ms. Barbara Fegley (University of Kansas Medical Center) for TEM facility, and Dr. Teide LeAnn, (school of dentistry) for helping me with confocal Microscopy.

I cannot find words to express my gratitude to my brothers Peter Owiti and late Frank Owiti for having selflessly put their interests aside to pave way for our dreams, and my mother Sulmena Owiti for constant prayers. My father Martin Owiti Oselu, who as a WWII veteran, waded through difficulties to ensure our well-being and academic progress. My siblings, Tom, Thadius, Ernest, Roseline, Joseph, Stella and Jairo. My late sister, Mary Lucy, who like a mother, took care of us when we were young. I am greatly thankful to my beloved wife, Erin Oselu and my little daughter, Harmony Leila Oselu for their continued love and support. I am also grateful to Mr. Shailen Visaria,

who through financial support, helped me through high school and aided my entry into University in Brazil. Finally, I would like to thank the almighty God for making all these possible.

DEDICATION

I dedicate this dissertation to my little daughter, Harmony Leila Oselu, my beloved wife, Erin Suzanne Oselu and the people of the great country of Brazil.

CHAPTER 1

STATEMENT OF PROBLEM

Overview

Prostate Cancer

Prostate cancer is the most abundant cancer among males, and the second most common cause of cancer deaths in men, with a projection that 164,690 new cases will be diagnosed, and 29,430 deaths will be registered in the United States within the year 2018 (1). About one man out of nine men will be diagnosed with prostate cancer in his lifetime. In the USA, for example, prostate cancer develops particularly in older men with high frequency among African-American men(2).

Approximately 6 in 10 cases are diagnosed among men aged 65 or older, but it is not common below age 40. The average age of diagnosis is about 66. Treatment of localized prostate cancer is currently faced with many treatment options available (3). The options include radical prostatectomy, hormonal manipulation, radiation therapy, brachytherapy or any combination of these treatments.

The list of currently used drugs includes: immunotherapy, chemotherapy, and radiotherapy. All diagnoses are done with routine screening of prostate-specific antigen (PSA) level conducted during a periodical physical examination (4, 5). Another cellular marker for prostate cancer is prostate specific membrane antigen (PSMA), whose levels become elevated on the surfaces of cancerous prostate cells. Various drugs have so far been approved by the FDA for prostate cancer treatment(4).

The efficacy of current cancer therapy is mostly limited due to toxicity related to anticancer drugs that sometimes end up in normal tissues and cells. This limitation is caused by lack of selectivity of the anticancer drugs currently used in chemotherapy towards the tumor cells (5). To ameliorate this situation, pharmaceutical researchers are working to find ways to deliver the drug more adequately to the prostate, where it may target the tumor tissues and cells while sparing the normal cells. Targeting of drugs specifically to the prostate is essential for the treatment of diseases related to the prostate such as prostatitis, benign prostatic hyperplasia (BPH) and prostate cancer(6).

A drug delivery system is usually associated with drug molecules carriers such as, liposomes, nanoparticles, and nanomicelles which are meant to ferry drugs to the target site. Hydrophobic drugs are in most cases difficult to administer and one of the ways of overcoming such barriers is nanomicelles. Until very recently, surfactants were the principal materials utilized in nanomicelle formation process in pharmaceutical industry. However, reports have indicated that surfactants are inadequate due to their cytotoxicity and high critical micellar concentrations (7, 8).

Due to this problem, a number of materials including various types of polymers and copolymers have been developed with the sole aim of making nanomicellar formulations in aqueous medium with lower critical micellar concentration(9).

Paclitaxel

Paclitaxel (PTX) is a drug used against various types of cancers, mostly by stabilizing the polymerization of the microtubules of cancer cells(10, 11). Paclitaxel has also proven to act directly on isolated mitochondria from cancerous cells as well as on mitochondria of normal cells resulting in apoptosis and death of cancer cells (12).

However, poor aqueous solubility of PTX significantly hinders its anticancer activity(13). Studies have shown that intravenous administration of currently used paclitaxel formulation cause allergic reactions and precipitation at the spot of injection (14, 15). Hydrophobic drugs are generally not easy to administer in aqueous solutions. Nanoformulation may be a strategy for improving the delivery of drugs with low solubility and absorption (16, 17).

One type of nanoformulation known as nanomicelles (NM) has recently attracted pharmaceutical researchers in their quest to achieve adequate blood drug levels (18). Currently, various polymers and non-polymers are utilized to prepare nanomicellar formulations in order to obtain good absorption and delivery of therapeutics *in vivo* (17).

Nanomicelles are formed as a result of micellization, which occurs when amphiphilic molecules undergo self-assembly in contact with a hydrophilic solvent. Polar parts of the amphiphile face towards the polar solvent, while the hydrophobic part of the molecule faces away from the solvent resulting in a nanomicelle with

hydrophobic core(19). Opposite orientation in a non-polar environment generates reverse nanomicelles with a hydrophilic core(19, 20). While normal nanomicelles are applied to encapsulate hydrophobic drugs, reverse nanomicelles may be designed to encapsulate and deliver hydrophilic drugs(19).

Doxorubicin

Doxorubicin (DOX), is a drug used in treatment of various cancers. Doxorubicin is a member of anthocyanin family and is grouped under anthracycline with both antitumor and antibiotic activities. It works by interfering with DNA function causing intercalation and alkylation of DNA, causing disruption to both RNA and DNA polymerase, inhibition of topoisomerase II which consequently kills the tumor cells (21, 22).

DOX is applied mostly in the treatment of breast and bladder cancers. It is also used in cases of sarcomas, lymphomas, and acute lymphatic leukemia. It is normally used as combination with other drugs by intra-venous application. However, there are many serious side effects associated with doxorubicin (23).

These side effects include but not limited to allergic reactions when applied to patients that are allergic to doxorubicin and tissue damage at the site of injection. The most notorious side effect of doxorubicin is its ability to cause tissue and heart injuries due to drug accumulation and redox cycling and oxidative stress in the heart tissue resulting in dose-dependent cardiotoxicity(24). This irreversible dose-dependent, side effect may cause toxicity to cardiac and respiratory tissues, resulting in cardiomyopathy, dyspnea and intolerance to exercise due to the production of

mitochondrial reactive oxygen species (ROS)(25). Other common collateral effects are: loss of hair, suppression of bone marrow, skin eruptions, vomiting, and mouth inflammation. Patients often experience red coloration of the urine for a few days during treatment with DOX.

Doxorubicin is a widely used drug in clinical setting. However, less entry and low distribution of doxorubicin in tumor tissue are the principal factors for its therapeutic backlash (23).

Due to low pH in the tumor interstitial environment, weak base drugs like doxorubicin, are likely to ionized before entering the cells leading to reduced cell uptake (26). In addition, serious cytotoxic effects may be caused to healthy cells due to non-targeted delivery. These may result in: dose-dependent cardiac damages, multidrug resistance, and myelosuppression thus, restricting its therapeutic application (27).

It is important to develop new delivery systems that is capable of ferrying sufficient amount of drug to the tumor cells, thereby avoiding the multidrug resistance and frequent dose administrations of chemotherapeutics. One of the attempts to elevate the drug bioavailability in tumor tissue is the application of site-specific delivery systems that may release the encapsulated drugs within tumor cells.

Another way is to attain higher accumulation of drug by specific tumor cell targeting. However, this may be difficult to achieve without using a ligand that is unique to the target on the cell surface. This lack of proper ligand may end up delivering the drug to the undesired site (28).

Some intrinsic variations in the tumor microenvironment such as enzymes, pH and oxidative stress, and the extrinsic factors i.e., light, temperature and magnetic fields, are known to cause site-specific drug release within the tumor cells and tissues (29). pH triggered drug release from a nanocarrier is the most acceptable way of drug release directly inside the cell cytoplasm(29).

This strategy of using the acidic tumor microenvironment to trigger drug release has shown some short falls due to the acidity of the interstitial region of the tumor tissue which may result in drug release outside the cancer cells (30). Since the interstitial region of a tumor has a pH lower than 6.5, the ability nanocarrier might be restricted as well. For instance, some carriers such as liposomes become unstable and are altered before arriving at their intended targets. Another promising type of nanoformulation for delivery of hydrophobic drugs is nanomicelles(31, 32).

Nanomicelles display higher efficiency compared to other carriers like liposomes. They also possess many advantages, which include: high bioavailability, improved stability of the encapsulated drug, better encapsulation and loading efficiencies and better delayed release profile (33).

Furthermore, most of the materials utilized in its production are biologically safe for all forms of administration. The application of these nanomicelles is with respect to ability of nanoformulations to improve drug entry into the tumor tissue, while reducing dosage and enhancing drug efficacy by limiting non-selective cytotoxicity (34-37).

Objectives

The main objectives of this study are:

1. Development of drug-loaded nanomicelles with PCL-PLA- PEG-PCL-PLA Pentablock copolymers for delivery of paclitaxel, a hydrophobic drug. Use monomers of lactide, ε-caprolactone and polyethylene-glycol to prepare pentablock copolymer by ring opening technique.

2. Preparation of pentablock nanomicellar (PBNM) formulation by evaporation-rehydration method. This results in pentablock Nanomicelles

3. Development of PSMA antibody conjugated drug-loaded nanomicelles using MPEG--PLA-PCL-PLA-PEG-NH2 Pentablock copolymer for targeted delivery of hydrophobic anticancer (paclitaxel) drug to prostate cancer cells.

4. Analysis of both block copolymers and the nanomicelles by H-NMR, FTIR and XRD, and determination of the nanomicelles size and zeta potential using dynamic light scattering (DLS) as well as H-NMR and TEM analyses.

5. Conjugation of PSMA antibody on the pentablock nanomicelles, this resulted in PSMA-Ab-PTX-PBNM for targeted delivery to prostate cancer.

6. Development of a hydrophobic ion paring complex (HIP) of doxorubicin using hydrophobic retinoic acid. This was conducted to obtain a

hydrophobic (DOX-RA) complex for the preparation of rug-loaded nanomicelles by co-precipitation and evaporation-rehydration methods.

7. Analysis of DOX-RA complex using H-NMR and FTIR. Determination of the nanomicelles size and zeta potential using dynamic light scattering (DLS), and morphology using transmission electron microscopy (TEM).

8. In-*vitro* cytotoxicity and uptake studies of nanomicelles in PC-3 and T47D Cells. This involved confocal microscopy and it was conducted to determine the entry and distribution of the drug molecules in the cytoplasm of the cells. While cytotoxicity test was carried out to examine the toxicity of Pentablock Nanomicelles to PC-3 and T47D cells.

9. Cell proliferation assay. This test should indicate the extent to which drug loaded nanomicelles can be uptaken into the cells and their enhancement of the drug amount and efficacy inside the cells. A higher cytotoxicity is expected with Pentablock nanomicelle formulation in both PC-3 cells and T47D cells compared to normal cells. Proliferation of PC-3 and T47D cells in presence and absence of drug loaded pentablock nanomicelles PBNM were compared.

CHAPTER 2

LITERATURE OVERVIEW

Prostate cancer is the development of tumor in the prostate gland of male reproductive system resulting adenocarcinoma (38). Most prostate cancers progress slowly; however, some proliferate relatively faster. The cancer cells may migrate from the prostate gland to other parts of the body, mainly to the bones and lymph nodes. In the initial stages, it may display no symptoms. In advanced stages, it can lead to urination difficulty, inflammation, blood stained urine or pain in the pelvis, back or when urinating. Similar symptoms may also be seen in other diseases such as benign prostatic hyperplasia(39, 40).

Other late symptoms may include tiredness due to reduced levels of red blood cells. Prostate cancer may be caused by changes in the DNA of prostate cells. Some genes called oncogene are responsible for controlling cell growth, cell division, and cell death. Genes that keep tumor cell growth under control, by trying to repair mistakes in DNA, or cause cells to die at the right time are called tumor suppressor genes. Cancer can be caused in partly by DNA changes (mutations) that turn on oncogenes or turn off tumor suppressor genes(41). DNA changes can either be inherited from a parent or can be acquired during a person's lifetime(42). Many guidelines have been established to ensure a more standardized diagnostic, classification and management of prostate cancer(43)

Nanoformulations Used in Drug Delivery Systems

Over the last two decades, many promising strategies such as liposomes, polymeric nanoparticles, dendrimers, nanoemulsions, nanomicelles, nanosuspensions, and combination of techniques have been studied in order to develop a sustained tumor drug delivery system. These colloidal nanoformulations offer numerous advantages over conventional dosage forms, such as higher drug solubility, enhanced bioavailability, improved physical and chemical stability, and sustained drug delivery (44). Furthermore, nanoformulations have proven to lower toxicity and irritability related to drug and/or formulation, and eventually these delivery systems can improve *in vivo* performance and patient compliance. Such delivery systems can significantly evade the blood-tumor barriers, overcome the efflux related problems of the drugs, and reduce frequency of administration. Nanoformulation has also been attributed to oxidative stress evasion(45)

However, a clear understanding of the size, charge, and affinity of drug molecules towards various tumor tissues and pigments are crucial for the development of effective tumor formulations. For example, for cancer delivery, it is important to understand the structure and properties of the tumor such as pH of tumor microenvironment which might pose a great challenge to the drug independent of whether the drug is hydrophobic or hydrophilic(46, 47).

Permeability of a drug molecule across the tissues depends upon various physicochemical properties such as hydrodynamic radius, molecular weight, surface charge, and hydrophilicity. Studies revealed that larger molecules, may not cross the

cellular pores easily, while smaller molecules e.g. 20 nm particles cross the cellular pores quite easily into the tissue at very high extent(48). Similarly, the performance of nanocarriers is also affected by peripheral circulations (dynamic barrier: blood and lymphatic flow), surface modifications with endogenous molecules, size, and abundance of various enzymes particularly for biodegradable nanocarriers.

Liposomes

Research on liposomes has expanded considerably in the last thirty years. Liposomes are spherical biphasic vesicular system where the internal aqueous phase is surrounded by phospholipid bilayer membrane. Hydrophilic drugs can be encapsulated in the inner aqueous core while the hydrophobic drugs tend to stay in the lipid bilayer (49). Depending on the size, liposomes can be classified into small unilamellar vesicles (SUV) (10-100 nm), large unilamellar vesicles (LUV) (100-300 nm) and multilamellar vesicles with more than one bilayer(50). Liposomes can be formulated from sphingolipids, long chain fatty acids, cholesterols, glycolipids, membrane proteins, and non-toxic surfactants(50).

Therapeutic molecules such as proteins, nucleotides, small molecules, and even plasmids can be delivered with liposomes. These delivery systems can be employed to control and sustain the release of therapeutic molecules, and more importantly, they can be used to protect the therapeutic agent from metabolic degradation. Due to numerous advantages, liposomes have been extensively investigated in anticancer treatments. Investigators have studied transtumor permeation of neutral, anionic and cationic liposomes (51). Cationic liposomes interact

more efficiently with negatively charged tumor epithelial membrane relative to the anionic or neutral liposomes, and eventually provide higher transport across the tumor tissue. Along with small molecule drug delivery, liposomes have also been investigated as non-viral vectors for gene transfections and as a carrier for the delivery of monoclonal antibodies (50, 52).

Of late, laser was applied to monitor the release of drug and dyes from liposomes at the target site. In the future, laser-targeted delivery system may be utilized for the treatment of neovascular vessel occlusion, choroidal and retinal blood vessel stasis, angiography, and selective tumors. Liposomes prepared with naturally derived phospholipids such as egg phosphatidyl ethanolamine or dioleoyl phosphatidyl ethanolamine (DOPE) are more suitable for the anticancer drug delivery purposes. Liposomes have been successfully utilized for drug delivery to the anterior segment of the eye. The therapeutic efficiency of liposomes depends on various factors, including size and charge, encapsulation efficiency, retention and stability in conjunctival sac and tumor tissues and affinity towards tumor surface. The surface charge of liposomes plays a key role in determining their affinity towards the tumor surface. According to Felt, et al. negatively charged tumor surface has higher affinity towards positively charged liposomes(50).

Studies conducted with liposomal formulation for use in eye disease have shown that drug elimination due to lachrymal flow get reduced as the cationic liposomes increased the viscosity and interacted with the negatively charged mucus(53). Still in eye disease therapy study conducted by Monem, et al; Liposomes-loaded with pilocarpine hydrochloride proved that neutral MLVs showed the most

prolonged effect when compared to negatively charged MLVs and free drug. Likewise, another study conducted with acyclovir (ACV) encapsulated in liposomes and evaluated for their in vitro permeation and in vivo absorption across the cornea in rabbits showed that positively charged liposomes formed a coating on the tumor surface. The morphology depicted that liposomes bound tightly to the tumor tissue and increased the residence time and thus improved the absorption and permeation than aqueous solution. This may be mainly attributed to the electrostatic interaction between positively charged liposomes and the negatively charged tumor membrane (50, 54, 55).

In the case of a study conducted with ofloxacin liposomal hydrogel, the permeation was seven-fold higher than that of aqueous solution. Hence liposomal hydrogels can overcome all the tumor barriers and ensures steady and prolonged tumor permeation of the drug. Like other delivery systems, liposomal treatment is also associated with few drawbacks, such as possible toxicity and irritability. Lipid components of the liposomes are believed to be a primary source of toxicity, while charge of the liposomes is a main reason for irritability. These constraints may restrict their chances for becoming popular anticancer dosage form of the future. Moreover, commercial success of liposomes is also limited because of the difficulties in sterilization and their relatively short shelf life (49).

Nanomicelles

Nanomicelles are self-assembling spherical systems comprised of amphiphilic polymers, block copolymers or surfactants. Development of anticancer drug delivery systems with nanomicelles is very promising, particularly because of their advantages such as high thermodynamic and kinetic stability, the sustain release ability, and the enhancement of drug solubility and permeability across the tumor tissues(56).

Furthermore, nanomicelles can be functionalized with endogenous molecules for targeted tumor delivery. Normally, particle size of the nanomicelles ranges from 5 to 50 nm. In recent study, Vitamin-E was applied to increase the solubility of the poorly soluble drugs, while octoxynol-40 reduced tumor discomfort and also provided extra stability with higher optical clarity when applied to the nanomicellar formulation for optical use. Investigators suggested that any buffer system with adjusted osmolality and physiological pH could be used to prepare an external aqueous phase. Rapamycin has very low aqueous solubility (2.6 µg/mL). However, after preparation of nanomicelles, its solubility improved to 2 mg/mL (~1000 fold). An average diameter of the nanomicelles was around 25 nm. In a separate study nanomicellar formulation of 14C rapamycin was instilled in rabbit eyes, and 60 min tumor distribution of the drug was determined by liquid scintillation counter (31).

Evidently, a higher concentration of 14C rapamycin was observed in the choroid/retina (~360 ng/g), while very negligible radioactivity was found in the lens, aqueous humor and vitreous humor (57). Higher accumulations of rapamycin in the posterior segment of the eye was believed to be a result of the smaller mean diameter

of nanomicelles. Thermodynamically stable nanomicellar formulation could be a promising innovation for the non-invasive treatment of the posterior segment diseases (58-62).

In another disclosure (US 2009/0092665), Mitra and his team developed mixed micellar formulation of calcineurin inhibitors (voclosporin) for anticancer applications. Various concentrations of Vitamin-E and octoxynol-40 were used to prepare nanomicelles. Dilution studies were performed to evaluate the stability of voclosporin-loaded mixed nanomicelles (0.2 wt. %), and micellar stability was confirmed up to a 20 fold dilution in saline. In addition, results have demonstrated that nanomicelles dissociated at around 44 °C and the formulation was re-stabilized well within 8 min. Additionally, formulation remained stable in polypropylene and polyvinylchloride containers at room temperature for 48 h. The particle size of the voclosporin-loaded (0.2 wt. %) nanomicelles was between 13-33 nm. In vivo tumor tissue distribution studies were performed in two groups (single dose and 7 days repeat dose) of rabbits after topical application of mixed micellar formulation-loaded with 14C-radio labeled voclosporin (63). Almost 2 fold higher Cmax were observed in all tumor tissues (cornea, aqueous humor, sclera, upper eyelid, lower eyelid, retina/choroid, lacrimal gland, optic nerve and lower bulbar conjunctiva) of a group with 7 days repeated dosing over to the single dose group. No signs or serious symptoms of irritation were observed in any rabbits after a tolerability and tissue irritability study (56).

According to the results discussed in this disclosure, nanomicellar formulation seems to be very promising in the treatment of anterior and/or posterior segment tumor diseases including age related macular degeneration (AMD) and degenerative

macular edema (DME). Results discussed in these patent applications explained that the nanomicellar drug delivery systems can effectively change the course of tumor treatment.

Polymeric Nanoparticles

In order to address the problems of possible toxicity and irritability associated with liposomes, drug-loaded nanometer sized polymeric particles may be considered a viable alternative for the development of sustained release anticancer formulation(64). Nanoparticular systems comprise of particles with less than one-micron particle size in which therapeutically active agent is entrapped, absorbed, encapsulated, attached or adsorbed.

Aqueous suspension of drug-loaded polymeric nanoparticles can either be delivered as topical drops in the cul-de-sac or can be administered via trans-scleral, intra-vitreal or intraperitoneal routes. Development of sustained release biodegradable dosage form for intra-vitreal delivery may evade the limitation of frequent administration and it may also improve patient compliance. Polymeric nanoparticles can sustain drug release by diffusion, dissolution, or mechanical disintegration and/or erosion of the polymer matrix (18). Nanoparticles can circumvent the limitation of poor solubility of therapeutics. Additionally, the Nanoparticle can also protect the drug (e.g. peptides and proteins) from enzymatic degradation, and eventually, improves tumor bioavailability (65).

Various biodegradable and non-biodegradable polymeric systems have been developed for sustained delivery of non-steroid anti-inflammatory drugs (NSAIDs),

such as ibuprofen, flurbiprofen, and indomethacin in the treatment of anterior chamber inflammations(66).

In a recently published study, investigators have utilized Eudragit RS100 to prepare ibuprofen Nanoparticles for inhibition of an inflammatory response to surgical trauma(67). Results from in vivo efficacy studies performed on the rabbit eye model demonstrated a significantly higher aqueous humor concentration than the control aqueous eye drop. Similar studies were performed with flurbiprofen as an active agent for the prevention of myopia induced by extracapsular cataract surgery (53). A higher interaction of positively charged Nanoparticles (zeta potential +40–60 mV) with an anionic corneal surface was observed. A higher precorneal retention achieved with controlled release formulation was noted to be a primary reason for improvement in flurbiprofen tumor bioavailability. Tumor applications of indomethacin are limited by its poor bioavailability(67).

In an attempt to improve tumor bioavailability Calvo, et al. have examined three different colloidal carrier systems, that is, nanoparticles, nanocapsules, and nanoemulsions. Results of ex vivo transport studies across the excised rabbit cornea demonstrated higher indomethacin tumor bioavailability, due to the colloidal nature of the carrier system. Two different biodegradable polymers (PLGA and PCL) were utilized to formulate flurbiprofen-encapsulated Nanoparticles to improve tumor availability. Significantly enhanced corneal transport of flurbiprofen was observed in case of a nanocarriage system relative to free drug. Additionally, PLGA Nanoparticles demonstrated a lot higher transport of flurbiprofen compared with the PCL Nanoparticles in a study conducted with PLGA nanoparticles (68).

Subsequently, flurbiprofen-loaded PLGA Nanoparticles were prepared and evaluated by Vega, et al. Incorporation of Poloxamer 188 in nanoparticle preparation has significantly enhanced stability of Nanoparticles. Additionally, topical application of nanoparticle formulation in the rabbit eyes, enhanced anti-inflammatory efficacy without any signs of irritation or toxicity to tumor tissues. Enhanced efficacy could be due to an improvement in the bioadhesive property of Nanoparticles.

Cyclosporin-A (CS-A)-loaded chitosan Nanoparticles were successfully prepared and evaluated for topical tumor applications. Significantly positive zeta potential and a smaller particle size enhanced precorneal retention of Nanoparticles. In another study, Higher nanoparticle retention at the precorneal surface was confirmed by single photon emission computed tomography and scintillation counter measurement with nanoparticle probe. In another study, the same research group has disclosed physical mixture of PLA/chitosan to prepare rapamycin-loaded Nanoparticles (68, 69).

Incorporation of PLA significantly enhanced nanoparticle encapsulation efficiency (~13-fold) due to stronger hydrophobic interactions. In vivo studies were conducted in rabbits with topical dosing of rapamycin-loaded Nanoparticles, empty Nanoparticles, and no treatment. Post-treatment inflammation or blood vessel development was monitored. Results for treatment with rapamycin-loaded Nanoparticles demonstrated clear and transparent corneas. On the contrary, studies pertaining to the eye therapy with nanoparticles observed that corneas, which received no treatment or empty nanoparticle treatment were found obscured with stromal edema and/or neovascularization, within first 10 days.

Prednisolone is one of the most effective agents in a group of glucocorticoids, and it is marketed as tumor suspensions and drops. This product inhibits a wide variety of inflammatory responses, such as fibrin disposition, leukocyte migration, fibroblast proliferation, edema, capillary dilation, and capillary proliferation. Gemifloxacin and prednisolone were simultaneously encapsulated in mucoadhesive polymer (HA)-coated Eudragit nanoparticles (RS 100 and RL 100) in the treatment of bacterial keratitis. Evidently, enhanced tumor bioavailability (corneal and aqueous humor) for gemifloxacin was observed after topical instillation of nanoparticle suspension (25-27).

However, investigators did not evaluate tumor tissue distribution of prednisolone. Specific components such as chitosan and lecithin have shown positive charge to Nanoparticles and also enhanced stability of the formulation. Various block copolymers have recently been developed for use in various types of delivery systems including the block copolymers with temperature-dependent gelling capacity with varying polymer block ratio and pattern. These polymeric nanoparticles may be utilized for various chemotherapeutic interventions and treatment in cancer management(70).

Biodegradable Polymers

Many biodegradable polymers can be applied in the development of various drug delivery systems which include but not limited to cancer drug delivery systems(71). They are classified as being of natural and synthetic origins(72). The use of polyglycolic acid as a post-surgery polymer in the mid-20th century paved way for the discovery and development of new synthetic biodegradable polymers(72).

Synthetic biodegradable polymers can be designed in various structures and different molecular weights. The composition and molecular weight dictate degradation trend of a polymer. The important weight loss occurs due to cleavage of the structural chains. Most researchers have studied many types of biodegradable polymers and researched their applicability in the development stable formulation for drug delivery to tumor tissue in a more predictable manner with techniques which include thermosensitivity (73).

Polyalkylcyanoacrylates (PACA)

Polyalkylcyanoacrylates (PACA) derived from a category of acrylate polymers that are synthesized from alkylcyanoacrylic monomers by anionic polymerization technique. The quick degradation rate of PACA is due to the potential instability of its carbon-carbon sigma bond and presence of electron withdrawing neighboring groups in its structure. It has been very useful as surgical glue and skin adhesive(74).

PACA was also utilized for the development of nanoparticles. The PACA degradation rate varies from hours to days depending on the length of alkyl side chain. For instance, PACA with shorter alkyl chain length such as polymethyl-cyanoacrylate degrades in few hours whereas higher alkyl chain length derivatives such as octyl and isobutyl cyanoacrylates degrade slowly. Nanoparticles that are made of PACA are essential for preparation and utilization in drug carriers (74, 75).

Polyanhydrides

Numerous investigations have elucidated the role of polyanhydrides (POA) for drug delivery applications. These polymers exhibit faster degradation and limited mechanical strength, which make them an ideal candidate for fabrication of sustained

release devices. Low molecular weight polyanhydrides were synthesized through dehydrative coupling and dehydrochlorination whereas melt polycondensation polymerization was employed for synthesis of high molecular weight polymers(72).

The degradation rate of polyanhydrides can be easily modulated by changing the polymer composition and depends on the crystallinity and hydrophilicity of the final polymer. These polymers undergo surface erosion and generate monomeric acids that are non-toxic (76). Homo-polyanhydrides have limited application in controlled drug delivery due to their crystalline nature. In contrast, copolymers such as poly-(carboxyphenoxy) propane-sebacic acid (PCPP-SA) demonstrated controlled degradation rates. Polyanhydrides have also proven to prevent formation of reactive oxygen species (77, 78). This polymer was approved by the FDA for human applications for the delivery of carmustine in the treatment of brain cancer. Other approaches based on aromatic monomers composed of hydrophobic aliphatic linear fatty acids were also investigated for drug delivery applications(79).

Polyesters

Polyesters are biodegradable polymers having short aliphatic, ester-linked backbones(80). These classes of polymers are generally produced by either ring-opening or condensation polymerization. Ring-opening polymerization technique is most used compared to condensation reaction to for production of high molecular weight polyesters. Homo- or co-polymers derived from lactone rings and anhydrides with low molecular weights may be produced through ring-opening polymerization technique (81).

The molecular weight of the final polymer can be controlled by varying the ratio of monomers. The molecular weight of the polyesters regulates the hydrolytic cleavage that follows bulk erosion kinetics to produce metabolic products which are eliminated through normal metabolic pathways (82). The hydrolytic degradation rate of the polymers may be altered by varying the molecular weight, crystallinity and structure of the polymeric chain. Among polyesters, poly-α-hydroxyesters are the most widely studied category of polymers for cancer drug delivery applications; they include PGA, PLA and their respective copolymers(83).

Polycaprolactone (PCL)

PCL is a semi-crystalline polymer synthesized by ring-opening polymerization of ε-caprolactone (81, 84, 85). It has a glass transition temperature of -60 °C and a melting temperature in the range of 59 to 64 °C. PCL was investigated for long term delivery due to higher permeability to many drugs, excellent biocompatibility and extremely slow hydrolytic cleavage of polyester backbone (84, 86). The PCL based Capronor® implant has been developed for controlled delivery of levonorgestrel. It has a low tensile strength of 23 MPa and an extremely high elongation factor, more than 700%. Numerous investigations were attempted to improve the slower degradation of PCL. Copolymers of ε-caprolactone with lactide or glycolide exhibits remarkably better degradation profile (81, 85, 86).

Polyglycolide (PGA)

Polyglycolic acid (PGA) is a relatively hydrophilic polymer compared to other polyesters with high crystallinity and low solubility in organic solvents (81). The low solubility in organic solvent is attributed to its higher tensile module. It has a high

melting point of 225 °C and glass transition temperature of 36 °C. with a comparatively faster degradation rate than other polyesters and generates glycine upon degradation, which eventually eliminates through the citric acid cycle (87, 88). Major losses in the mechanical strength of PGA usually take place in one to two months and it completely degrades in vivo within six to twelve months.

PGA was initially explored for developing sutures because of their fiber-forming properties and excellent mechanical strength. However, it has limited role in prostate cancer drug delivery due to its faster degradation rate and higher crystallinity. PGA implants can be easily fabricated by widely applicable processing techniques such as solvent casting, compression and extrusion techniques(86).

Polylactic Acid (PLA)

PLA is comparatively more hydrophobic than PGA due to the presence of an additional methyl group(86). It is chiral in nature because of the structure of lactic acid and commonly exists in three isomeric forms the D (-), L (+) and racemic (D, L) lactide. The crystalline nature of PLA depends upon the isomeric forms and molecular weight of the polymer. PLA (L) is crystalline in nature and hydrolyzed through normal metabolic pathway due to presence of naturally occurring isomer (L-lactide). It has a melting point of 175 °C and glass transition temperature of 60 to 65 °C(89).

It also bears a good tensile strength of 50-70 MPa and high modulus of 4.8 GPa. On the other hand, PLA (DL) is amorphous in nature due to presence of the racemic mixture. It has glass transition temperature of 55 to 60 °C and comparatively faster degradation rate than PLLA. All isomeric forms of PLA follow bulk erosion

kinetics and generate lactic acid upon hydrolytic cleavage. Researchers have often utilized PLA for cancer drug delivery system applications(90).

Poly (lactide-co-glycolide) (PLGA)

Poly (lactide-co-glycolide), commonly known as PLGA is produced through the copolymerization of monomers of lactide and glycolide(90). This copolymer has low hydrolytic stability compared to the available homopolymers such as PLA and PGA. A well-defined research on a variety of these copolymers indicate their implication in drug delivery system(91). These copolymers are subdivided into two main compositions which contain lactide and glycolide. PLGA demonstrates an eroding kinetics, and its degradation is dependent on molecular weight apart from its lactide to glycolide ratio (92). As the level of glycolide in copolymer goes down, the hydrolytic degradation rate decreases (92). PLGA copolymers are FDA approved for human applications because of the excellent biocompatibility and controlled degradation profiles(89). PLGA is negatively charged and thus has adhesive nature (93).

Polyorthoesters

Polyorthoesters (POE) are hydrophobic polymers composed of a hydrolytically unstable polyester linkage(92). However, they exhibit slower degradation due to surface erosion. This degradation characteristic is ideal for designing sustained release devices. In this polymer the degradation profile can be easily adjusted by employing different diols for polymerization(94). The POE group is hydrolytically unstable in acidic conditions and requires basic additives to inhibit autocatalysis (92).

Degradation profile of POE II can be easily altered by incorporation of acidic additives such as adipic acid. POE III upon hydrolysis generates diol and pentaerythriol dipropionate, which subsequently generate propionic acid and pentaerythriol. This class of polymers is biocompatible and follows pH dependent degradation behavior. They do not require organic solvents for the incorporation of drugs due to their semisolid nature. However, there are difficulties in scale up processes that limit their application in drug delivery (94, 95).

CHAPTER 3

STRATEGIC PENTABLOCK NANOMICELLAR FORMULATION FOR PACLITAXEL DELIVERY SYSTEM.

Rationale

Paclitaxel (PTX) is a natural plant product obtained from the bark of western *Taxus brevifolia*. It is active against various types of cancers, mostly by stabilizing the polymerization of the microtubules of cancer cells (11). Paclitaxel has also proven to act directly on isolated mitochondria from cancerous cells as well as on mitochondria of normal cells resulting in apoptosis and death of cancer cells (12). However, poor aqueous solubility of PTX significantly hinders its anticancer activity(13). Studies have shown that intravenous administration of currently used paclitaxel formulation cause allergic reactions and precipitation at the spot of injection (14, 15). Hydrophobic drugs are generally not easy to administer in aqueous solutions.

Nanoformulation may be a strategy for improving the delivery of drugs with low solubility and absorption (16, 17). One type of nanoformulation known as nanomicelles (NM) has recently attracted pharmaceutical researchers in their quest to achieve adequate blood drug levels (18). Currently, various polymers and non-polymers are utilized to prepare nanomicellar formulations in order to obtain good absorption and delivery of therapeutics *in vivo (17).* Nanomicelles are formed as a result of micellization, which occurs when amphiphilic molecules undergo self-assembly in contact with a hydrophilic solvent. Polar parts of the amphiphile face towards the polar solvent, while the hydrophobic part of the molecule faces away from the solvent

resulting in a nanomicelle with hydrophobic core (17). Opposite orientation in a non-polar environment generates reverse nanomicelles with a hydrophilic core(19). While normal nanomicelles are applied to encapsulate hydrophobic drugs, reverse nanomicelles may be designed to encapsulate and deliver hydrophilic drugs. Reverse nanomicelles can be applied to deliver proteins and peptide drugs and hydrophilic small molecules (17, 81).

Until recently, surfactants were the main materials for nanomicelle formation. However, these surfactants have proven inadequate due to high cytotoxicity and critical micellar concentrations (CMC) (8, 96). High CMC means that nanomicelles can easily disintegrate in blood circulation after administration. Due to this obstacle, various materials including amphiphilic copolymers are being developed with the aim of forming nanomicellar structures in aqueous environments with lower CMC (9, 96). Various polymers such as Ɛ-polycaprolactone, polylactide, chitosan and many others can be employed for preparing nanomicelles with suitable biocompatibility (97). Nanomicelles exhibit several advantages as a delivery system i.e. Simple preparation, enhanced drug solubility, reduced toxicity, increased circulation time and better tissue penetration and targetability (56, 98).

However, conventional nanomicelles have several disadvantages such as system instability over certain periods of time, sustained release for short periods of time, unsuitability for hydrophilic drugs and the need for system optimization with each drug (86). It is for this reason we sought to synthesize pentablock copolymers that are stable, less cytotoxic, and that can provide better entrapment for the hydrophobic paclitaxel drug(99).

Materials and Methods

Materials

Poly ethylene glycol-PEG of different molecular weights, L-lactide and ε-caprolactone monomers, stannous octoate, triton X100 and coumarin-6 were purchased from Sigma-Aldrich (St. Louis). A Cyquant™ cell proliferation assay kit was obtained from Invitrogen Life Technologies Inc. through Thermos-Fisher Scientific. Paclitaxel was procured from ADOOQ Bioscience, Irvin, CA, USA. All other reagents utilized in this study were of analytical grade.

Methods

Pentablock copolymers were prepared in two steps. The first step involved the preparation of triblock and in the second step, the synthesized triblock was used to prepare pentablock.

Synthesis of Triblock Copolymers

Triblock copolymers composed of monomers of ε-caprolactone and poly (ethylene glycol), (PCL-PEG-PCL) were synthesized by a reaction involving ring-opening polymerization of ε-caprolactone, where PEG was utilized to commence the reaction and stannous octoate acting as a catalyst (100). Before polymerization, a specific amount of PEG (4.0 g) was heated in a round bottom flask at 130^{o} C until melting of the polymer, followed by addition of ε-caprolactone (8.0 g).

The reactants were degassed under vacuum for 30 minutes at every stage while being heated at 130°C. The flask was then purged with nitrogen gas, followed by addition of stannous octoate (0.5 wt. %). The reaction was carried out continuously

for 24 h with a temperature maintained at 130°C. The resultant polymer was then dissolved in dichloromethane and precipitated by transferring dropwise into a tube containing cold diethyl ether. Precipitates were centrifuged at 1200rpm and the sediments were vacuum-dried for 12 hours to remove any residual solvents. The purified polymers were stored at −20°C for future use (97, 101).

Synthesis of Pentablock Copolymers

To prepare pentablock copolymer, the triblock copolymer (PCL1250-PEG1500-PCL1250) which was first synthesized (Table 3.1) was used(18). Briefly, the whole amount (3g) of synthesized triblock copolymer was added into a round bottom flask and heated until melting point. A predetermined amount (0.8g) of L-lactide (250Da) was added into the flask containing the melted triblock copolymers.

This step was then followed by degassing under vacuum for 30 min while heating at 130°C. The flask was then injected with nitrogen gas followed by addition of stannous octoate (0.5 wt. %). The reaction was continued at 130°C for 24 h. The resultant pentablock copolymers were purified and stored in a similar manner as described earlier (81).

Table 3. 1 Triblock and pentablock copolymers with their respective chains and molecular weights.

COPOLYMER	CHAIN	MW(Da)	TOTAL MW(Da)
Triblock 1	PCL-PEG-PCL	1250-1500-1250	4000
Pentablock 1	PLA-PCL-PEG-PCL-PLA	250-1250-1500-1250-250	4500

H^1-NMR Analysis for Block Copolymers

To ascertain molecular structure of the formed block copolymers, samples of both triblock and pentablock copolymers were analyzed with a ^{1}H-NMR spectrometer. Spectra were acquired at room temperature using a Varian Inova 400 MHz spectrometer (Varian, Palo Alto, CA). Briefly, triblock and pentablock copolymers were dissolved in deuterated chloroform CDCl3 and samples solutions were transferred into NMR glass tubes before being submitted to the NMR chamber one by one. Chemical shift values were reported in parts per million (ppm) (102).

X-Ray Diffraction (XRD) Analysis of Pentablock and Triblock Copolymers

Physical states of synthesized pentablock and triblock copolymers were determined by XRD analysis. Triblock and pentablock copolymers were analyzed at room temperature by MiniFlex automated X-ray diffractometer (Rigaku, The Woodlands, and Texas- USA) equipped with Ni-filtered Cu-kα radiation (30 kV and 15 mA). The diffraction angle (2θ) ranged from 5° to 45° with 1° per min of increment(103).

Cytotoxicity Studies on Pentablock Copolymer

Human prostate tumor cells (PC-3) were cultured and maintained according to a protocol provided by ATCC. In brief, PC-3 cells were cultured in Dulbecco's F-12 medium containing 10% heat-inactivated fetal bovine serum (FBS), sodium bicarbonate, HEPES, streptomycin (100 mg/L) and penicillin (100mg/L). The solution samples of PB copolymer (20mg/mL) and triton-X100 (0.005mg/mL) were then transferred into 96 well plate containing already cultured PC-3 cells.

The plate was incubated under humidified environment at 37°C and 5% CO_2 for 24h. The wells were then washed three times with PBS followed by addition of Cyquant ™ cell proliferation assay reagent in each well and incubation for 4h before being analyzed using fluorescent plate reader at 480 and 520nm excitation and emission wavelengths respectively (104).

Viscosity Measurements

Rheological properties of 15wt% aqueous solution of pentablock copolymers was determined with the help of Oswald capillary viscometer at room temperature (25°C). The viscometer temperature was kept constant. Viscosity values were noted as average of triplicate measurements (kinematic viscosity, cP±1 standard deviation) and the values calculated by applying the equation 1.

$$\text{Vis}_{(\text{liq})} = (\text{density}_{(\text{liq})} \times \text{time}_{(\text{liq})} \times \text{Vis}_{(\text{water})}) / (\text{density}_{(\text{water})} \times \text{time}_{(\text{water})}) \quad \text{Eq.1}$$

Statistical Analysis of Pentablock Copolymer

In order to measure the cytotoxic effect of PB on the PC-3 cells, statistical analysis of the data obtained from the cytotoxicity assay was conducted using analysis of variance (ANOVA). Depending on the results of the ANOVA Student–Newman–Keuls comparison test, the evaluation data was applied to ascertain significance of differences. To make comparison on the significance of the difference between the means of 2 groups, Student's *t*-test $p < 0.05$ was considered as significant.

Preparation of Nanomicelles

Nanomicelles were prepared by hydration-dehydration method (16). Briefly: a small amount (0.1%w/v) of drug (paclitaxel) was dissolved in 1ml of ethanol. Separately, 2%w/v of pentablock copolymer was dissolved in 1 mL ethanol. The two solutions were mixed together, homogenized and evaporated in speed vacuum until a thin film was formed. Deionized (DI) water was then added to the resultant thin film followed by vortexing until complete dissolution was achieved(103). Solution was then filtered using 0.22μm filter membrane to obtain uniform sizes in a clear solution. It was further freeze-dried using glucose as a cryo-protectant (Fig.3.1 and Fig. 3.2)

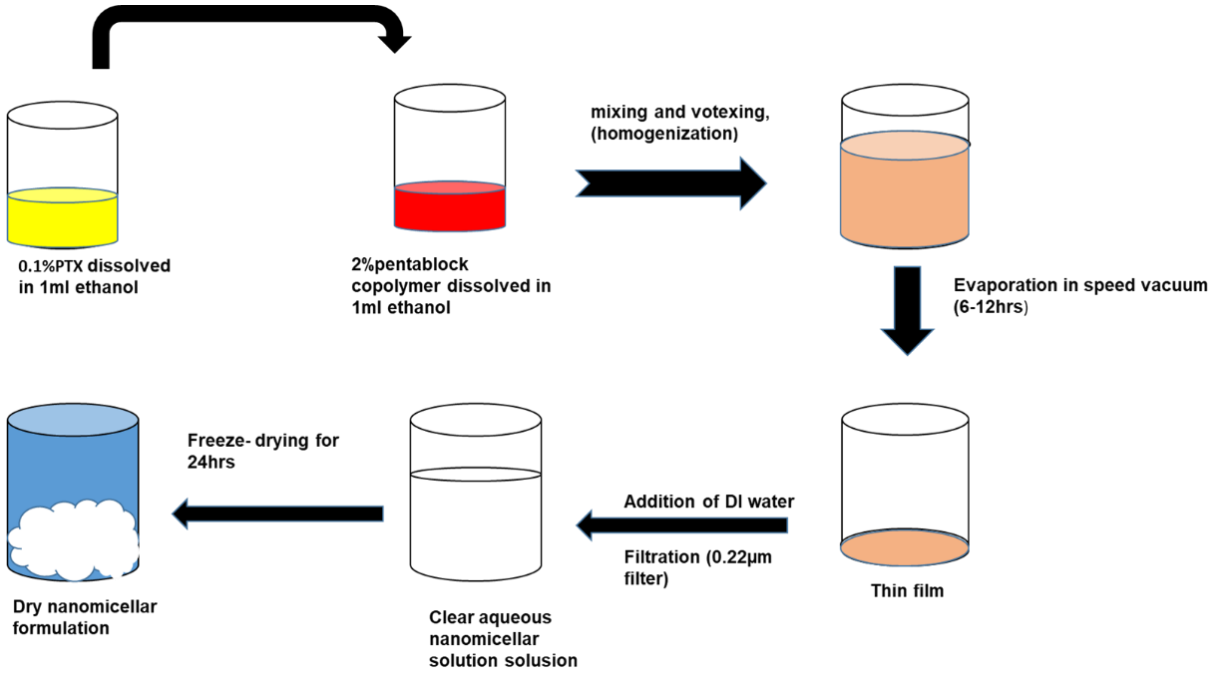

Figure 3. 1: A schematic illustration showing the preparation procedure for PTX-loaded Pentablock nanomicellar formulation.

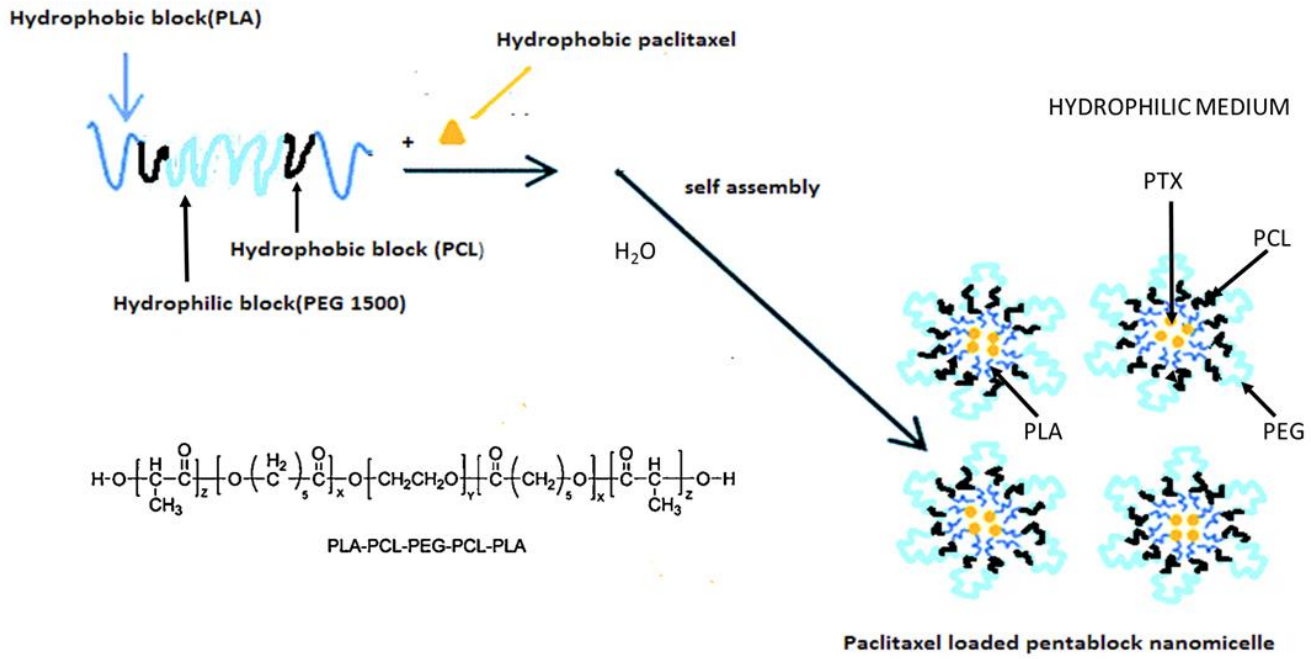

Figure 3. 2: Micellization process of pentablock copolymer with paclitaxel drug in aqueous environment

Freeze-drying of Paclitaxel-loaded Pentablock Nanomicelles

During the freeze-drying process, 1 mL of nanomicelle suspension was transferred to a 5mL freeze-drying bottle. On the other hand, 0.2 % w/v of glucose solution was prepared with deionized water(105). A specific amount (1mL) of glucose solution was then added to the nanomicelle suspension. The solution was homogenized before being submitted to a freeze-dryer (Labconco Corporation, Kansas City, MO,USA) for 24h to obtain powdered NM which was then collected and stored at 4°C for future use(106-108).

Critical Micellar Concentration (CMC) Determination

The micellization mechanism of the pentablock copolymer was monitored by iodine as a hydrophobic probe. A standard solution of KI/I_2 was prepared by dissolving 0.5 g of iodine and 1 g of potassium iodide in 50 mL of DDI water. Pentablock solution with different concentrations were prepared.

To each of the pentablock solution, 25 µL of KI/I_2 solution was added. Mixed solutions were then kept for 12 h at room temperature away from light. Values of UV absorbance for varying pentablock concentrations were measured with a UV-Vis spectrometer at 400 nm. The absorbance values were plotted against logarithm of PB concentration. CMC values correspondent to the concentration of PB copolymer with significant increase in absorbance was noted and registered. CMC of Pentablock copolymer was calculated in weight percentage (84, 85)

Nanomicelles Size and Zeta Potential Determination

Mean diameters and polydispersity indices (PDI) of both Paclitaxel-loaded pentablock nanomicelle PTX-PBNM and the empty pentablock nanomicelles (PBNM) were determined by dynamic laser scattering (DLS) using a Zetasizer HS 3000 (Malvern Instruments, UK), with a detection angle of 90 degrees at 25^{o} C. The average values of 3 measurements in 12 runs were calculated for all samples. The peaks for zeta sizes, PDI and zeta potentials were recorded accordingly(109).

^{1}H-NMR for PTX- PBNM

PTX-PBNM and empty PBNM were dissolved in either CDCl3 or D_2O then subjected to H^1-NMR analysis. An adequate amount of pure paclitaxel sample was dissolved in $CDCl_3$ before being analyzed. The spectra were acquired at room temperature using a Varian Inova 400 MHz spectrometer (Varian, Palo Alto, CA, USA). Chemical shift values reported in parts per million (ppm)(102). ^{1}H-NMR spectra were recorded from 12 to 0 ppm with a delay time of 4 seconds.

Fourier-Transform Infrared Spectroscopy (FT-IR) Analysis for Pentablock Nanomicelles

To determine structural properties of nanomicelles, samples of synthesized pentablock nanomicelles were subjected to FT-IR (Thermo-Scientific Nicolet iZ10) with an ATR diamond and DTGS detector. Freeze-dried samples of paclitaxel-loaded pentablock nanomicelles, empty nanomicelles and pure paclitaxel drug were analyzed at a scanning range of 650–4000 cm^{-1}.

Drug Encapsulation Efficiency

The amount of paclitaxel encapsulated in the nanomicelles was measured by UV-vis. briefly, a portion of the nanomicellar formulation was freeze-dried. Then 2mg of the dry formulation was dissolved in 1mL dichloromethane (DCM) to break the nanomicelle structure followed by centrifugation at 10,000rpm for 5min and then eventually evaporation to remove DCM. Subsequently, dry content was dissolved in ethanol. The resultant ethanolic solution was then filtered through 0.22-mm nylon

syringe filter. The filtrate was analyzed with UV-spectrophotometry at 221nm (Beckman, DU® 530, UV-vis spectrophotometer, Life science, CA, USA), for the determination of paclitaxel concentration. This process was performed in triplicate and a calibration curve with pure paclitaxel dissolved in ethanol at different concentrations produced an equation Y=38.059+0.029 and R^2 =0.9984 (110). Percentage encapsulation efficiency (%EE) and drug loading were calculated according to the equations below.

$$\text{Encapsulation efficiency (\%)} = \text{Total } \frac{\text{drug (mg)} - \text{Free drug (mg)}}{\text{Total drug (mg)}} \times 100$$

$$\text{Drug loading (\%)} = \frac{\text{Mass of PTX in nanomicelles}}{\text{Mass of PTX used + Mass of PB used}} \times 100$$

Statistical Analysis

A statistical program called JMP was applied for analyzing six different formulations. The polymer amount was the main determinant of nanomicelles size, showing the P-value of 0.0435 with the intercept probability greater than [t] <0.0001* (Tab.3.2), where $p < 0.05$ is considered significant.

Table 3. 2 Prediction profiler and parameter estimates showing the effect of drug%, and PB copolymer percentages on EE, LD, PDI, size and overall desirability of the PTX-Loaded pentablock nanomicelles.

EFFECT SUMMARY

Source	LogWorth	PValue
Polymer%(0.5,2)	1.361	0.04351
Drug%(0.05,0.2)	1.180	0.06614

Parameter Estimate

Term	Estimate	Std Error	tRatio	Prob>|t|
Intercept	19.442857	0.609659	31.89	<.0001*
Polymer%(0.5,2)	2.35	0.806503	2.91	0.0435*
Drug%(0.05,0.2)	-0.3	0.806503	-0.37	0.7288

Transmission Electron Microscopy Analysis

Morphology of nanomicelles was determined by transmission electron microscopy (TEM; Philips CM12 STEM, Hillsboro, OR.). Briefly, freeze-dried drug-loaded and empty nanomicellar formulations were separately dissolved in DI water to prepare aqueous solutions. The samples were further stained with 1% uranium salt. One drop of each solution containing nanomicelles was placed on a carbon-coated

copper grid, and excess fluid was removed with a piece of filter paper. TEM images were then obtained after the samples on the grids were completely dried.

Statistical Analysis for Pentablock Nanomicelles

Statistical analysis was conducted with full factorial design on JMP® software. Six formulations of pentablock nanomicelles with PB concentrations varying from 0.5% to 2.0% and paclitaxel concentrations varying from 0.05% to 0.2 % were treated as independent variables and their respective sizes, zeta potentials, percentage drug loading and entrapment efficiencies were recorded as dependent variable factors.

In vitro Drug Release Studies

Aqueous solutions of paclitaxel-loaded pentablock nanomicellar formulation samples (2%w/v), were poured into a dialysis bag. Equal volume (1mL) of Paclitaxel solution (0.1%w/v) was prepared and placed in dialysis bag(111). The bags were dipped in separate 15mL tubes containing 10ml buffer solution (PBS) each. Tubes were closed and placed in oscillating water bath at 37 degrees Celsius(112). Buffer containing released drug was collected and completely replaced at different time intervals (3 h, 6 h, 12 h, 24 h, 48 h, 72 h, 120 h, 168 h, 240 h) respectively(112). PTX content was detected by UV-Vis spectrophotometry as described above, and a calibration curve was generated to calculate the PTX concentrations.

Release Kinetics

In order to determine the release mechanisms, release data were fitted to various kinetic models, i.e., Korsmeyer-Peppas ($M_t / M_\infty = kt^n$), Higuchi ($Qt = Kt^{1/2}$), Hixon-Crowell ($C_0^{1/3} - C_t^{1/3} = K_t$), First-order ($LogC = LogC_0 - Kt/2.303$), and Zero-

order (C = K0t). Best fit model was identified based on R^2 values. Exponent of diffusion (n) of Korsmeyer-Peppas equation was applied to determine the release mechanism (85).

Cell Uptake Studies for Coumarin6-loaded Pentablock Nanomicelles

Coumarin6-loaded PBNM at different concentrations of 10µg/mL and 20µg/mL and two solutions of coumarin-6 at 10µg/mL and 20µg/mL were used in the uptake experiment. These solutions were transferred into 4 chamber slides with PC-3 cells grown for 72 h. Drug uptake was carried out at 37^{o} C for 1 h. Then the drug was removed before washing the slides 3 times with cold PBS to stop further uptake.

The slides were further treated with 4%paraformaldehyde, washed 3 times with PBS, and then kept in mounted with cover slip and kept at 4^{o} C. The slides were then observed using confocal laser scanning microscopy (LEICA ®, microsystem, Weitzler , Germany) with 488 and 536nm excitation and emission wavelengths respectively for coumarin-6 detection(102, 108)

Cell Proliferation Assay for PTX-PBNM

Cell proliferation assay analysis was conducted using a DNA based Assay Kit called CyquantTM® Cell Proliferation (C7026) that contains fluorescent dye called CyquantTM® GR dye (113). Briefly; PC-3 cells were cultured in a 96 well plate with Dulbecco's F-12 medium as described previously. Cells were incubated in 96 well plate at 37 ^{O}C and 5%CO_2 until confluence. The medium was then removed followed by addition of different medium solutions made of empty PBNM (10 µg/mL,

20μg/mL), pure PTX (5μg/mL, 10 μg/mL, 20μg/mL and 30μg/mL) and PTX-loaded PBNM (5μg/mL, 10 μg/mL, 20μg/mL, and 30μg/mL) in specific row of the plate.

The plate was then incubated under humidified atmosphere at 37°C and 5% CO_2 for 24h. The wells were then washed with PBS 3 times. Cyquant reagent solution was prepared and added in each well. The plate was then kept for 1h at 4^o C. The plate was submitted to the fluorescent plate reader where detection of cell proliferation is caused by fluorescence enhanced when the dye is bound to cellular nucleic acids (DNA).

Results and Discussions

Pentablock Synthesis and Analysis

^{1}H-NMR Analysis for the Block Copolymers

^{1}H-NMR was applied to determine the structure of the synthesized PCL-PEG-PCL triblock copolymer and PLA-PCL-PEG-PCL-PLA pentablock copolymers (97). Fig. 3 depicts ^{1}H-NMR spectra of TB, and PB copolymers dissolved in deuterated chloroform. As described in the Fig. 3.3, ^{1}H-NMR characteristic peaks of the copolymers observed at 1.40, 1.65, 2.30 and 4.06 δ ppm which represent methylene protons of -(CH_2)3-, -$OCOCH_2$-, and -CH_2OOC- of ε-caprolactone, respectively. A well pronounced peak at 3.65 δ ppm designated to methylene protons (-CH_2CH_2O-) indicating the presence of PEG in both TB and PB. Characteristic signals at 1.50 (-CH_3) and 5.17 (-CH-) δ ppm designate L-lactide blocks of pentablock. Deuterated chloroform (-CH) shows at 7.25ppm. While a peak at 3.38 δ ppm depicts methyl terminal of (-OCH_3-) of PEG.

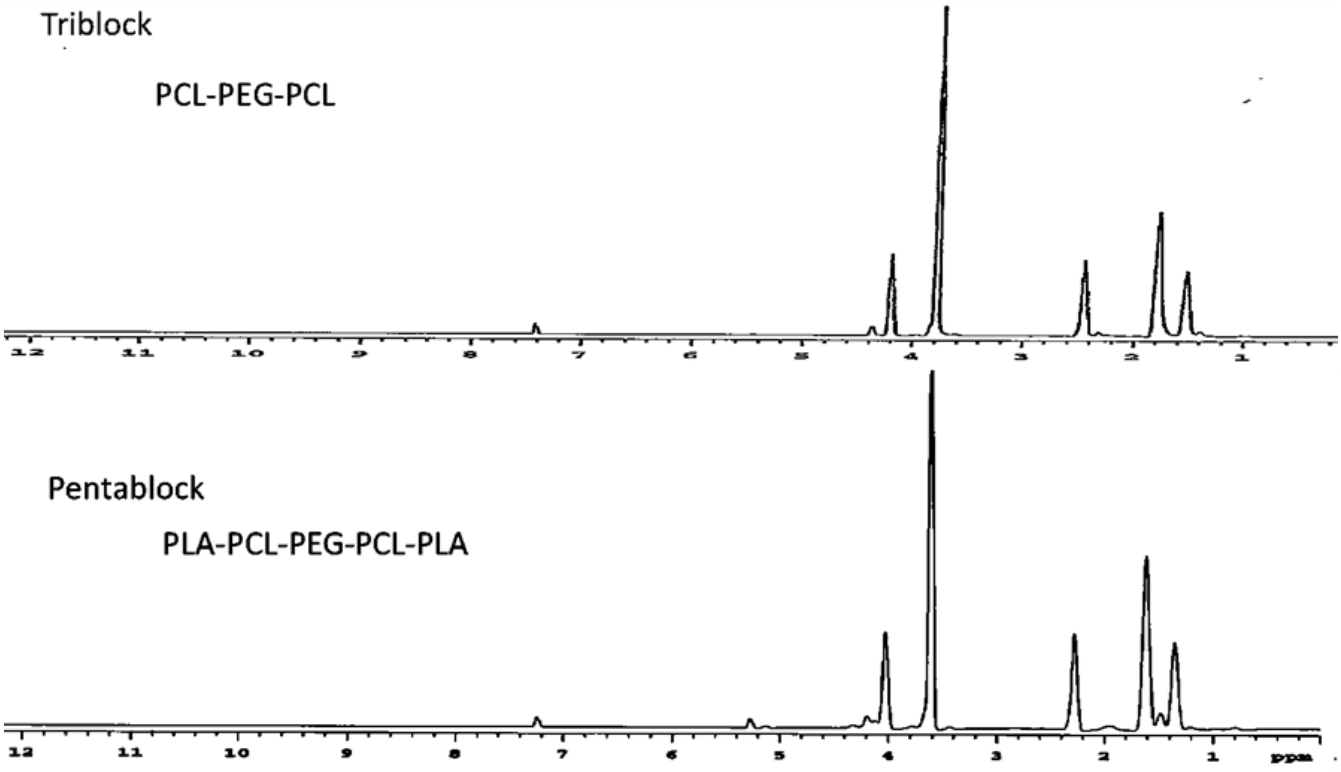

Figure 3. 3: H-NMR peaks showing protons for PB and TB copolymers.

Viscosity Determination of Pentablock Copolymer

Rheological characteristics of pentablock copolymers were analyzed with Oswald glass viscometer and the result generated a value of 0.7883 which is close to the water viscosity (0.8880). These results suggest that pentablock is suitable for IV nanoformulations (81).

X-ray Diffraction Analysis for Block copolymers

Crystallinity and phase composition of triblock and pentablock copolymers were evaluated with XRD analysis (Fig.3.4). There were no peaks corresponding to PEG in all block copolymer samples analyzed. All block copolymers provided more pronounced crystallinity peaks of PCL at two-theta (2θ) between 21^{o} and 22° for both TB and PB. PLA showed crystallinity peaks between 2θ of 22^{o} and 24^{o} for PB copolymer. XRD peaks for TB on the other hand did not show PLA blocks in the composition as it was not used during its synthesis.

Therefore, only the PCL crystallinity peak was present in TB at 2θ around 23^{o}. Attachment of PLA blocks at the terminals of triblock copolymers showed a small reduction in the peak intensity indicating semi-crystalline structures of the triblock. Crystallinity of block copolymers can be determined by the arrangement of monomer blocks in its structure. Furthermore, recently published reports suggest that reduction in crystallinity significantly influences degradation of block polymer (114).

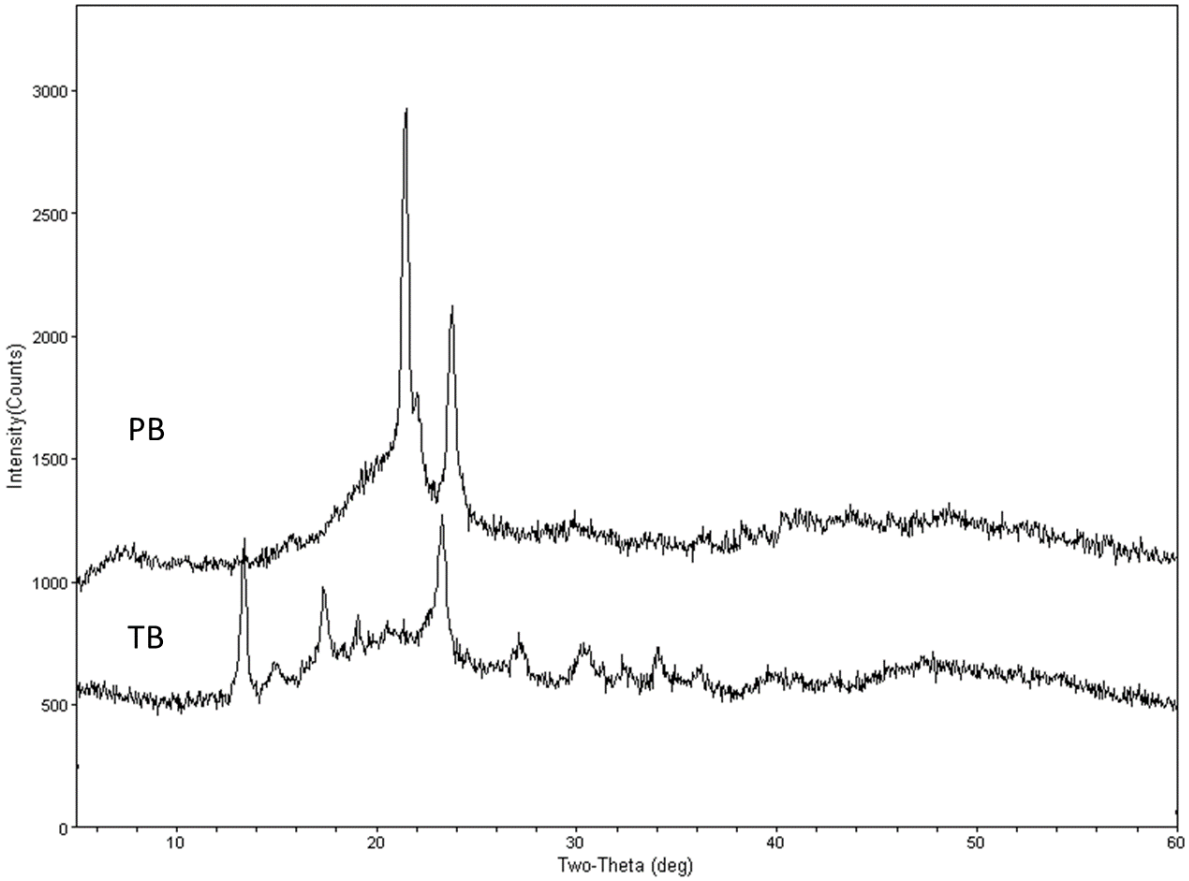

Figure 3. 4: The XRD peaks showing a comparison between TB and PB copolymers.

Pentablock Cytotoxicity Analysis

Cytotoxicity assay was performed on the pentablock copolymers for a period of 48h to evaluate the cytotoxic effects of both the pentablock copolymers. The test was conducted using cell proliferation assay (Cyquant) Kit. Triton X-100 was used as positive control. Pentablock copolymer did not demonstrate any cytotoxic effects (Fig. 3.5). Furthermore, the results observed in assay were again confirmed by statistical test (Anova) which revealed F greater than F-critical. This depicted no significant deference between the pentablock copolymer and the negative control after the

Anova results were submitted to Tukey post Hoc test and revealed no significant difference between the pentablock samples and the negative control(table 3.3) . The results from this assay clearly suggest that pentablock copolymers are safe and therefore can be used for formulation to be used in both topical and intravascular application(86). The constituents of this pentablock copolymer has also been studied in previous work conducted by Sulabh P. Patel *et al*.., in our laboratory, where the block copolymers were studied against various cell lines using MTT and LDH analyses. The results obtained demonstrated nontoxicity in both assays (84, 85)

Table 3. 3;Tukey post Hoc test results for the cytotoxicity analysis of samples of PB copolymers against both positive (triton X100) and negative control(media)

Comparison	Absolute difference	Critical Range	Significance, Reject μ=0
A vs B	0.0205	0.01384601	TRUE
B vs C	0.00125	0.01384601	FALSE
A vs C	0.02175	0.01384601	TRUE

Tukey post Hoc test results for the cytotoxicity analysis where B) represents samples of PB copolymers, A) represents positive (triton X100) and C) represents negative control (media)

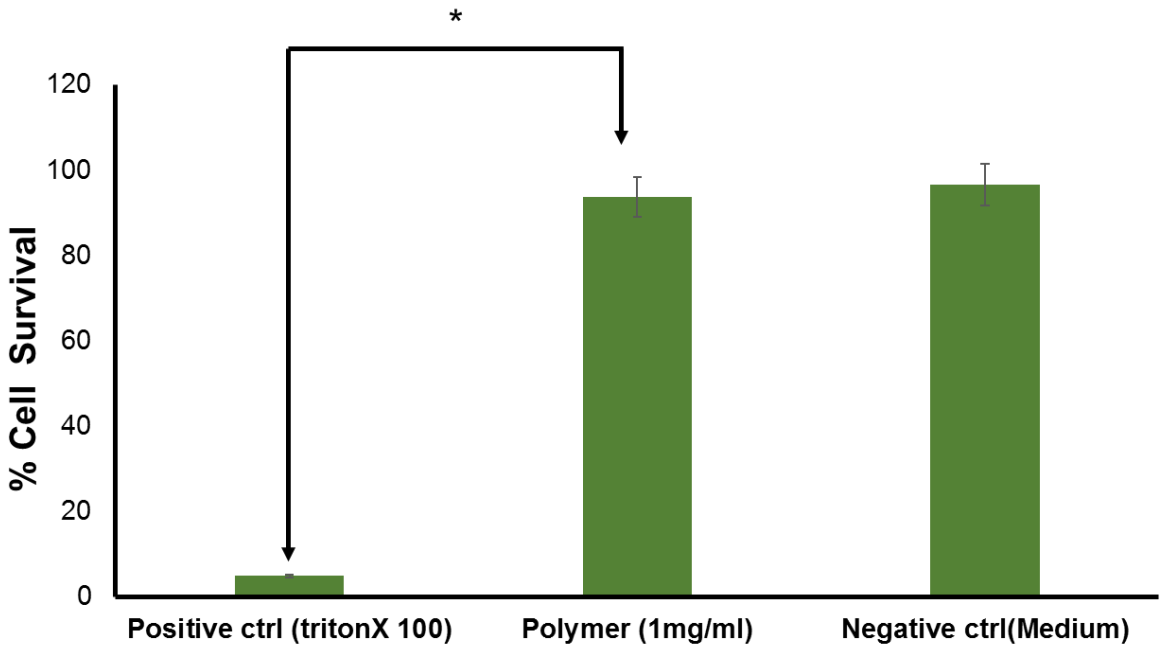

Figure 3. 5: Cytotoxicity in % cell survival of pentablock copolymer relative to negative and positive control (triton X 100). Negative control has 100% cell survival. Asterix denotes significant difference between the positive control and the polymer sample.

Freeze-drying of Pentablock Nanomicelles

Freeze-drying (also known as lyophilization) serves to ensure the preservation of physical and chemical characteristics of a product, i.e. neat appearance, short time of reconstitution, acceptable suspension, narrow size distribution of Nanomicelles and un-altered encapsulated drug activity. Furthermore, it ensures adequate relative humidity and sufficient stability(115). Cryoprotectants are stabilizer that are added to nanosuspensions during freeze-drying process to prevent stresses related to freezing and drying. The recommended cryoprotectants used in pharmaceutical industry include: Sucrose, lactose, glucose, trehalose, glycerol,

mannitol, sorbitol, glycine, alanine, lysine, polyethylene glycol, dextran, and PVP(105). These sugars tend to vitrify at specific temperature ($T_{g'}$)(116).

The immobilization of nanomicelles within a glassy matrix of cryoprotectants limits their aggregation and prevents mechanical stress of the formed ice crystals. Generally, freezing should occur below $T_{g'}$ of frozen amorphous sample or below eutectic crystallization temperature (T_{eu}), which denotes the crystallization temperature of soluble component as a mixture with ice, if in a crystalline state to achieve total sample solidification (105, 117). In this study, the freeze-drying process, glucose was use as cryoprotectants to achieve the same effect (105). The freeze-drying process lasted 24h and the paclitaxel-loaded pentablock nanomicelle (PTX-PBNM) powdered was obtained and stored at 4 °C for future use (106-108).

CMC Determination

CMC is a characteristic of *in vitro* and *in vivo* stability of nanomicelles(118). Low CMC values of pentablock copolymers cause high stability of nanomicelles in solutions upon dilution (31). Nanomicellization mechanism of pentablock copolymer can be studied with Iodine as a hydrophobic probe for determination of critical micellar concentration of pentablock copolymer. Solubilized I_2 tends to partition in microenvironment of the pentablock copolymer which is amphiphilic.

The results in the conversion of I_3 to I_2 causes excessive KI in the solution. CMC of Pentablock copolymer was calculated to be 0.035 wt. % (Fig 3.6). This low CMC of pentablock suggests that the PB copolymer displays stability and ability to maintain integral structure even after dilution (119).

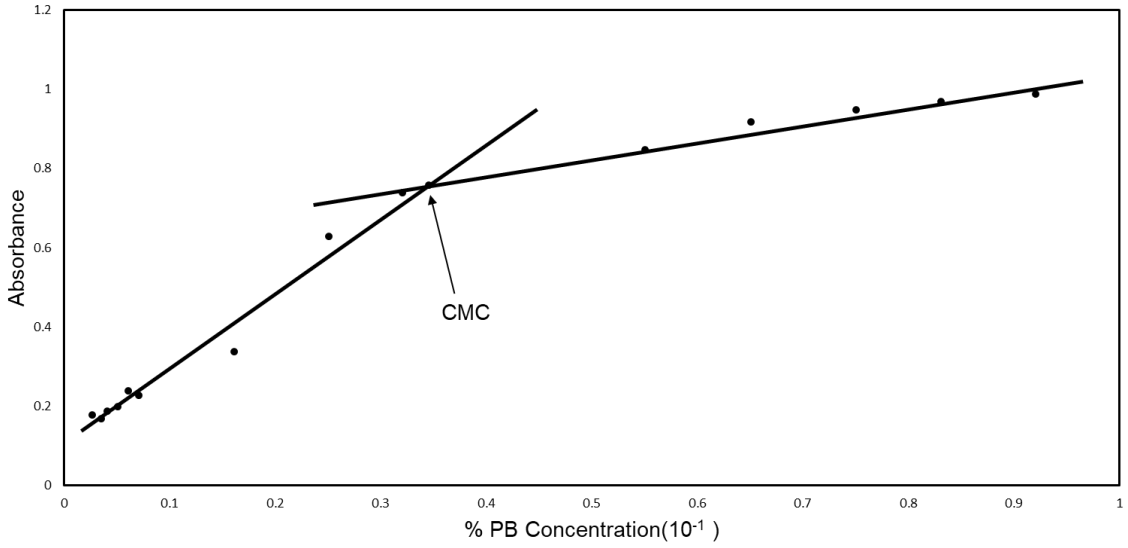

Figure 3. 6: CMC graph showing % pentablock concentration versus UV-Vis absorbance.

Drug Encapsulation Efficiency

Percentage of drug encapsulation efficiency (EE) is a crucial factor for drug delivery carriers. The percentage EE of paclitaxel loaded in pentablock nanomicelles was calculated to be 99% while the drug loading was found to be approximately 11%. These results demonstrate that pentablock nanomicelles achieved high paclitaxel entrapment efficiency and adequate drug loading which might be attributed to the hydrophobic core formed by hydrophobic PCL and PLA. This property allows for efficient entrapment of the hydrophobic paclitaxel drug.

FTIR Analysis for PTX-PBNM

FTIR spectra were obtained for freeze-dried samples of PTX-PBNM and empty NM as well as pure paclitaxel drug and PB samples. The result show absorption band

at 1700 cm−1 and multiple bands that range from 1000–1500 cm−1 depicting the presence of ester bonds in pentablock copolymer (Fig.3.7). C-O bands at 1100 cm−1 and O-H band stretching at 3300 cm−1 are for PEG and PLA and PCL. C-H stretching bands at 2940 and 2900 cm−1 indicate the presence of PCL blocks.

Bands manifested in the region around 3000cm $^{-1}$ can be assigned to aromatic C-H stretching of PTX**,** The C-C ring stretching of PTX occur in the region from 1652-1579 cm-1. However, primary aliphatic amines in PTX are present in the region 3450-3250 cm-1.

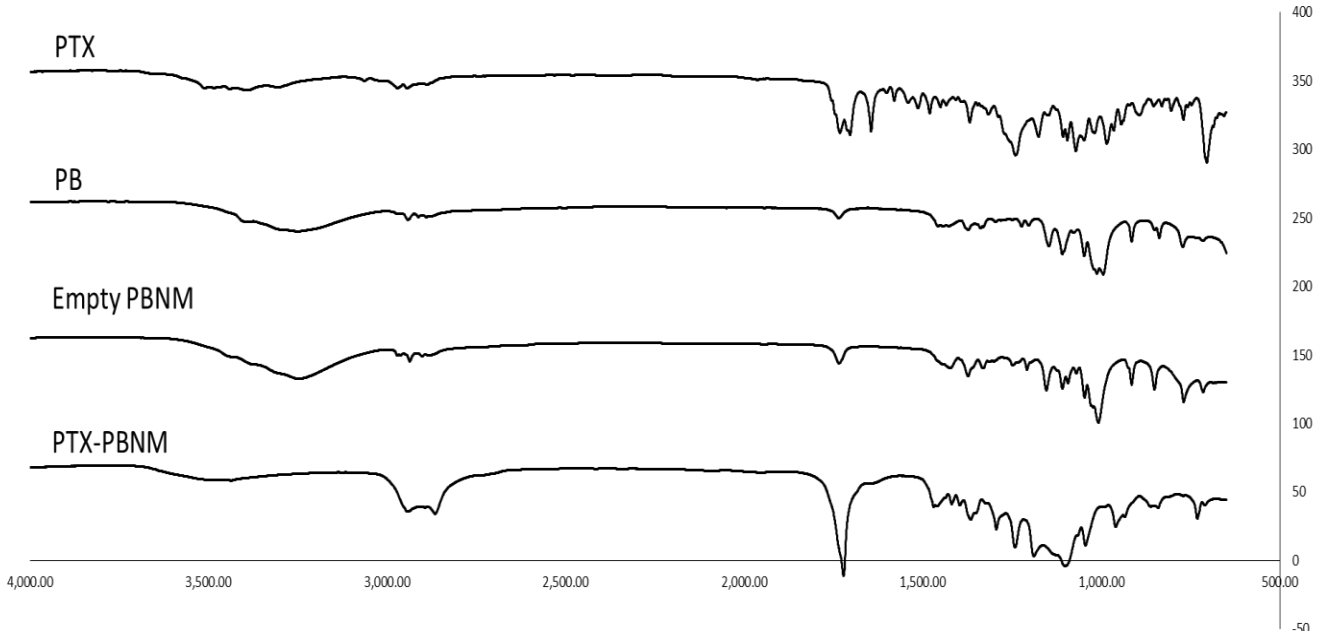

Figure 3. 7: FT-IR spectrum for the samples of PTX-PBNM compared to the empty PBNM, and pure PTX drug.

Size Distribution for Pentablock Nanomicelles

Solvent evaporation method was applied for the preparation of both PTX-PBNM and empty PBNM. These PBNM formulations were analyzed to determine the size, polydispersity index (PDI), and zeta-potential (Table 3.3). Average mean diameters for empty PBNM and PTX-PBNM are11.96±5.00nm, and 20.98±5.00nm respectively (Fig 3.8A and Fig 3.8 C). Small negligible peaks appeared at regions beyond 1000nm for PTX-PBNM, perhaps due to a small aggregation in the sample, but still the majority peak (around 98%) was 20.98±5.00nm (fig.8C).

Average PDI for PTX-PBNM and empty PBNM are 0.049±0.005 and 0.042±0.005 respectively. PDI values suggest that the nanomicelles exhibit uniform particle size distribution with less aggregation. Both unloaded and drug-loaded nanomicelles display neutral zeta potential (around 0±2.5 mV) as shown in Fig.3. 8B and 3.8D. This makes it possible for the pentablock nanomicelles to be an excellent candidate for intravenous application since it is unlikely to produce interactions with blood components (120, 121)

Table 3. 4 Zeta analysis results showing the sizes, zeta potentials and PDI of both the empty and the paclitaxel-loaded pentablock nanomicelles.

Sample	Size (nm)	Zeta potential(mV)	PDI
PTX-PBNM	20.98±5.00	0±2.5	0.049±0.005
EMPTY PBNM	11.96±5.00	0±2.5	0.042±0.005

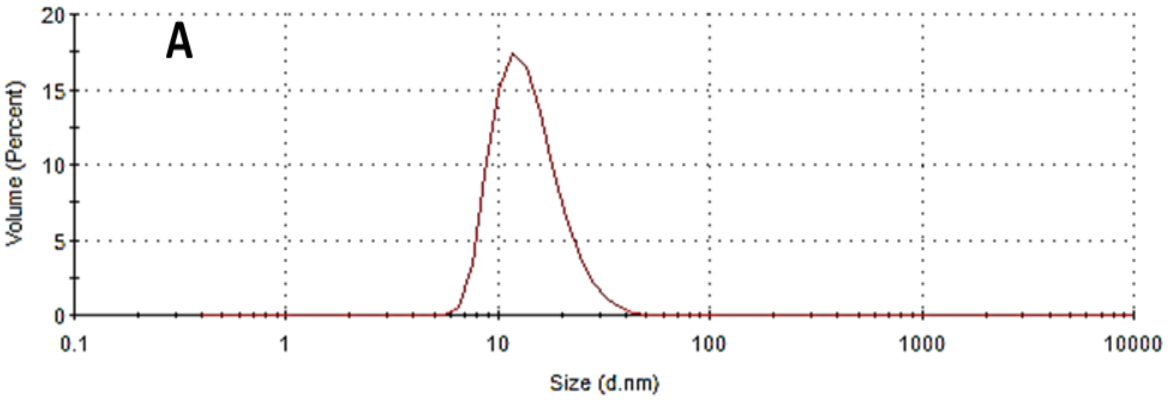
A
Volume (Percent)
20
15
10
5
0
0.1
1
10
100
1000
10000
Size (d.nm)

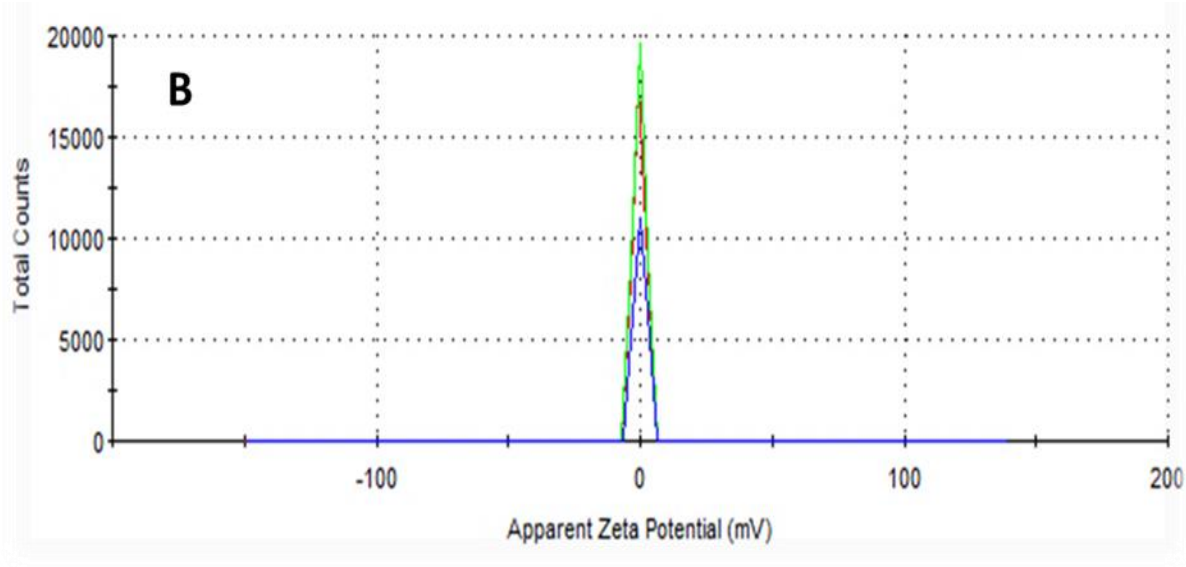
B
Total Counts
20000
15000
10000
5000
0
-100
0
100
200
Apparent Zeta Potential (mV)

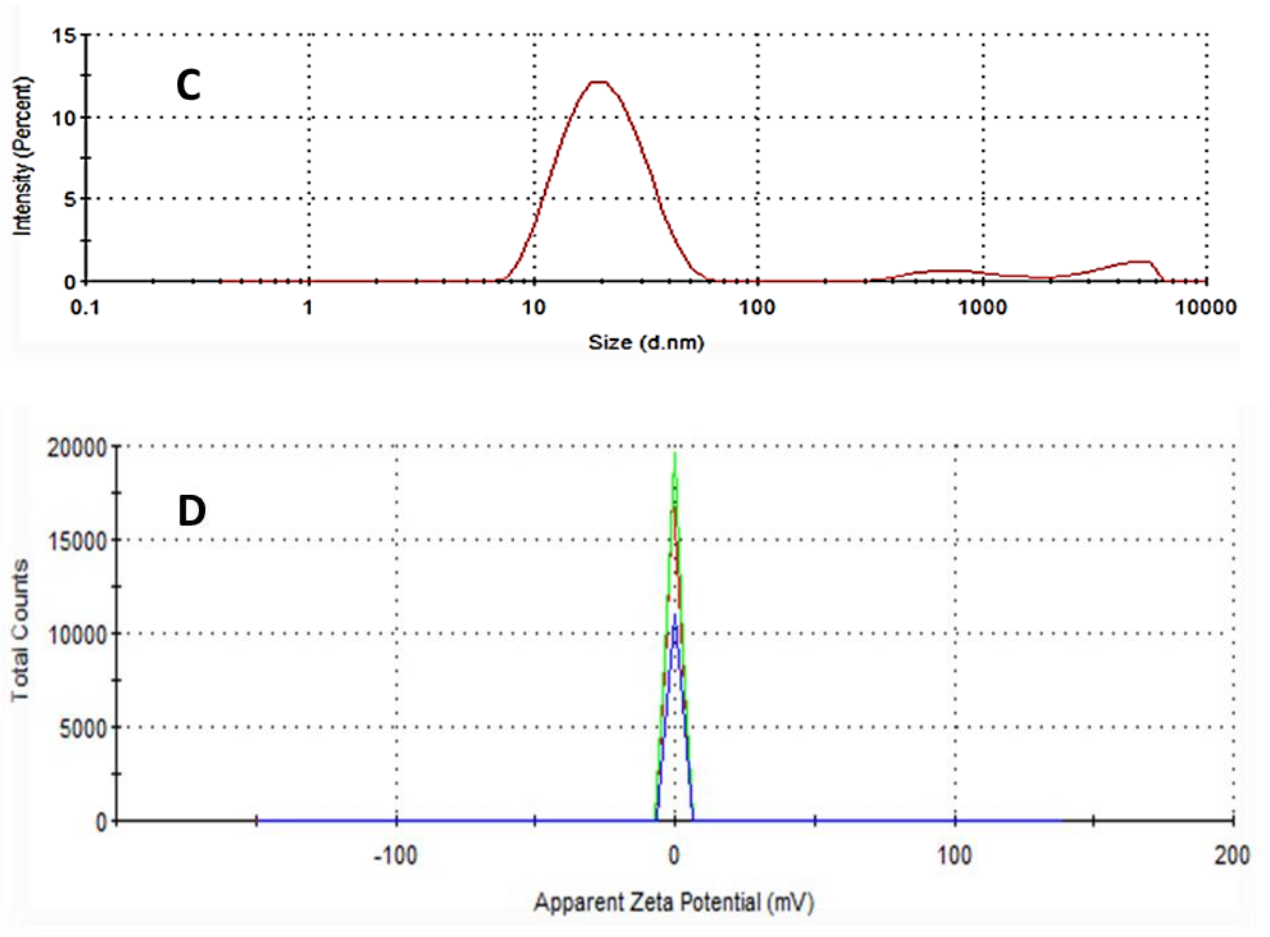

Figure 3. 8: Comparison between two pentablock nanomicelles in terms of size and zeta potential, where A and B denote the respective size and zeta potential distribution curves for the empty PBNM. C and D show the size and zeta potential curves for PTX-loaded PBNM.

^{1}H-NMR Analysis for Pentablock Nanomicelles Formulation

H-NMR analysis was conducted in order to understand the structure and polymerization of PTX drug and PB copolymer during NM formation. Both $CDCl_3$ and D_2O were applied as solvents to analyze samples. PTX-PBNM, and empty PBNM were dissolved in D_2O while free PTX was dissolved in $CDCl_3$ due to its hydrophobicity (Fig. 3.9).

Although known to be insoluble in water, the solubility in D_2O was significantly improved in the presence of PB copolymer as a result of nanomicellization. Samples containing PB copolymer and paclitaxel in $CDCl_3$ showed sharp peaks representing various protons of PEG, PCL, PLA and paclitaxel. Interestingly, a sample containing PB copolymer and paclitaxel in D_2O was devoid of paclitaxel signal suggesting that paclitaxel is inside the nanomicellar core.

Broad peaks observed at 3.75 δ ppm and 2.30 δ ppm were attributed to the protons of PEG (-CH2-CH2-) and PCL (-OCO-CH2-), respectively. Proton peaks for PLA and PTX were absent. NMR analysis carried out in CDCl3 exhibited sharp peaks for all the protons indicating free movement of polymer chains and paclitaxel in organic solvent.

However, NMR spectra carried out in D_2O exhibited very few broad peaks representing PEG and PCL blocks only and no paclitaxel or PLA. These results suggest that paclitaxel was located in the core of nanomicelle along with PLA blocks, hence very weak NMR signals for PCL in D_2O. This could as well be due to their restricted molecular movement in the structure. Strong peak of PEG in D_2O indicate the location of PEG in outer surface of nanomicelles. Results from this study suggest

that PBNM are solubilized in water via micellization process where core is composed of PCL-PLA and shell is of PEG.

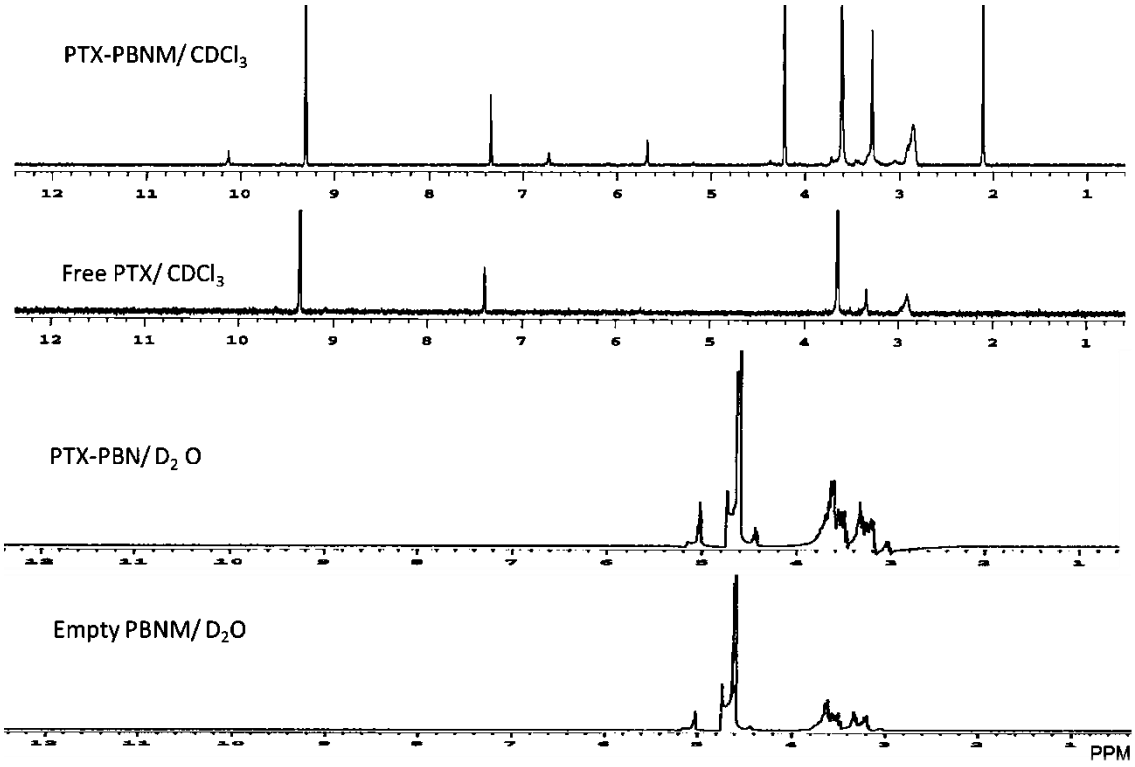

Figure 3. 9: HNMR peaks of PTX-PBNM in both $CDCl_3$ and D_2O, free PTX in $CDCl_3$ and empty PBNM in D_2O.

Transmission Electron Microscopy Analysis

Morphology of pentablock nanomicelles was investigated by transmission electron microscopy (TEM). This analysis showed that the nanomicelles were spherical, homogenous, and did not produce aggregates (Fig 3.10). In regard to size, paclitaxel-loaded pentablock nanomicelles had an average of 20±2.5nm and the empty pentablock nanomicelles were around 10±2.0nm.

Unloaded (empty PBNM) and PTX-PBNM did not differ in terms of morphology, with both having uniform appearance. The particle sizes visualized in the TEM images corroborate with the sizes obtained by DLS which already depicts the PTX-PBNM and the empty PBNM sizes as 20.98±5.00nm and 11.96±5.00nm respectively.

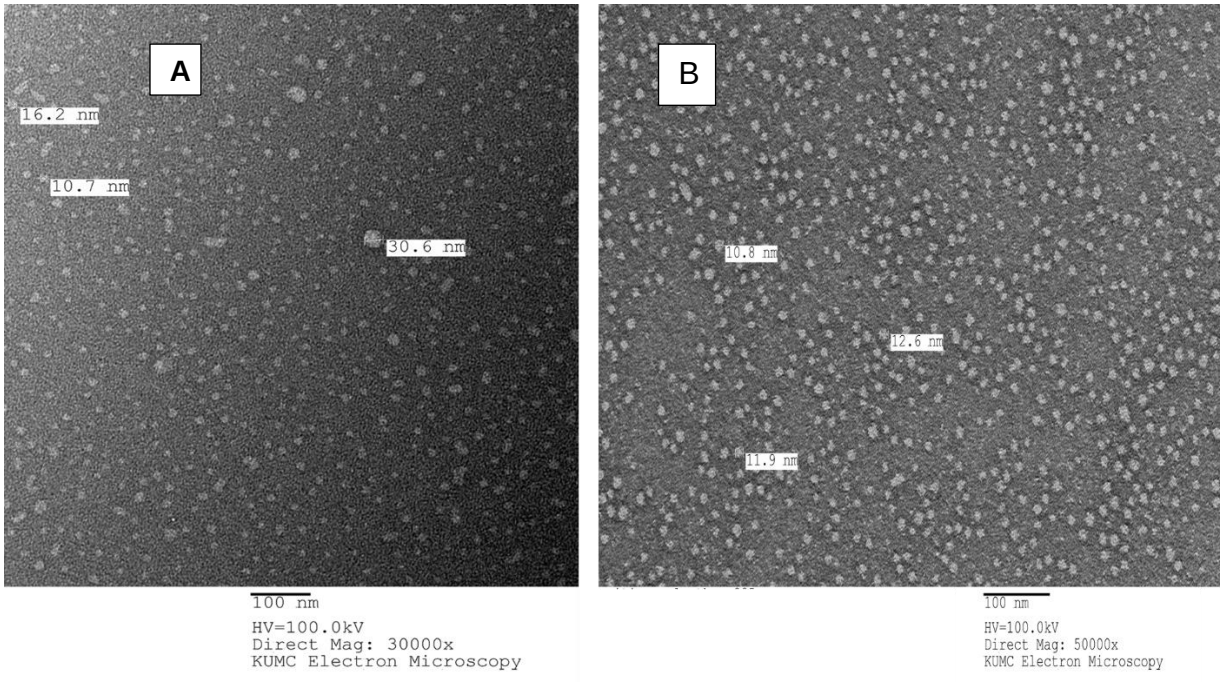

Figure 3. 10: TEM images of A) paclitaxel-loaded pentablock nanomicellar formulation and B) empty PBNM.

In vitro Drug Release Studies

In vitro release profile of paclitaxel from pentablock nanomicelles was investigated at a physiological pH of 7.4 at 37 ^{o}C. A substantial quantity of pure PTX (0.1%w/v) dissolved in 1mL of ethanol/water (0.5: 9.5) was used as a control. Equal amount of freeze-dried PTX-loaded PBNM formulations with different PB copolymer concentrations (0.5%, 1%, 1.5% and 2%) were also dissolved in DI water under the same condition. PTX release from hydroethanolic solution was rapid in comparison to PTX in PBNM, with almost 100% drug release occurring within 72h.

Release trend of paclitaxel from the pentablock nanomicelles were slow with no significant burst effect. Results suggest a sustained release of the PTX drug from the pentablock nanomicelles (PTX-PBNM) over a period of 200 h (Fig 3.11). A small amount ethanol (5%w/v) was added to overcome the hydrophobicity of PTX resulting in a homogenized drug solution. All the four PTX-PBNM formulations could be dissolved in DI water easily. The presence of PEG in the pentablock structure affords interactions with aqueous environment, resulting in a clear homogenized solution.

There were variations in the release trend among the PTX-PBNM formulations. At a time point of 172 h, the formulation containing 0.5%PB released around 95% of the drug followed by 80%, 50% and 40% for formulations containing 1%PB, 1.5%PB and 2%PB respectively. This trend shows that the more the polymer in the formulation, the longer it takes for the nanomicelles to release the drug (Fig. 3.11). This may be attributed to the thick wall which forms with higher polymer concentrations.

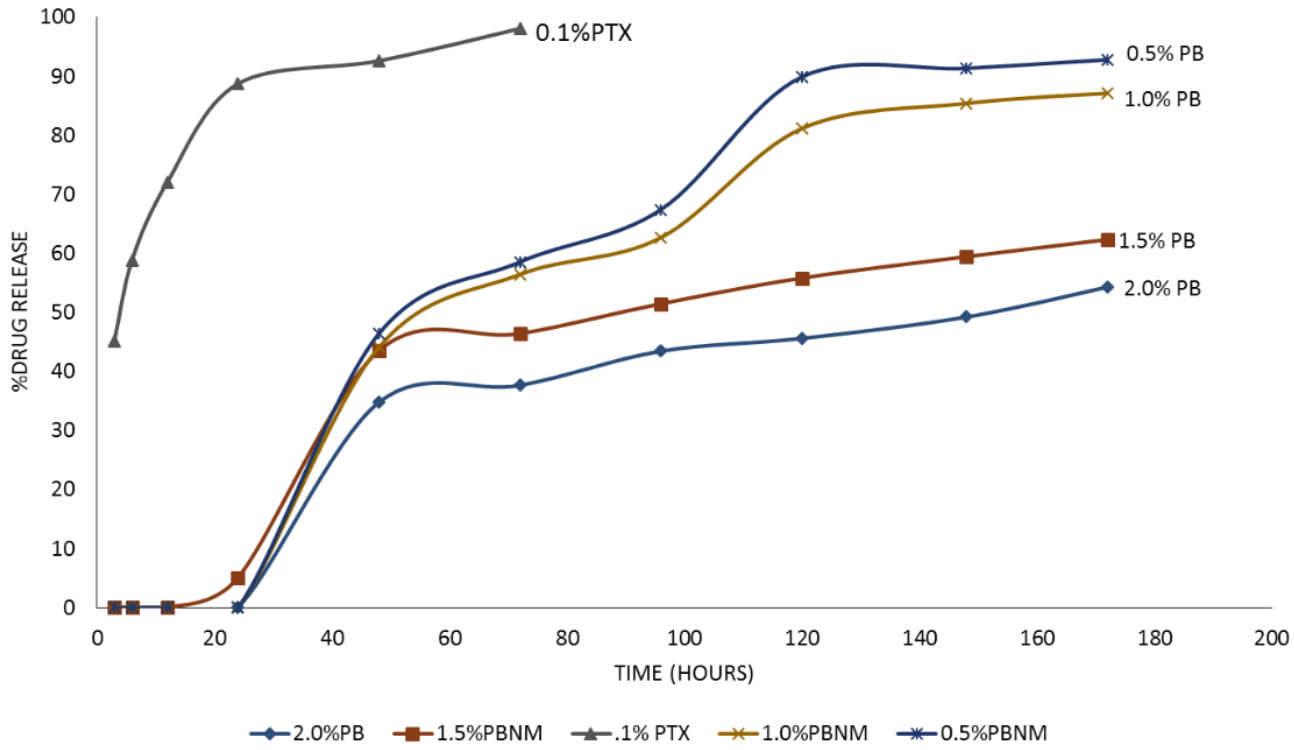

Figure 3. 11: Cumulative drug release from PTX-loaded nanomicelles in PBS (pH 7.4), at 37 ± 0.5°C. Each point represents the mean value of three different experiments ± standard deviation.

Release Kinetics

The data obtained from *In vitro* release profile were applied to, Higuchi, Korsmeyer-Peppas, Hixson-Crowell as well as zero and first order models to determine the kinetics of Paclitaxel release. Our best fit model was the Korsmeyer Peppa's based on average R^2 value (0.995). The diffusion exponent, n value ranged from 0.267–0.372 for the PB copolymer samples tested. The n-values below 0.43 depicts diffusion dependent mechanism of paclitaxel release (85).

In vitro Cell Uptake Studies

Studies were conducted in order to analyze nanomicelle uptake by PC-3 prostate cancer cells. In this study, PTX was replaced with coumarin-6 due to its ability to emit fluorescence compared to the non-fluorescent paclitaxel. Cell monolayers were incubated in chamber slides with coumarin-6 loaded pentablock nanomicelles or coumarin-6 only. Coumarin-6 loaded nanomicelles were prepared in the same manner as described previously.

Cell uptake of nanomicelles was monitored by fluorescent confocal microscopy. Images were taken after incubation of confluence PC-3 cells with 0.25 mg/ml coumarin-6 loaded nanomicelles formulation and naked coumarin-6 for 48h at 37^{o}C (Fig. 3.12 A&B). In figure 3.12 B, green coumarin-6 was observed with high intensity all over the cytoplasmic region excluding the nucleus (DAPI stained).

This indicates that nanomicelles are internalized by PC-3 cells. A large amount of coumarin-6 was taken inside the cells with pentablock nanomicelle formulation compared to less intensity of coumarin-6 concentration observed with naked coumarin-6 (Fig. 3.12 A).

Therefore, it can be concluded that fluorescent coumarin-6 loaded nanomicelles are in the intracellular space. There was a significant ($p < 0.05$) intracellular accumulation of coumarin-6 loaded nanomicelles when compared to free coumarin-6. This observation suggests that high accumulation of coumarin6-PBNM may be due to endocytosis or pinocytosis that may have allowed coumarin-6 loaded pentablock nanomicelles to generate higher uptake in comparison to free coumarin-6.

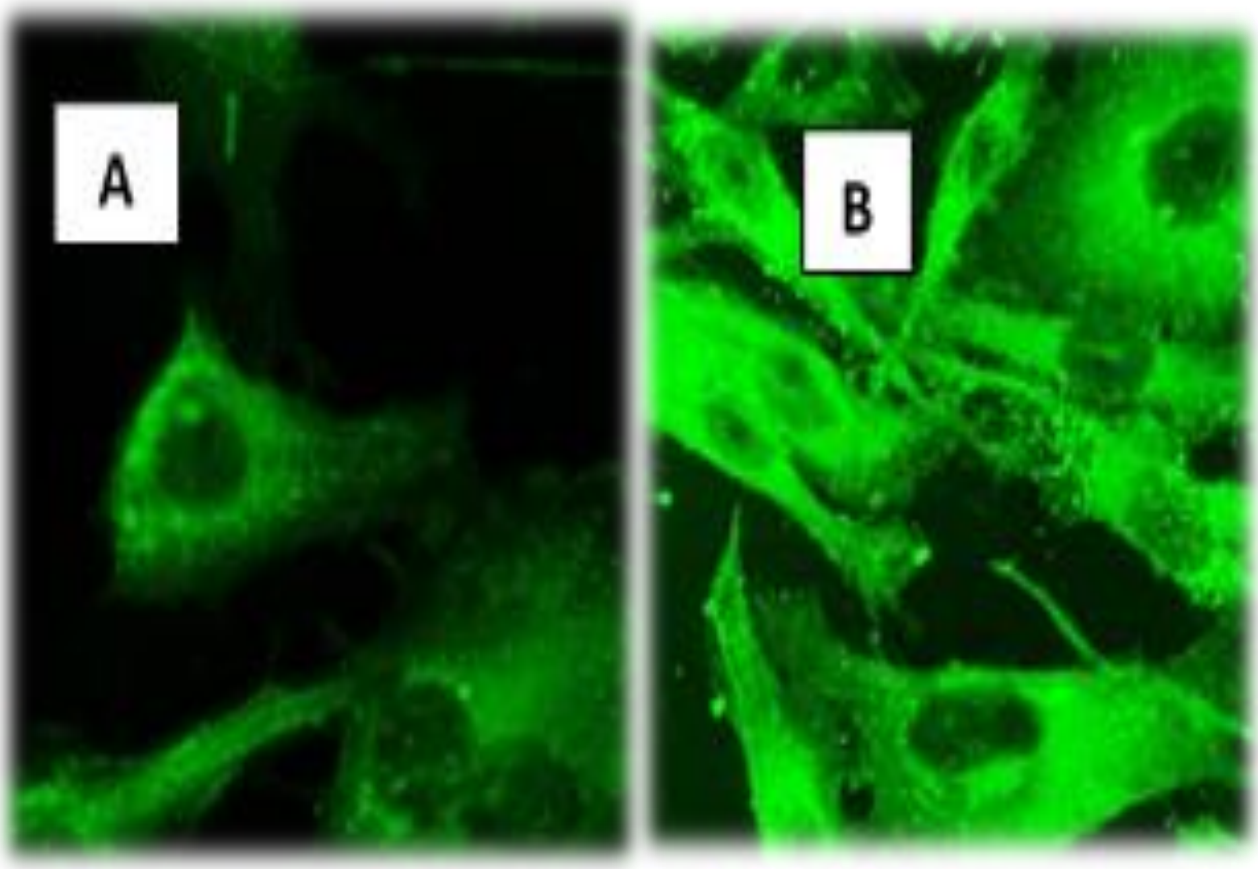

Figure 3. 12: Confocal imaging depicts a comparison between A) Cell uptake of naked coumarin-6(10µg) and B) Cell uptake of coumarin-6 loaded in PBNM (10µg) in PC-3 cells.

Cell Proliferation Assay of PTX-PBNM

Cytotoxicity of paclitaxel-loaded pentablock nanomicelles formulation was evaluated in PC-3 cell lines using a CyquantTM cell proliferation assay. It works under a principle of interactions of fluorescence emitted by DNA with a special dye in the assay. Percentage of cell growth inhibition was measured by fluorescence caused by DNA of surviving cells after 48 h incubation. Paclitaxel concentration in the formulations was adjusted to the same as that of free drug.

PTX-PBNM formulation showed significant cytotoxic effect in PC-3 cells as the free drug after 48h incubation ($p < 0.05$) as shown in Fig. 3.13. It is worth noting that at 48 hours, the drug is not completely released from the PTX-PBNM (only 30%-40%was released) as earlier depicted by the release profile. Nanomicelle formulation showed a significant difference in reduction of cell proliferation than the free drug ($p < 0.05$). One of the reasons for this difference may be due to the multi-drug resistance effect on free drug (efflux) through *p*-glycoprotein which may have resulted in lower intracellular concentration of paclitaxel drug(122). Large amount of PTX within the PTX-PBNM was delivered into PC-3 cells by endocytosis, causing cytotoxic effect (123). Direct impact of efflux mechanism on paclitaxel inside the cells may have been reduced by loading drug into the core of the PTX-PBNM(110).

Empty nanomicelles (without drug), showed no cytotoxicity in PC-3 cells. These results demonstrate that incorporation of drug in pentablock nanomicelles strongly enhanced the cytotoxic effect, probably due to more drug molecules ferried into the cells by nanomicelles. Furthermore, sustained drug release within the cell and reduction of efflux may have played a great role on effectiveness of the delivery system. This might be because a large amount of drugs ferried into the cells at a time by the nanomicelles may have overwhelmed the activity of the efflux proteins present in the cells . The concentration of PTX was calculated based on its IC_{50} which is 3.3±1.2nM (124).

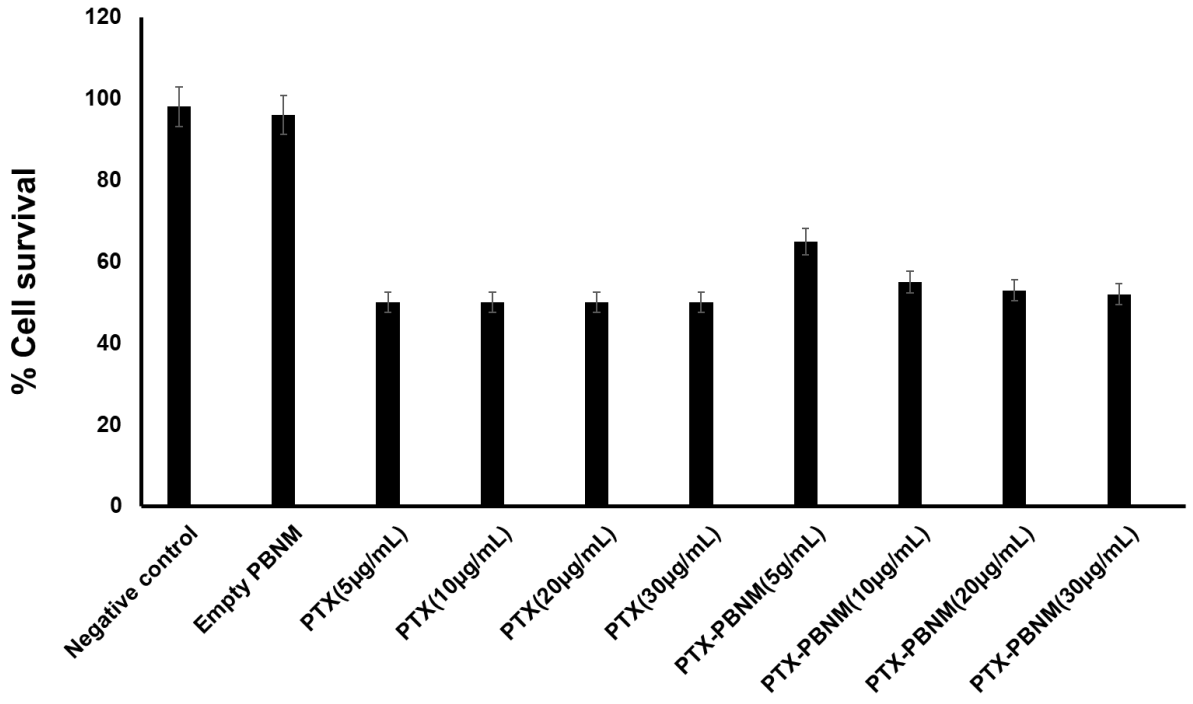

Figure 3. 13: Cell proliferation assay showing % cell survival after 48 h involving: Control (cells only), empty PBNM, and pure PTX at concentrations of 5µg/mL, 10 µg/mL, 20µg/mL and 30µg/mL respectively and PTX-PBNM at 5µg/mL, 10 µg/mL, 20µg/mL, and 30µg/mL respectively.

Conclusions

From the results obtained in this study, it can be concluded that synthesized pentablock copolymers are safe for cellular delivery as confirmed by Tukey post Hoc test. Pentablock copolymers can be utilized for preparation of drug-loaded nanomicelles of adequate sizes (20.98±5.00nm). This formulation can be ideal for delivering drugs into specific cells if conjugated with a targeting moiety. Viscosity of the formulation is similar to that of water. Hence it is suitable for application through IV route.

Cell analysis displayed an excellent uptake profile demonstrating that the nanomicelles facilitated the entry of more drug(coumarin 6) molecules into the cells. Release studies showed long term release profile, which can be significant in cancer chemotherapy. Cell proliferation assay showed a high effectiveness of this drug delivery system. In general, this method can be directed to delivery of hydrophobic anticancer drugs like paclitaxel in cancer therapy. This strategy may reduce side effects, diminish frequency and drug dosage.

CHAPER 4

PSMA ANTIBODY CONJUGATED PENTABLOCK NANOMICELLES FOR TARGETED DELIVERY TO PROSTATE CANCER

Rationale

Prostate cancer is the most abundant cancer among males, and the second most common cause of cancer deaths in men, with a projection that 164,690 new cases will be diagnosed, and 29,430 deaths will be registered in the United States within the year 2018 (1). About one man out of nine men will be diagnosed with prostate cancer in his lifetime. In the USA, for example, prostate cancer develops particularly in older men with high frequency among African-American men (2).

Approximately 6 in 10 cases are diagnosed among men aged 65 or older, but it is not common below age 40. The average age of diagnosis is about 66. Treatment of localized prostate cancer is currently faced with many treatment options available (3). The options include radical prostatectomy, hormonal manipulation, radiation therapy, brachytherapy or any combination of these treatments.

All diagnoses are done with routine screening of prostate-specific antigen (PSA) level conducted during a periodical physical examination (4, 5). Another cellular marker for prostate cancer is prostate specific membrane antigen (PSMA), whose levels become elevated on the surfaces of cancerous prostate cells. Over 20 drugs have been approved by the FDA for prostate cancer treatment (6).

However, paclitaxel is not among the first priority drugs for prostate cancer, this is because paclitaxel drug does not reach the target site in effective concentrations due to its poor aqueous solubility which significantly hinders its anticancer activity (7).

Intravenous administration of its current formulation has also proven to cause allergic reactions and precipitation at the spot of injection (8, 9). Its use in other cancers is also limited as it may require increased dosage which may lead to unnecessary consequences.

The efficacy of current cancer therapy is mostly limited due to toxicity related to anticancer drugs that may end up in normal tissues and cells. This limitation is caused by lack of selectivity of the anticancer drugs currently used in chemotherapy towards the tumor cells. To ameliorate this situation, pharmaceutical researchers are working to find ways to deliver the drug more adequately to the prostate, where it may target the tumor tissues and cells while sparing the normal cells. Targeting of drugs specifically to the prostate is essential for the treatment of diseases related to the prostate such as prostatitis, benign prostatic hyperplasia (BPH) and prostate cancer (125).

A drug delivery system is usually associated with drug molecule carriers such as, liposomes, nanoparticles, and nanomicelles which are meant to ferry drugs to the target site (10). Hydrophobic drugs are in most cases difficult to administer and one of the ways of overcoming such barriers is nanomicelles. Until very recently, surfactants were the principal materials utilized in nanomicelle formation process in pharmaceutical industry. However, reports have indicated that surfactants are inadequate due to their cytotoxicity and high critical micellar concentrations (CMC)(126).

Nanomicelles possess several advantages as a delivery system i.e. enhanced drug solubility, Simple preparation, reduced toxicity, better tissue penetration,

increased circulation time, and easy targetability (4, 5). However, traditional nanomicelles have shown various disadvantages such as: short–term sustained release, system short stability periods, low suitability for hydrophilic drugs and the need for system adjustment for each drug (6).

To avoid these shortfalls, we decided to synthesize and use pentablock copolymer that possess adequate stability and low cytotoxicity as well as the ability to provide high entrapment for the hydrophobic drugs such as paclitaxel drug.

Targeted delivery of paclitaxel may reduce the side effects and provide safe and effective therapy for prostate cancer by reducing the dosage and duration of treatment. Based on this logic, paclitaxel as a drug was loaded into pentablock nanomicelles whose surfaces were attached to an antibody against prostatic specific membrane antigen (PSMA-Ab) used for prostate cancer cell targeting.

This pentablock copolymer is composed of FDA approved biocompatible, biodegradable and non-toxic materials. This paper details the preparation and characterization of a drug delivery system containing paclitaxel for prostate cancer targeting. The therapeutic efficacy and the biocompatibility of drug-loaded pentablock nanomicelles were evaluated by in vitro cytotoxicity by using PC-3 prostate cancer cell line.

Materials and Methods

Materials

Poly ethylene glycol-methyl ether (MPEG), L-lactide and ε-caprolactone monomers, stannous octoate, triton X100, coumarin-6 and paclitaxel drug were obtained from Sigma-Aldrich (St. Louis). NH2-PEG-COOH was acquired from NECTAR ™ Huntsville, AL, USA. EDC was obtained from ACROS ORGANIC, NJ, USA. Cyquant™ cell proliferation assay kit was obtained from Invitrogen Life Technologies Inc. and distributed by Thermos-Fisher Scientific. Paclitaxel drug was obtained from ADOOQ Bioscience, Irvin, CA, USA. Invitrogen PSMA-monoclonal antibody-Alexafluor 488 was obtained from thermo-fisher scientific, Human recombinant bFGF was purchased from Invitrogen through thermo-fisher scientific, USA. All other reagents utilized in this study were of analytical grade.

Methods

Synthesis of Pentablock Copolymers

The preparation of pentablock containing MPEG-PLA-PCL-PLA-PEG-NH2, commenced by melting MPEG by heating at 130^{o}C in a round bottom flask. Poly lactide (PLA) was then added to the molten MPEG together with stannous octoate followed by vacuuming and addition of nitrogen gas for 5min while heating at 130^{o} C for 24h. The resultant diblock (MPEG-PLA) was cooled, purified then heated again at 130^{o}C until melting point. Polycaprolactone (PCL) was added followed by vacuuming and nitrogen gas before heating for 24h.

The resultant triblock (MPEG-PLA-PCL) was collected and purified as described above before being heated at the same temperature followed by addition of another shot of PLA then degassing by vacuuming and filling with nitrogen gas. The heating was continued again for 24h giving rise to tetrablock. The obtained tetrablock (MPEG-PLA-PCL-PLA) was treated as described previously, followed by addition of PEG-NH2 and subsequently vacuuming and addition of nitrogen gas.

The reaction was carried out continuously for another 24 h with temperature maintained at 130°C. All the reactions were catalyzed by 0.5 wt % stannous octoate in every step. The final resultant pentablock copolymer (MPEG-PLA-PCL-PLA-PEG-NH2) was dissolved in dichloromethane and precipitated by transferring dropwise into a tube containing cold diethyl ether (81). Precipitates were centrifuged at 1200rpm and the sediments were vacuum-dried for 12 hours to remove any residual solvents. The purified pentablock polymer was stored at −20°C for future use (97, 101).

H^1-NMR Analysis for Block Copolymers

To determine molecular structure of the synthesized block copolymers, samples of both triblock (MPEG-PLA-PCL) and pentablock (MPEG-PLA-PCL-PLA-PEG-NH2) copolymers were analyzed using ^{1}H-NMR spectrometer. The analysis was conducted at room temperature using a Varian Inova 400 MHz spectrometer (Varian, Palo Alto, CA), briefly: the synthesized triblock and pentablock copolymers samples were dissolved in deuterated chloroform CDCl3. The chloroformic solutions were transferred into a standard NMR glass tubes before submission to the NMR chamber one at a time. values of chemical shift were reported in parts per million (ppm) (102).

X-ray Diffraction (XRD) Analysis of Block Copolymers

Synthesized pentablock and triblock copolymers were analyzed by XRD to determine their physical crystallinity. Triblock and pentablock copolymers samples were analyzed at room temperature using a MiniFlex automated X-ray diffractometer (Rigaku, Woodlands, Texas- USA) equipped with Ni-filtered Cu-kα radiation (30 kV and 15 mA). Diffraction angle (2θ) used ranged from 5° to 45° increasing by 1° per min (103).

Cytotoxicity Studies on Pentablock Copolymer

Cells from human prostate tumor cell line (PC-3) were cultured and maintained according to a protocol provided by ATCC. In brief, PC-3 cells were cultured in Dulbecco's F-12 medium containing 10% heat-inactivated fetal bovine serum (FBS), sodium bicarbonate (29 mM), HEPES (15mM), streptomycin (100 mg/L) and penicillin (100 U/L). The solution samples of PB copolymer (20mg/ml) and triton-X100 (5µg/mL) were then transferred into 96 well plate containing already cultured PC-3 cells.

The plate was incubated under humidified environment at 37°C and 5% CO_2 for 24h. The medium was then removed and the plate washed with PBS three times and kept in the fridge for 4h before being analyzed using UV-laser analyzer Benchmark plus ^{TM} microplate spectrophotometer, BIO-RAD, Japan (104).

Viscosity Measurements for Pentablock Copolymer

During the analysis to determine the viscosity of the synthesized pentablock, the copolymers was dissolved in deionized water before being submitted to Oswald capillary viscometer at room temperature (25°C). The viscometer temperature was kept constant. The values of viscosity were recorded as averages of triplicate measurements (kinematic viscosity, cP±1 standard deviation) and calculated by applying the equation below.

$$\text{Vis}_{(\text{water})} = (\text{density}_{(\text{liq})} \times \text{time}_{(\text{liq})} \times \text{Vis} \; / \; (\text{density}_{(\text{water})} \times \text{time}_{(\text{water})})$$

Preparation of Nanomicelles

Nanomicelles (NM) were prepared using hydration-dehydration method (16). Briefly, a specific amount (0.1%w/v) of paclitaxel drug was dissolved in 1ml of ethanol in an Eppendorf tube. On the other hand, 2%w/v of pentablock copolymer was dissolve in 1 mL ethanol in a separate tube. The two solutions were then mixed together, homogenized and evaporated in the speed vacuum for 24h to form a thin film.

The resultant thin film was suspended in deionized (DI) water followed by vortexing until complete dissolution was achieved(103). The solution was filtered using 0.22μm filter membrane to acquire uniform nanomicelle sizes and eliminate the polymer residues. The nanomicelle suspension was further freeze-dried using

LABCONCO freeze-dryer, USA, using glucose or trehalose as cryo-protectants as shown in figure 4.1.

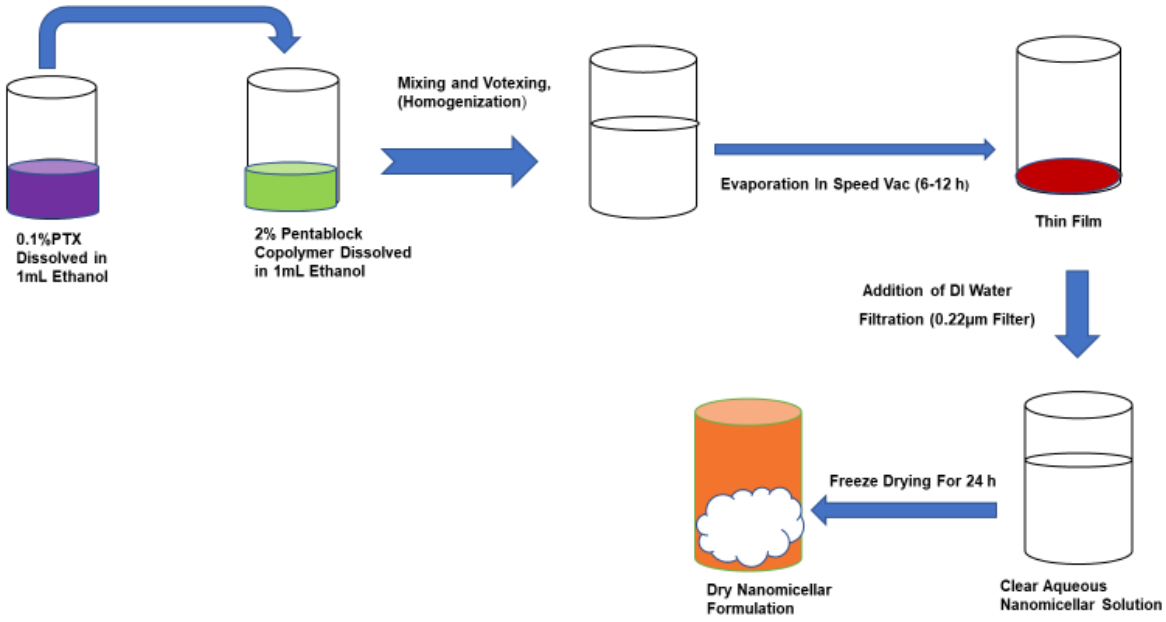

Figure 4. 1: A schematic illustration showing the preparation procedure for PTX-loaded Pentablock nanomicellar formulation.

Thermal Stability Analysis of PB and PTX-PBNM

Thermogravimetric analysis (TGA) was carried out to evaluate the thermal stability of the synthesized pentablock copolymers and the nanomicelle formulation. Thermogravimetric analyzer (Nietzsche Corporation, TG209, Goliaths, Germany), was applied for the analysis. Samples of pentablock, PTX-PBNM and pure paclitaxel were analyzed, where 10mg of each dry sample was placed in an alumina pan and heated from 0°C to 700°C (127).

The TGA analysis was performed under nitrogen atmosphere at a constant flow rate of 10 mL/min. The heating rate was maintained at 10 °C/min as heating continued

between 0 and 700 °C (128). The analysis was conducted for all the 3 samples in triplicates (129, 130).

PC-3/PSMA

During the prostate cancer development, the expression of prostate specific membrane antigen (PSMA) increases with the development of tumor(131). However, during metastasy, there is the emergence of metastatic prostate cancer cell lines such as PC-3 and Du 145 cell lines which do not express this PSMA protein(131, 132). Estradiol (E2) and basic fibroblast growth factor (bFGF) have been reported to restore the PSMA expression ability of PC-3 cells due to their significant engagement in the growth and developemnet of prostate gland(131-133).

In order for the expression of PSMA in the PC-3 cells, 10 mL of medium containing 0.2µg/mL of fibroblastic growth factor(bFGF) was prepared and used to culture the cells to restore the expression of PSMA on the surfaces of prostate cancer PC-3 cell line used in the experiment(131, 133). The culturing process was done for 48 h and 72 h resulting in PSMA/PC-3 cells. This was then tested with PSMA antibody before being incubated with antibody-conjugated pentablock nanomicelles. The tested cells were observed under confocal microscopy as shown in fig 4.2 below.

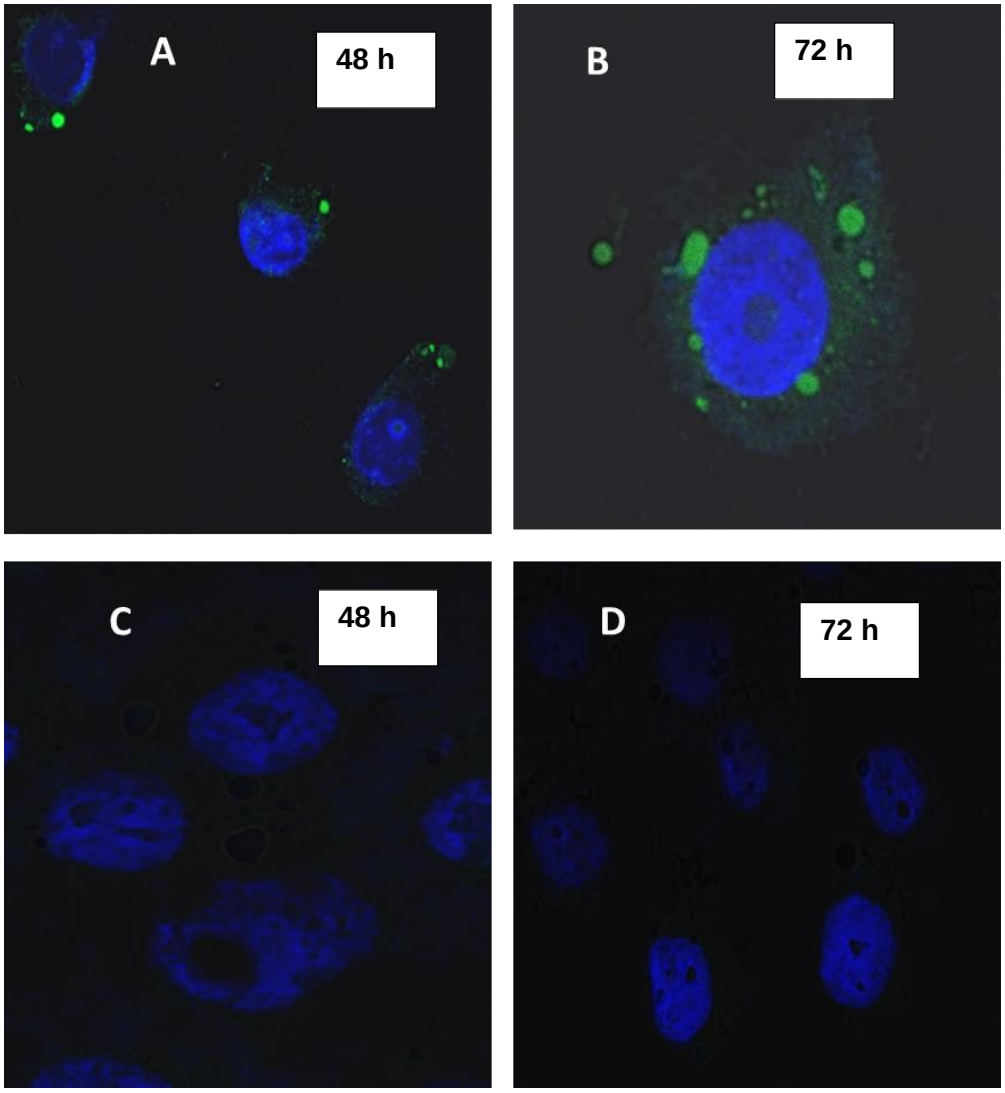

Figure 4. 2 confocal image showing PSMA expression (green) in PC-3 cells after incubation for 48 h and 72 h. A & B were treated with 0.2µg/mL bFGF and C &D without bFGF.

Conjugation of PSMA Antibody to the Surface of PTX-PBNM

Covalent coupling of carboxyl group of PSMA antibody with free amine group present on the surface of nanomicelles was achieved using EDC as coupling agent (Fig.4.2). Briefly, freeze-dried drug loaded pentablock nanomicelles (PTX-PBNM) were suspended into PBS (pH 7.4) containing antibody (NM/Ab) ratio: 100:10 v/v). EDC (20 mg/ml of NM/Ab mixture) was added and vortexed and kept for 2 h at room temperature. The antibody-conjugated nanomicelles were separated from unconjugated ligand using mini column centrifugation (Sephadex G-75 packed column) technique followed by washing thrice with deionized (DI) water.

The antibody-conjugated nanomicelles were collected after ultracentrifugation (Hitachi, Himac CP100 MX, Japan) at 60,000 rpm for 45 min and the resultant pellet was re-dispersed in distilled water and subsequently freeze-dried resulting in nanomicelles named PSMA-Ab coupled paclitaxel-loaded pentablock nanomicelles (PTX-PBNM-Ab) as shown in figure 4.3. The amount of PSMA-Ab coupled to the surface of the PTX-PBNM was assessed by change in the zeta potential.

The two process variables (incubation time and total nanomicellar formulation to antibody ratio) were optimized by measuring the change in zeta potential (the surface charge density) of the dispersion (Zetasizer 3000 HS, Malvern Instruments Co., UK).

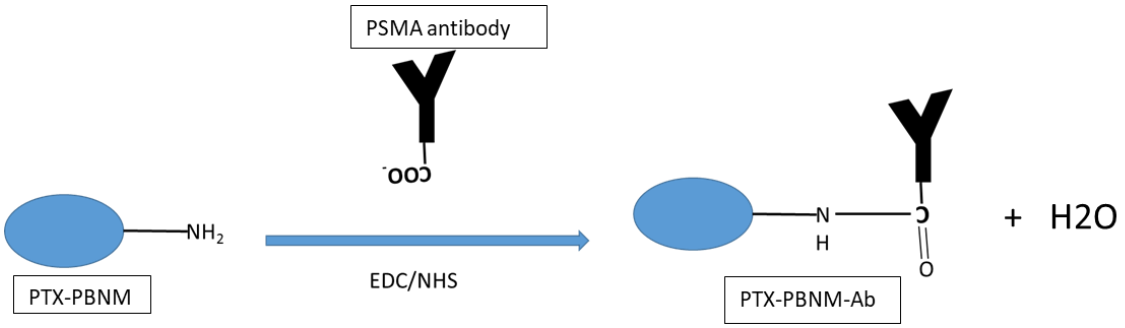

Figure 4. 3: Schematic illustration of antibody conjugation to the amine group on the surface of the pentablock Nanomicelles.

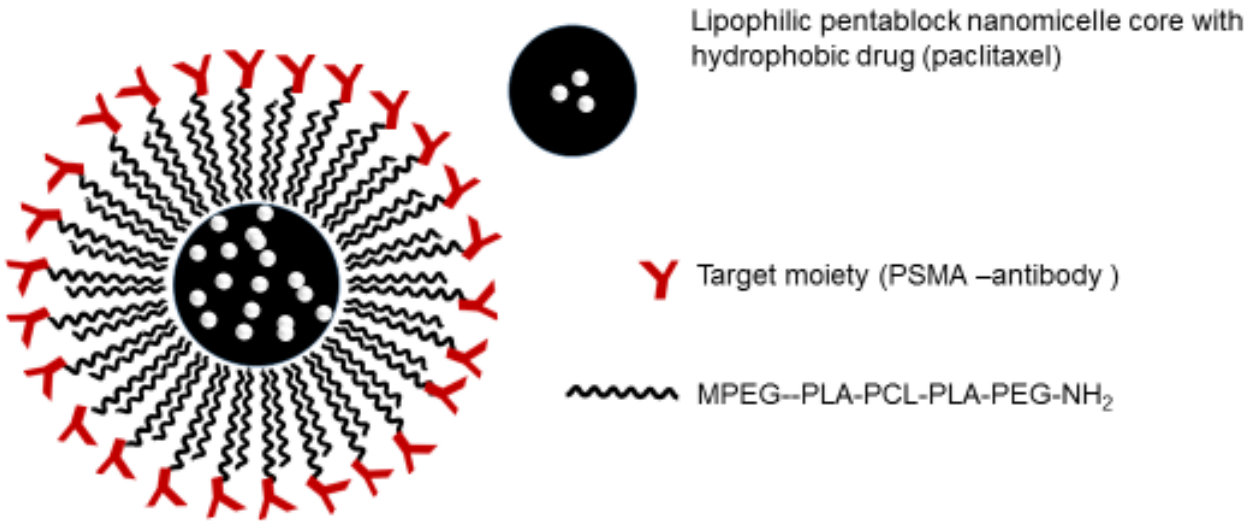

Figure 4. 4: PSMA antibody coupled paclitaxel-loaded pentablock nanomicelle after conjugation.

Critical Micellar Concentration (CMC) Determination

The critical micellar concentration (CMC) of the synthesized pentablock copolymer was determined by use of iodine as a hydrophobic probe. Standard KI/I_2 solution was prepared by dissolution of 0.5 g of iodine and 1 g of potassium iodide in 50 mL of DDI water. Samples of pentablock solution at different concentrations were also prepared.

A volume of KI/I_2 (25 µL) solution was added to each tube containing pentablock copolymer solution. Solution mixtures were then kept at room temperature in a dark room for 12 h. UV absorbance values for different pentablock concentrations were measured using a UV-Vis spectrometer at 400 nm. The absorbance values were plotted against logarithm of Pentablock concentrations.

The CMC values correspondent to the PB copolymer concentration bearing significant absorbance increase was recorded and registered. CMC of Pentablock copolymer was expressed in weight percentage (84, 85)

Nanomicelles Size and Zeta Potential Determination

The sizes, zeta potentials and polydispersity indices (PDI) of both PSMA antibody coupled Paclitaxel-loaded pentablock nanomicelle (PTX-PBNM-Ab) and the unconjugated pentablock nanomicelles (PTX-PBNM) were obtained using dynamic laser scattering (DLS) with the help of Zetasizer HS 3000 (Malvern Instruments, UK), at a detection angle of 90 degrees at 25^{o}C. The samples were dissolved in deionized water, homogenized and filtered using 0.22µL before being transferred into a transparent cuvette for analysis. Average values of three measurements were

obtained for all samples and the peaks for zeta sizes, PDI and zeta potentials were obtained and recorded accordingly(109).

H^1-NMR Analysis for PTX- PBNM-Ab

PTX-PBNM-Ab and empty PBNM-Ab were analyzed using either deuterated water(D_2O) or Deuterated chloroform (CDCl3) as solvents then subjected to H^1-NMR analysis. An adequate amount of pure paclitaxel was dissolved in $CDCl_3$ before analysis. The spectra were obtained at room temperature upon submission to a Varian Inova 400 MHz spectrometer (Varian, Palo Alto, CA, USA). Values of chemical shifts were reported in parts per million (ppm)(102). ^{1}H-NMR spectra were recorded from 0 to 14 ppm using a delay time of 4 seconds.

Fourier-Transform Infrared Spectroscopy (FT-IR) Analysis for Pentablock Nanomicelles

To determine structural characteristic of the nanomicelles. Samples of synthesized pentablock nanomicelles were subjected to FT-IR, Thermo-Scientific Nicolet iZ10 with an ATR diamond and DTGS detector. Where freeze-dried samples of PTX-PBNM-Ab and PTX-loaded pentablock nanomicelles PTX-PBNM, and pure paclitaxel drug were analyzed with FT-IR with scanning range of 650–4000 cm^{-1}.

Drug Encapsulation Efficiency

The amount of encapsulated paclitaxel in the nanomicelles was measured by UV-vis. Before and after attachment of PSMA antibody. Briefly, 2mg freeze-dried nanomicellar formulation was dissolved in 1mL dichloromethane (DCM) to break the

nanomicellar structure. The solution was submitted to centrifugation at 10,000rpm for 5min followed by washing and finally evaporation to eliminate DCM.

The resultant dry residue was dissolved in ethanol and the ethanolic solution was filtered using 0.22µm nylon syringe filter and then analyzed using UV-spectrophotometry at 221nm wavelength (Beckman, DU® 530, UV-vis spectrophotometer, Life science, CA, USA), to determine the concentration paclitaxel.

This process was conducted in triplicate and the calculation was done using a standard curve with the equation Y=38.059+0.029 and R^2 =0.9984, drawn using ethanolic solutions of pure paclitaxel at different concentrations (110). Percentage encapsulation efficiency (%EE) and percentage drug loading were calculated according to equations below.

$$\text{Encapsulation efficiency (\%)} = \text{Total } \frac{\text{drug (mg)} - \text{Free drug (mg)}}{\text{Total drug (mg)}} \times 100$$

$$\text{Drug loading (\%)} = \frac{\text{Mass of PTX in nanomicelles}}{\text{Mass of PTX used + Mass of PB used}} \times 100$$

Transmission Electron Microscopy Analysis

Nanomicelles morphology was determined by transmission electron microscopy (TEM; Philips CM12 STEM, Hillsboro, OR.). Briefly; a small amount of freeze-dried paclitaxel-loaded and unloaded antibody coupled pentablock nanomicellar formulations were dissolved in DI water separately to form aqueous solutions.

The samples were then stained with 1% uranium salt. The resultant solution containing nanomicelles was then placed on a carbon-coated copper grid, and excess liquid was removed using a piece of filter paper. TEM images were subsequently obtained after the samples on the grids were dried completely.

Statistical Analysis for Pentablock Nanomicelles

Statistical analysis was conducted using full factorial design on JMP® software, where 21 formulations of pentablock nanomicelles with PB concentrations varying from 0.5% to 2.0% and paclitaxel concentrations varying from 0.05% to 0.2 % were used as independent variables and their respective sizes, zeta potentials, percentage drug loading and entrapment efficiencies were used as dependent variable factors.

In vitro Drug Release Studies

Aqueous solutions of paclitaxel-loaded pentablock nanomicellar formulation samples (2%w/v), was poured into a dialysis bag. Equal volume of Paclitaxel solution (0.1%w/v) was prepared and placed in a separate dialysis bag (111). Dialysis bags were then dipped into separate 15mL tubes containing 10ml phosphate buffer solution (PBS) each.

The tubes were closed and placed in oscillating water bath at 37 degrees Celsius(112). PBS media was collected and completely replaced at different time intervals (3 h, 6 h, 12 h, 24 h, 48 h, 72 h, 120 h, 168 h, 200 h) respectively(112). PTX content was analyzed by UV-Vis spectrophotometry as described above, and a calibration curve was drawn to calculate the PTX concentrations at each time interval.

Cell Uptake Studies for Coumarin6-loaded Conjugated Pentablock Nanomicelles

Coumarin6-loaded antibody coupled PBNM at different concentrations of 10µg/mL and 20µg/mL and two solutions of coumarin-6 at 10µg/mL and 20µg/mL were used in the uptake analysis. The solutions were transferred into 4 chamber slides previously incubated with PC-3 cells and to another chamber slide that contained cultured T47D cells. Each cell line was in separate chamber slides in a manner that avoids cross contamination.

The slides were treated with 4%paraformaldehyde, washed 3 times with PBS, and then kept in mounting medium for 48 h. The slides were then observed using confocal scanning microscopy (CLSM, 510 META, Carl Zeiss, Germany) with the excitation and emission wavelengths for coumarin-6 at 488 nm 540 nm respectively (102, 108).

Results and Discussions

Synthesis and Analysis of Block Copolymers

^{1}H-NMR Analysis for the Block Copolymers

^{1}H-NMR analysis was conducted to determine the structural arrangement of the synthesized triblock copolymer (MPEG--PLA-PCL) and pentablock copolymers (MPEG--PLA-PCL-PLA-PEG-NH_2) (97). Fig. 4 shows ^{1}H-NMR spectra of the two block copolymers dissolved in deuterated chloroform. The ^{1}H-NMR characteristic peaks of the copolymers representing methylene protons of -(CH_2)3-, -$OCOCH_2$-, and

-CH_2OOC- of ε-caprolactone were observed at 1.40, 1.65, 2.30 and 4.06 δ ppm respectively.

There was a presence of a well-defined peak for methylene protons of (-CH_2CH_2O-) at 3.65 δ ppm indicating the presence of PEG in both the triblock and pentablock samples. Characteristic peaks for L-lactide blocks of pentablock were observed at 1.50 (-CH_3) and 5.17 (-CH-) δ ppm. The proton for (-CH) of deuterated chloroform was visible at 7.25ppm. While a peak of methyl terminal of (-OCH_3-) of PEG was observed at 3.38 δ ppm.

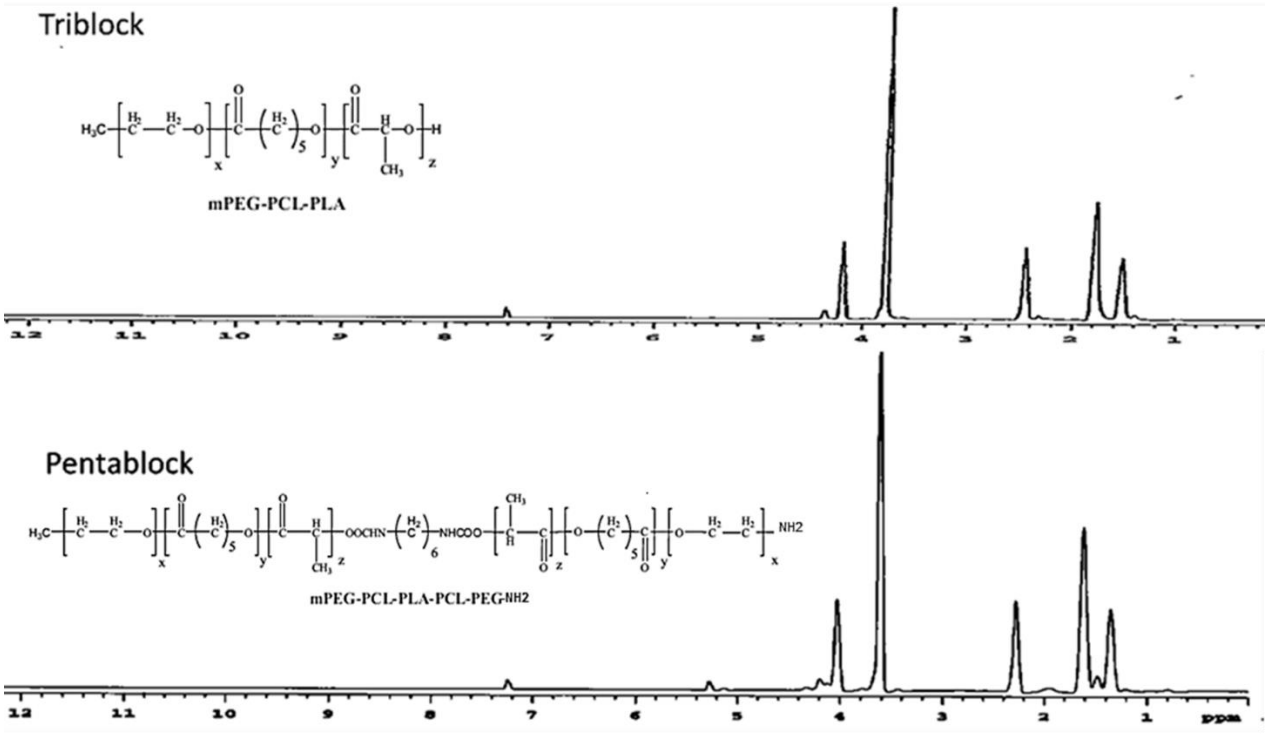

Figure 4. 5: H-NMR peaks showing protons shifts for triblock and pentablock copolymers.

Thermo-Gravimetric Analysis (TGA) for PB and PBNM

The TGA results of the Pentablock copolymer, paclitaxel-loaded pentablock nanomicelle and pure paclitaxel are illustrated in Fig. 4.5. The TGA curve shows a number of degradation stages for the samples. The changes during the first stage were different for each sample. The weights of all the samples remained unchanged past 100 ^{o} C. The first weight reduction was seen in paclitaxel which reduced to 97.3% at a temperature of 123.4 ^{o} C followed by the PTX-PBNM with 98.7 % at 190.2 ^{o}C and the PB with 98.7% at 238.7 ^{o} C. At this stage, the Pentablock copolymer, pentablock nanomicelle and paclitaxel undergoes moisture vaporization(130).

The decomposition temperatures were determined following an obvious weight reduction in the Pentablock copolymer, pentablock nanomicelle and paclitaxel during the test (Table 4.2). The TGA curve suggests that the decomposition temperatures causing reduction in weight percentages for the samples of pentablock copolymer, pentablock nanomicelle is due to de-polymerization of the polymer structure (134). Thermal decomposition of PTX at temperatures between 202.3^{o}C and 356.6^{o}C caused percentage residual weight reduction from 94.8% to 40.7%.

Decomposition for PTX-PBNM nanomicelle started from 200.8 ^{o}C -645.6 ^{o}C with a free fall in residual weight percentage from 95.4% -40.7%. The greatest stability was seen in PB copolymer, whose decomposition only started at 300.5^{o}C -356.6^{o}C, with decrease in residual weight from 90.4%- 40.7%, and further to 423.3^{o}C, where the weight falls to 10.2%. However, this was also the fastest decomposition process with a temperature change of only 26.1^{o}C. At 700^{o}C, the residual weight for pentablock

copolymer was only 6.2% while the remaining residues was 24.3% and 24.9 % for PTX-PBNM and PTX respectively.

This is due to the thermal de-polymerization of the block copolymers. Both PTX-PBNM and PTX have the same residual weight. At 645.6(weight 26.7%) and at 700^{o}C (around 24%) all the PB all in the PTX-PBNM is degraded leaving only PTX residues.

Table 4. 1 Percentage residual weights of PTX, PTX-PBNM and PB copolymer at different thermogravimetric temperatures.

PB		**PTX-PBNM**		**PTX**	
Temp (^{o}C)	TGA (% residual weight)	Temp (^{o}C)	TGA (%residual weight)	Temp (^{o}C)	TGA (%residual weight)
238.7	98.5	190.2	98.7	123.4	97.3
300.5	90.4	200.8	95.4	202.3	94.8
345.3	42.2	305.4	49.6	245.6	74.5
356.6	40.7	356.6	40.7	356.6	40.7 *
386.9	30.9	443.5	33.8	406.7	36.1
423.3	10.2	645.6	26.7	645.6	26.7 *
700.0	6.2	700.0	24.3	700	24.9

* Shared point

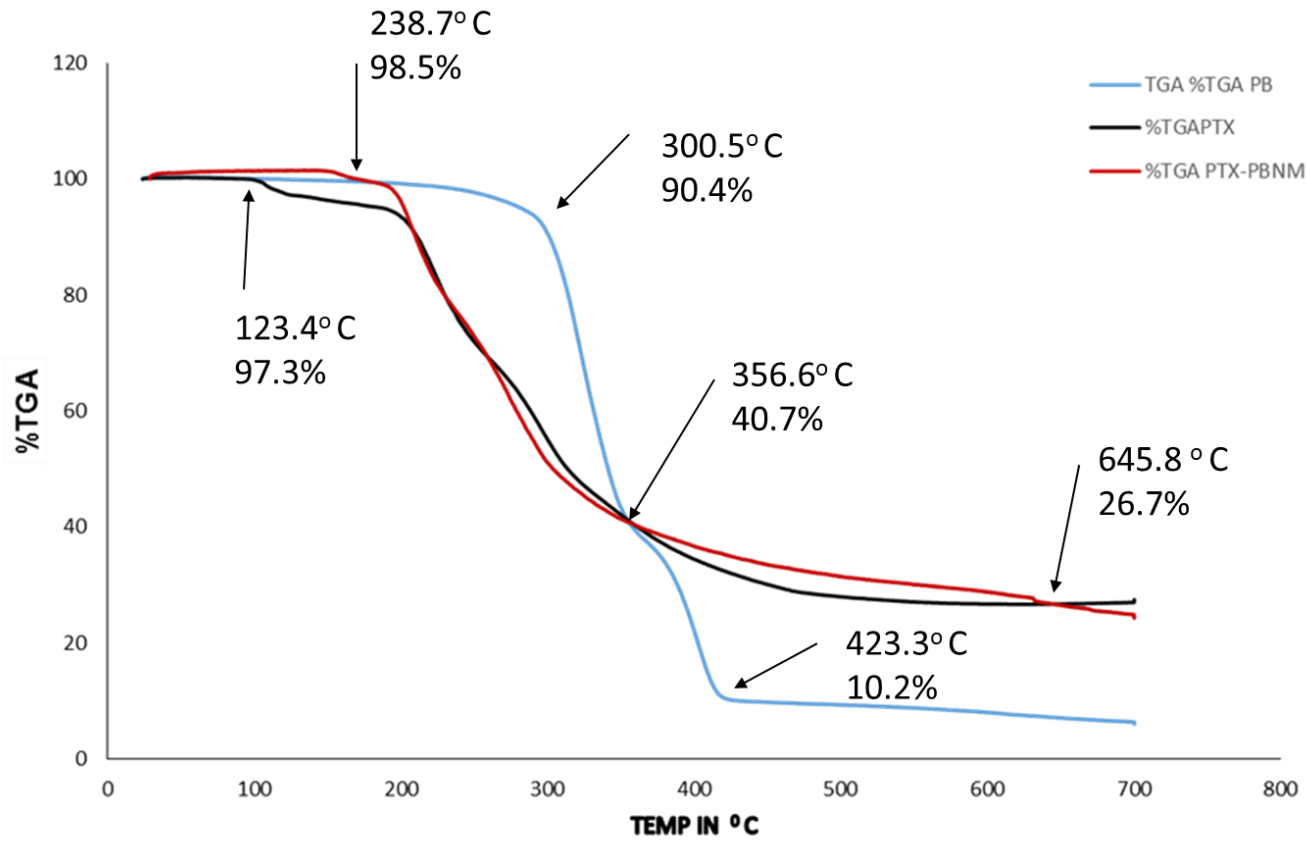

Figure 4. 6: The thermogram showing thermal degradation (TGA) of PTX, PB, PTX-PBNM as a function of temperature

Viscosity Determination of Pentablock Copolymer

The Rheological properties of pentablock copolymers were analyzed using Oswald glass viscometer and the viscosity a value obtained was 0.7883. This is close to the viscosity of water (0.8880). The results suggest that pentablock copolymer is suitable for preparation of nanoformulations meant for intravenous application (81).

X-ray Diffraction Analysis for Block copolymers

The phase composition crystallinity of diblock (DB), triblock (TB) and pentablock (PB) copolymers were determined using X-ray diffraction (XRD) analysis (Fig.4.6). The spectra show no peaks corresponding to PEG in all block copolymers analyzed. The triblock (TB) and pentablock (PB) copolymers showed well-elaborate crystallinity peaks for PCL at two-theta (2θ) of 21^{o}.

Crystallinity peaks of PLA were present at 2θ of 23^{o} in all the block copolymers (DB, TB and PB). XRD peaks for TB on the other also showed PCL blocks while diblock. DB showed PLA crystallinity but did not show PLA crystallinity as it was not added in its composition during its synthesis. PLA crystallinity peak was present in both TB and PB at 2θ around 23^{o} as shown in fig.6 (114).

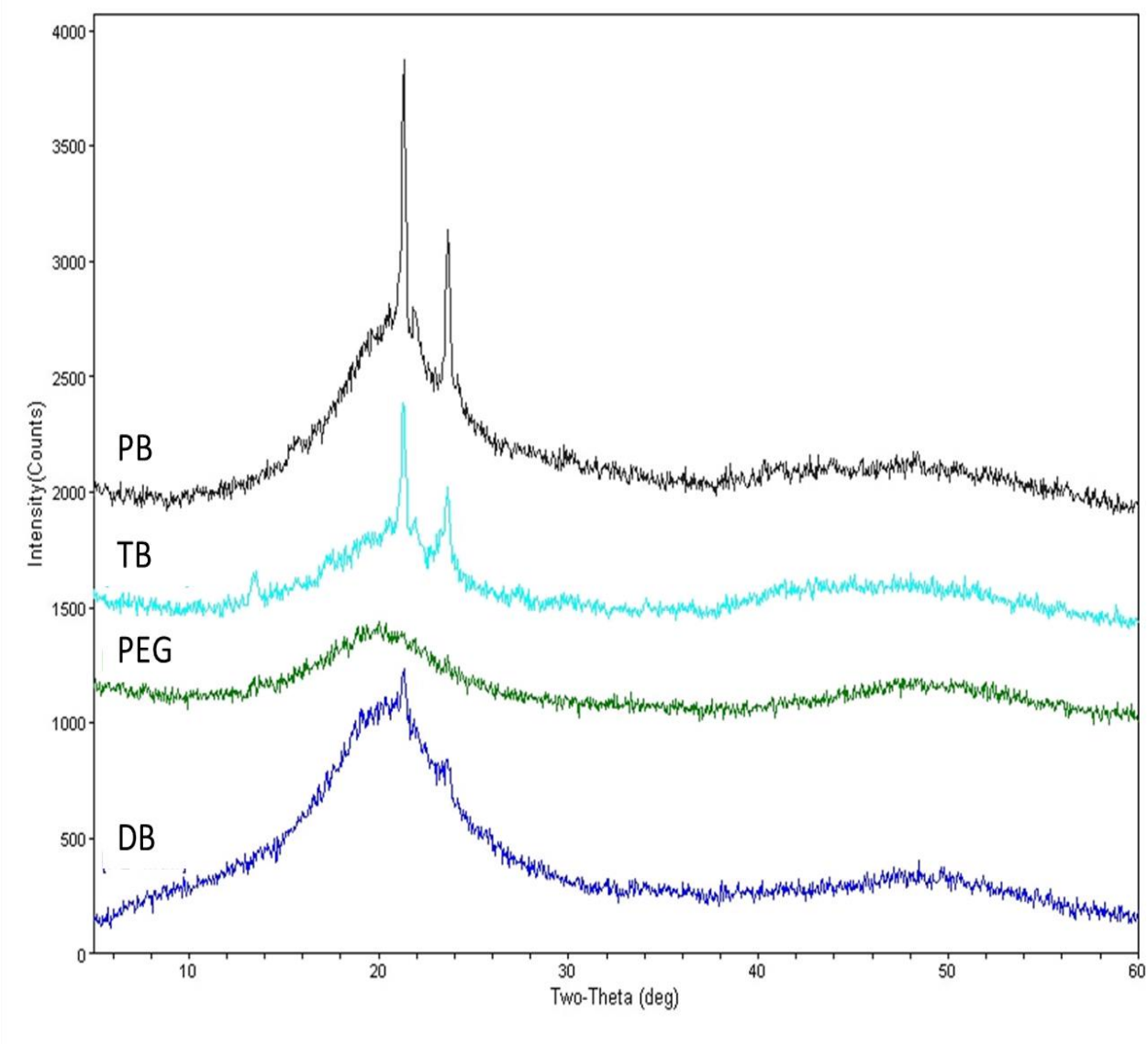

Figure 4. 7: The XRD peaks showing a comparison among DB, TB and PB copolymers.

Cytotoxicity Analysis of Pentablock Copolymer

Cytotoxicity assay was performed on the pentablock copolymers for a period of 48h to evaluate its cytotoxic effects on the human cells. The test was conducted using cell proliferation assay (Cyquant) Kit. Triton X-100 was used as positive control. Solution of Pentablock copolymer did not manifest any cytotoxic effects on

the cells (Fig. 4.7). Furthermore, the results observed in assay were again confirmed by statistical test (Anova) which revealed F value greater than F-critical.

The Anova results were submitted to Tukey post Hoc test using the equation below:

$$\frac{M_1 - M_2}{\sqrt{Ms_w}\left({}^{1}/_{n}\right)}$$

The results obtained indicated no significant deference between the pentablock copolymer and the negative control (untreated cells only) (Fig 4.7). This shown by comparative data in table 4.2. The results from this assay clearly suggest that pentablock copolymers are safe for intravascular and or topical application in human (31, 56, 57, 109).

In a Previously conducted Lactate dehydrogenase LDH assay with PB composed of similar components, where the cells were incubted for 48 h after treatment. The pentablockcopolymer did not triger significant LDH release (less than 10% LDH released) in the assayed cells indicating no cytotoxicity(86).

In vitro Safety and biocompartibility studies have also been carried out on these pentablock copolymers using MTS assay, where PB copolymers solutions at the concentration of 10mg/mL were prepared, aliquoted, and sterilized. After sterilization, ARPE-19 cells were incubated in 96-well plates at a cell density of 1.0×10^4 at 37^o C and 5% CO 2 in humidified atmosphere for 48 h. The same procedures were followed with other cell lines such as HCEC, SIRC, and RAW264 cells. Percent cell viability in

all these cases were found to be above 90% denoting that PB copolymers were nontoxic.(135)

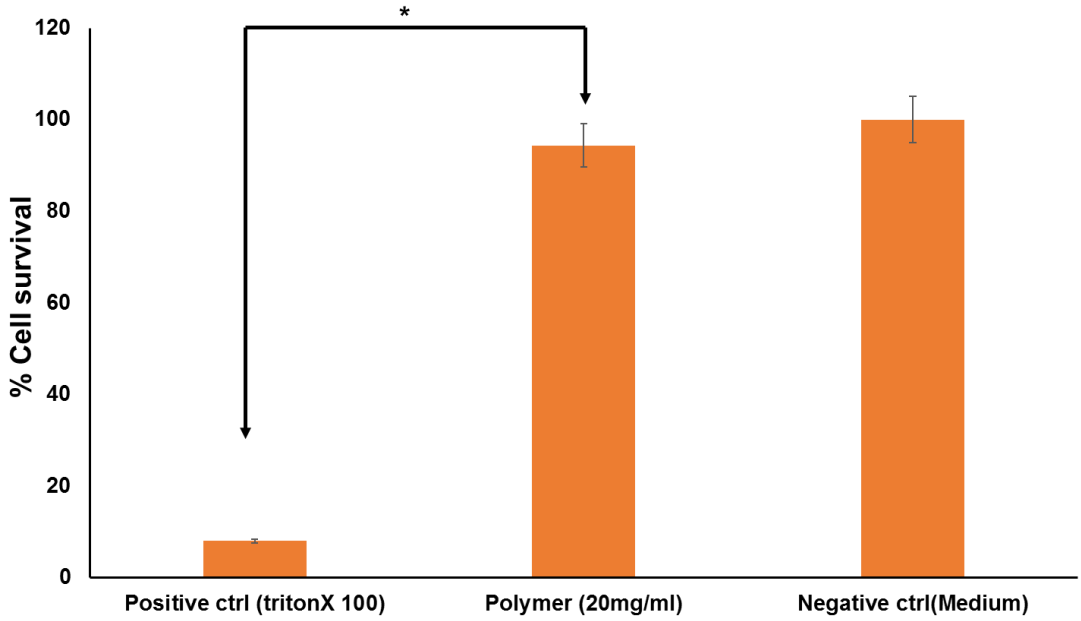

Figure 4. 8 : Cytotoxicity graph showing % Cell Survival of PC-3 cells treated with pentablock copolymer in relation to positive control (triton X 100). Negative control is 100% cell survival. Asterix denote significant difference between the polymer sample and the positive control.

Table 4. 2 Tukey post Hoc test values obtained on Anova results for the cytotoxicity analysis of pentablock copolymer samples against positive and negative controls tested in PC-3 cells.

Comparison	Absolute Difference	Critical Range	Significant Diff. Reject μ=0
A vs B	0.019263	0.014594	TRUE
B vs C	0.002488	0.014594	FALSE
A vs C	0.02175	0.014594	TRUE

The samples of triton X 100, PB copolymer and negative control are represented by A, B and C respectively

Analysis and Characterization of Pentablock Nanomicelles

Nanomicelles were prepared by hydration-rehydration method, where ethanolic solutions of both the synthesized pentablock copolymer and PTX drug were prepared in separate tubes then mixed together and homogenized, followed by evaporation in speed vacuum for 24h after which DI water was added to the resultant film.

The solution was filtered using 0.22 μm nylon filter, resulting in a clear aqueous solution of nanomicelles which was further freeze-dried giving rise to final white powder of paclitaxel-loaded pentablock nanomicellar formulation (fig.4.9)

Figure 4. 9:. Powdered form of freeze-dried PTX-PBNM-Ab nanomicellar formulation.

CMC Determination

Critical micellar concentration (CMC) is a property of *in vitro* and *in vivo* stability of nanomicelles (136). Low CMC cause high stability of micelles in solutions after dilution (31). Micellization mechanism can be determined using Iodine as a hydrophobic probe for the critical micellar concentration of pentablock copolymer.

Solubilized I_2 tends to partition within the microenvironment of the amphiphilic pentablock copolymer. The results after the conversion of I_3 to I_2 brings about excessive KI in the solution. CMC of Pentablock copolymer was found to be 0.035 wt. %. This low CMC of pentablock suggests that the PB copolymer displays stability and ability to maintain integral structure even after dilution(118).

Drug Percentage Encapsulation Efficiency and Loading

Drug percentage encapsulation efficiency (EE) and loading were analyzed to determine the precise amount of paclitaxel entrapped within the nanomicelle core. The percentage EE of paclitaxel drug within the pentablock nanomicelles was found to be 98% and the average drug loading was approximately 12%.

The values show that pentablock nanomicelles had a significant paclitaxel EE and substantial drug loading which may be due to the hydrophobic core hydrophobicity maintained by PCL and PLA, thus entrapping the hydrophobic paclitaxel while the hydrophilic PEG-NH2 interacted with the hydrophilic environment. This property can be applied to improve entrapment of other hydrophobic drugs.

FTIR Analysis for PTX-PBNM

FTIR was conducted on freeze-dried samples of unconjugated PTX-PBNM and empty PBNM as well as pure paclitaxel drug and PB samples. The resultant spectra in figure 4.10, show absorption band at 1700 cm−1 and some bands ranging from 1000–1500 cm−1 indicating the presence of ester bonds in the pentablock copolymer structure (Fig.4.10). C-O bands at 1100 cm−1 and O-H band observed at around 3300 cm−1 are for PEG, PLA and PCL. Stretching bands of C-H at 2940 and 2900 cm−1 indicate the presence of PCL blocks. Bands manifested in the region around 3000cm $^{-1}$ are attributable to aromatic C-H of PTX**,** The C-C ring stretching of PTX occur in the region from 1652-1579 cm-1. However, the amines in PTX and PEG-NH2 are visualized in the 3450-3250 cm-1 band regions.

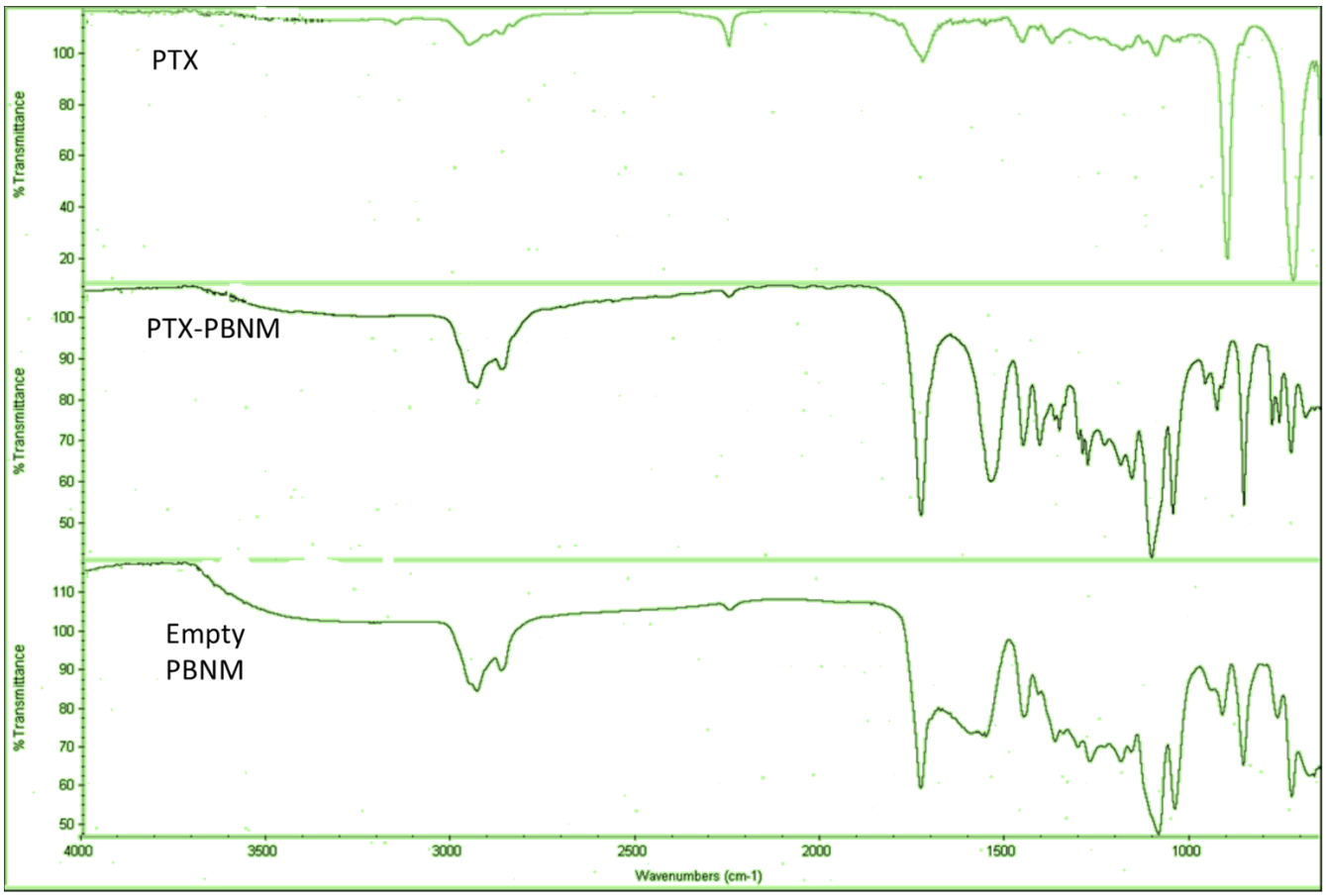

Figure 4.10. FT-IR spectrum for the samples of PTX-PBNM compared to the empty PBNM, PB and pure PTX drug.

Size Distribution for Pentablock Nanomicelles

Solvent evaporation method was used during the preparation of both PTX-PBNM-Ab and unconjugated PTX-PBNM. The pentablock nanomicelle formulations were analyzed to determine their sizes, zeta-potential and polydispersity indices (PDI), (Table 4.3). The mean diameters for unconjugated PTX-PBNM and conjugated PTX-PBNM-Ab were 26±3.5nm, and 45±5.00nm respectively (Fig 4.11).

Negligible peaks were observed beyond 1000nm for unconjugated PTX-PBNM, perhaps due to a little aggregation in the sample. However, majority peak (around 98.5%) was 26±3.5nm (fig.10). Average PDI for PTX-PBNM-Ab and unconjugated PTX-PBNM were 0.045±0.005 and 0.046±0.005 respectively. The PDI values indicate that the nanomicelles were uniform in size distribution with low aggregation levels. While the unconjugated PTX-PBNM displayed neutral zeta potential (around 0±2.5 mV), the conjugated PTX-PBNM-Ab had a zeta potential of-28.7± 0.5mV as shown in Fig. 10.

The electronegativity of the conjugated PTX-PBNM-Ab confirms the successful conjugation of the antibody on the surface of the nanomicelle thus turning the charge from neutral to negative (137-139). The adequate sizes and zeta potentials obtained here, make pentablock nanomicelles suitable candidate for intravenous administration due to unlikely interactions with blood components and the targetability of the conjugated Nanomicelles.

Table 4. 3 Zeta analysis results showing the sizes, zeta potentials and PDI of both the conjugated and the unconjugated paclitaxel-loaded pentablock nanomicelles.

Sample	Size (nm)	Zeta potential(mV)	PDI
PTX-PBNM-Ab	45±5.00	-28.5±2.5	0.045±0.005
PTX-PBNM	26±3.5	0±2.5	0.046±0.005

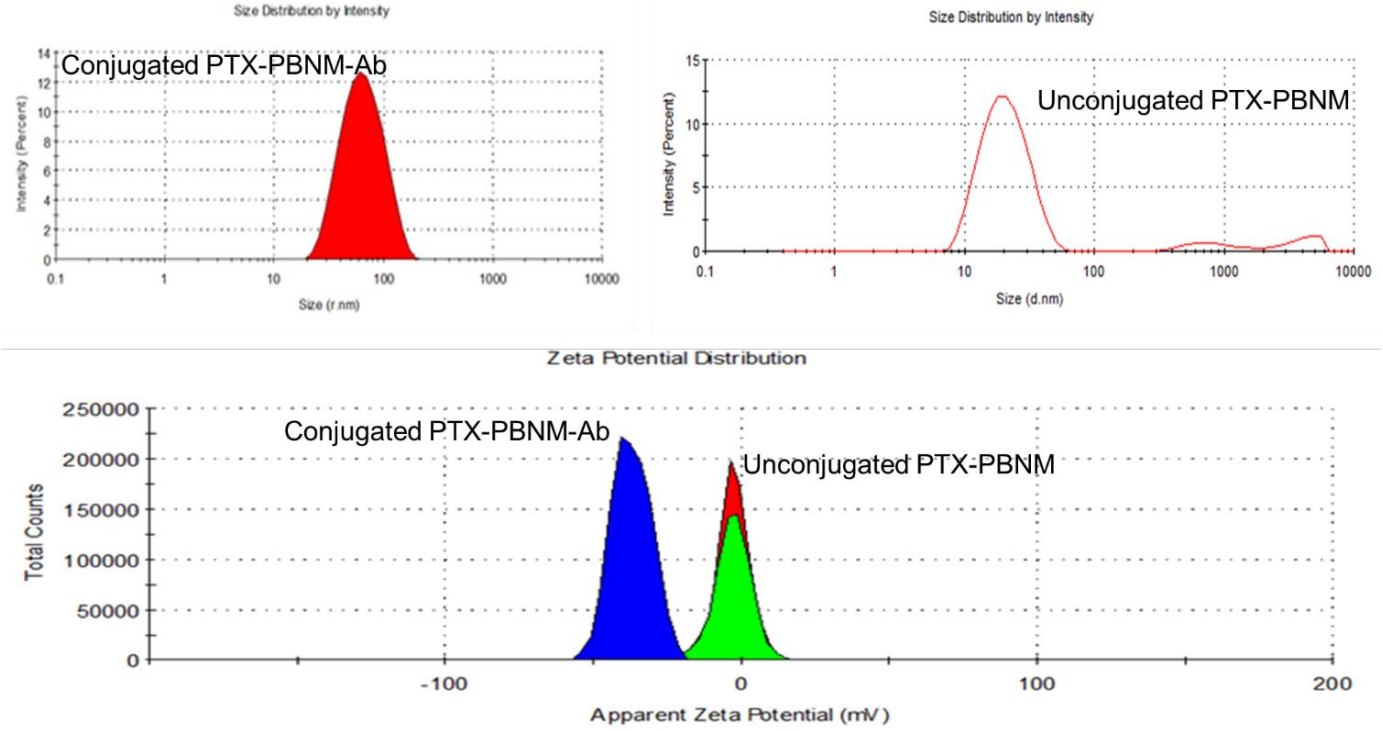

Figure 4. 11: Comparison between two pentablock nanomicelles in terms of size and zeta potential, with respective sizes and zeta potential distribution curves for the antibody conjugated PTX-PBNM-Ab, and for the Unconjugated PTX-PBNM.

^{1}H-NMR Analysis for Pentablock Nanomicelles

H-NMR analysis was conducted in order to understand the structure and polymerization of PTX drug with PB copolymer nanomicelles is formed. Here the nanomicelles were prepared and freeze-dried and then utilized without conjugation with antibody. Both $CDCl_3$ and D_2O were used as solvents to for the analysis of the samples. Unconjugated PTX-PBNM and empty PBNM were dissolved in D_2O while free PTX was dissolved in $CDCl_3$ due to its hydrophobicity (Fig. 12).

Although known to be insoluble in water, the solubility in D_2O was significantly improved in the presence of PB copolymer after micellization. Samples containing PB

copolymer and paclitaxel in $CDCl_3$ showed sharp peaks representing various protons of PEG, PCL, PLA and paclitaxel. Interestingly, a sample containing PB copolymer and paclitaxel in D_2O was devoid of paclitaxel signal suggesting that paclitaxel was inside the nanomicellar core. Broad peaks observed at 3.76 δ ppm and 2.32 δ ppm were attributed to the protons of PEG (-CH2-CH2-) and PCL (-OCO-CH2-), respectively. Proton peaks for PTX was absent.

NMR analysis carried out in CDCl3 exhibited sharp peaks for all the protons indicating free movement of polymer chains and paclitaxel in organic solvent. However, NMR spectra carried out in D_2O exhibited very few broad peaks representing PEG and PCL blocks only. These results suggest that paclitaxel was located in the core of the nanomicelle along with PCL and PLA blocks. Hence, very weak NMR signals for PCL blocks was observed in D_2O due to the restricted molecular movement, and no signals of PLA and paclitaxel were observed. Strong peak of PEG in D_2O indicate the location of PEG in the outer regions of nanomicelles. These results suggest that PBNM are solubilized in water due to micellization process where core is composed of hydrophobic PCL-PLA and shell is composed of PEG which interacts with water.

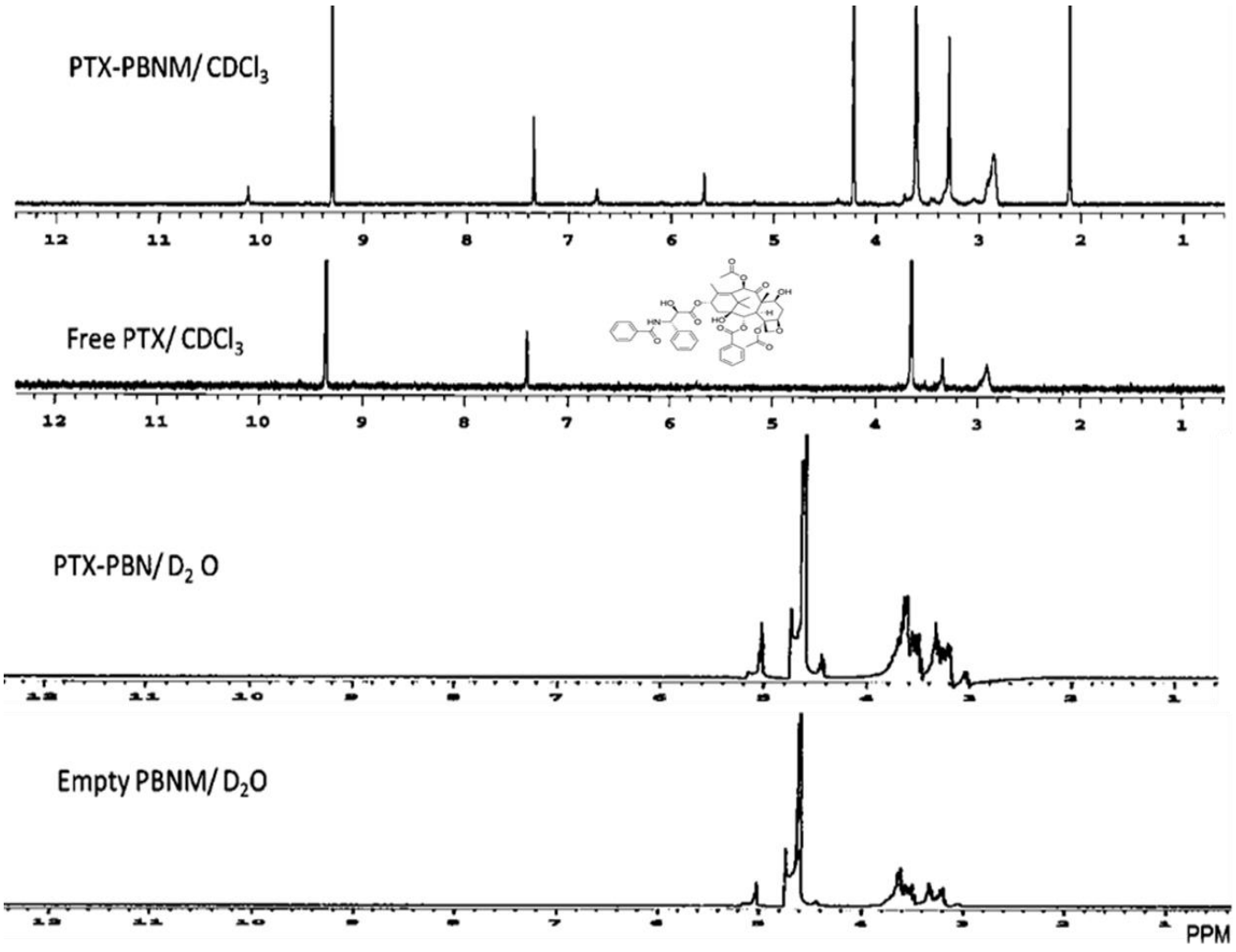

Figure 4. 10: HNMR peaks of PTX-PBNM in both $CDCl_3$ and D_2O, free PTX in $CDCl_3$ and empty PBNM in D_2O.

Transmission Electron Microscopy Analysis

The pentablock nanomicelles were investigated by transmission electron microscopy (TEM) to determine their shapes. This analysis showed that the nanomicelles were round and homogenous and did not produce aggregates (Fig. 4.11). Regarding size, the antibody conjugated paclitaxel-loaded pentablock

nanomicelles had an average of 35nm±2.5nm and the empty conjugated pentablock nanomicelles were around 26±2.0nm.

The Unloaded (empty PBNM-Ab) and PTX-PBNM-Ab had slight difference in terms of appearance as PTX-PBNM-Ab appeared to show some agglomeration perhaps due to high concentration caused by saturation during suspension, the empty PBNM-Ab manifested uniform in appearance. The particle sizes visualized in the TEM images corroborated with the nanomicelles sizes obtained by DLS which already depicted the sizes for PTX-PBNM-Ab and the empty PBNM-Ab as 35±3.5nm and 25±5.00nm respectively.

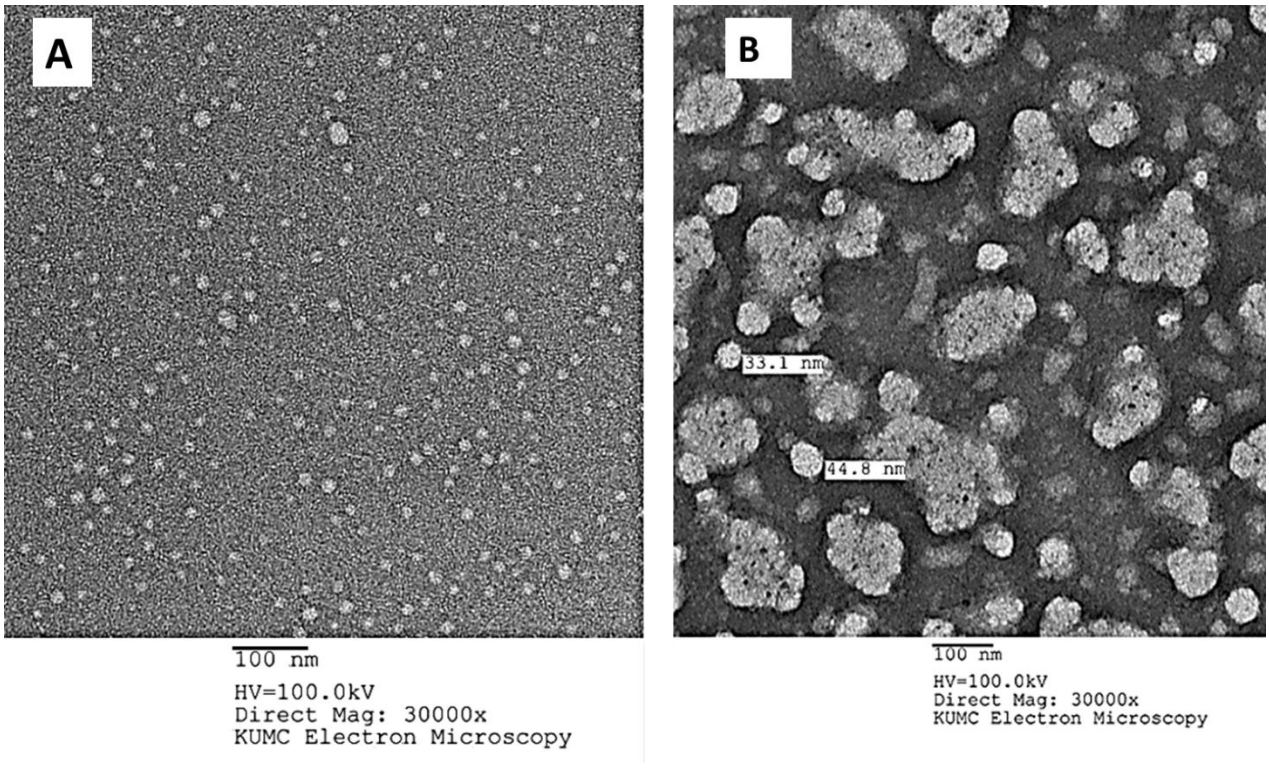

Figure 4. 11:. TEM images of A) conjugated empty PBNM-Ab and B) conjugated paclitaxel-loaded pentablock nanomicellar formulation.

In vitro Drug Release Studies

In vitro release profile of paclitaxel from pentablock nanomicelles was investigated at a physiological pH of 7.4 at 37 ^{o} C. A specific amount of pure PTX (0.1%w/v) dissolved in 1mL of ethanol/water (0.5: 9.5) was used as a control. Equal amount of freeze-dried PTX- PBNM-Ab with different PB copolymer concentrations (0.5%, 1%, 1.5% and 2%) were also dissolved in DI water under the same condition. The release of PTX from hydroethanolic solution was very fast in compared with paclitaxel from PTX-PBNM-Ab, with almost 100% drug release occurring within the first 72h.

Release trend of paclitaxel from the formulations of pentablock nanomicelles were slow with no significant burst effect. The results manifest a sustained release of the PTX from the pentablock nanomicelles (PTX-PBNM-Ab) over a period of 200h. Fig 13. In the initial step, a small amount ethanol (5%w/v) was added to overcome the hydrophobicity of PTX giving rise to a homogenized PTX drug solution. All the four formulations of PTX-PBNM-Ab were easily dissolved in DI water. The presence of PEG in the pentablock structure was responsible for the interactions with aqueous environment, resulting in a clear homogenized solution of the formulations.

There were variations in the release trend among the PTX-PBNM-Ab formulations. At a time point of around 170 hours, the formulation composed of

0.5%PB released around 96% of the PTX drug content followed by 80%, 50% and 40% for formulations bearing 1%PB, 1.5%PB and 2%PB respectively. This trend shows that the more the polymer in the formulation, the longer it takes for drug to get released from the nanomicelles (Fig.4.13). This may be due to the formation of a thick wall as the polymer concentrations increases.

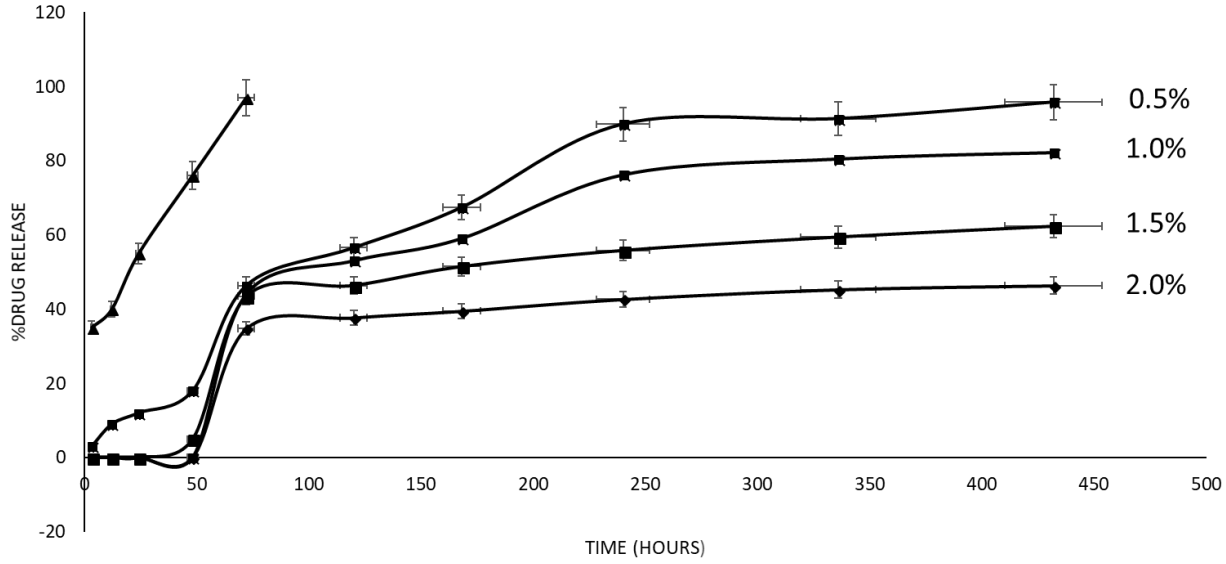

Figure 4. 12: Cumulative drug release from PTX-PBNM-Ab nanomicelles in PBS (pH 7.4), at 37 ± 0.5°C. Each point represents the mean value of three different experiments ± standard deviation.

In vitro Cell Uptake Studies of PSMA-Conjugated Nanomicelles in Prostate Cancer Cells

This experiment was done to enhance specificity of nanomicelles to make a targeted delivery of drug to prostate cancer cells. Prostate cancer cells are known to overexpress prostate specific membrane antigen (PSMA) on their surface (140, 141).

For this reason, cell uptake study was conducted in a specific manner, where, PSMA antibody (Ligand) was conjugated onto the surface of drug-loaded pentablock

nanomicelles then incubated for 24h and 48h, during which, coumarin-6 loaded pentablock nanomicellar formulation was incubated with breast cancer(T47D) cells for 48hs, Prostate cancer PC-3 cells for 24 h and, again with PC-3 cells for 48hs under conducive conditions of 5% carbon dioxide, 37 ^{o} C(142). An appropriate media for the growth of the two cell lines were used (142-144). In this study, PTX was replaced with coumarin-6 due to its ability to emit fluorescence compared to the non-fluorescent paclitaxel.

Cells were incubated in chamber slides with coumarin-6 loaded pentablock nanomicelles bearing PSMA antibody on their surface. The results of this study showed that there was no uptake of ligand conjugated nanomicelles into the breast cancer T47D cells, this may be because they do not overexpress PSMA on their surfaces (145-147) Fig.14A. There was a significant uptake into prostate cancer cell line (PC-3) cells with more drugs entering the cells after 48hs Fig.4.14C, compared to 24hs. Fig.4.14 B. In figure 4.14 B, green coumarin-6 was observed with high intensity all over the cytoplasmic region and not the nucleus (DAPI stained). Therefore, it can be concluded that fluorescent coumarin-6 loaded nanomicelles are inside the cells.

This indicates that nanomicelles were internalized by PC-3 cells. It is an evidence that a large amount coumarin-6 was taken inside the cells with pentablock nanomicelle formulation as shown in (Fig. 4.14 A). There was a significant amount of coumarin-6 loaded nanomicelles inside the cytoplasm ($p < 0.05$). This observation suggests that high uptake of the drug loaded nanomicelles may be due to endocytosis.

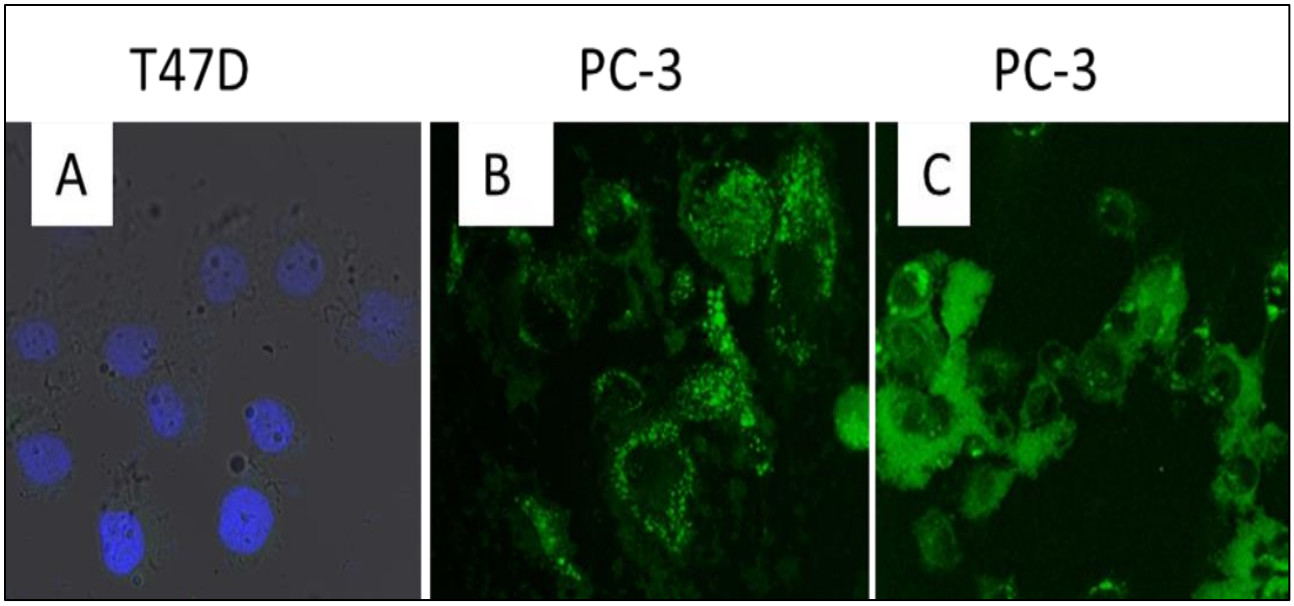

Figure 4. 13: Confocal images showing cell uptake of PSMA antibody (Ligand) conjugated pentablock nanomicelles incubated for 24 h and 48 h, where: A) The ligand conjugated paclitaxel-loaded pentablock nanomicelles incubated with T47D cells for 48h, B) Prostate cancer PC-3 cells incubated for 24 h with ligand conjugated paclitaxel loaded pentablock nanomicelles and, C) PC-3 cells incubated for 48hs in presence of ligand conjugated PTX-loaded PBNM.

Statistical Analysis

A statistical program called JMP was applied for analyzing six different formulations. The polymer amount was the main determinant of nanomicelles size, showing the P-value of 0.0020 with the intercept probability greater than [t] <0.0001* (Tab.3), where $p < 0.05$ is considered significant. Encapsulation efficiency was found to be influenced by the amount of drugs with p-Value of 0.01696 (Fig.4.14).The optimum combination produced for the formulation was 1.25% and 0.125% for PB and PTX respectively (Fig. 4.15).

Parameter Estimates

Term	Estimate	Std Error	t Ratio	Prob>|t|
Intercept	37.666667	1.157628	32.54	<.0001*
polymer%(0.5,2)	5.5833333	1.531398	3.65	0.0020*
Drug %(0.05,0.2)	2.0833333	1.531398	1.36	0.1915
polymer%*Drug %	-0.416667	1.531398	-0.27	0.7888

Effect Tests

Source	Nparm	DF	Sum of Squares	F Ratio	Prob > F
polymer%(0.5,2)	1	1	374.08333	13.2926	0.0020*
Drug %(0.05,0.2)	1	1	52.08333	1.8507	0.1915
polymer%*Drug %	1	1	2.08333	0.0740	0.7888

Effect Summary

Source	LogWorth	PValue
polymer%(0.5,2)	2.699	0.00200
Drug %(0.05,0.2)	0.718	0.19147
polymer%*Drug %	0.103	0.78884

Figure 4. 14 Parameter estimate, effect test and effect summary demonstrating the impacts of PB copolymers, Drug and their combination in relation to size and %EE of the pentablock Nanomicelles.

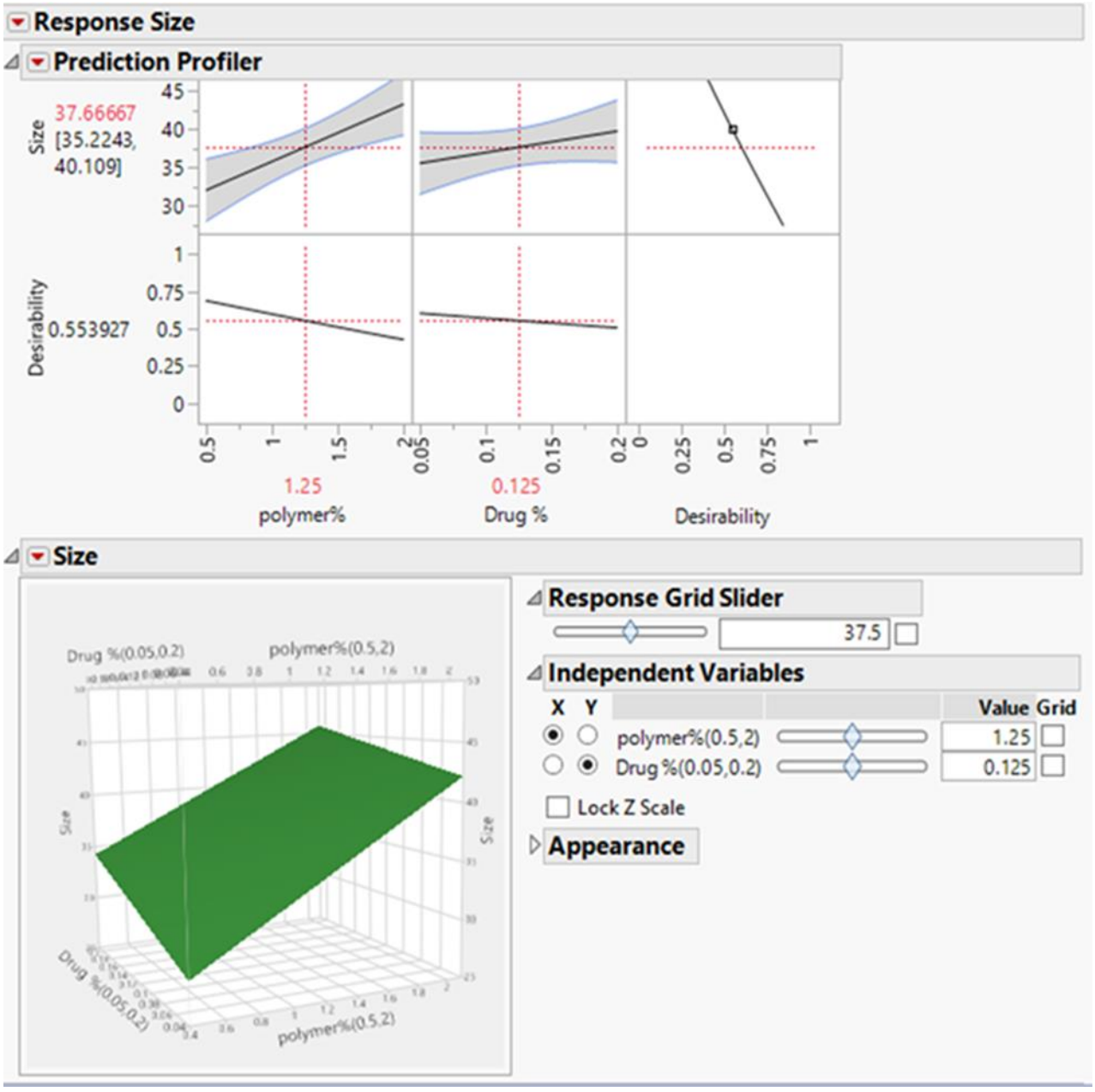

Figure 4. 15: Prediction profiler and parameter estimates showing the effect of drug%, and PB copolymer percentages on nanomicellar size and the desirability of the PTX-PBNM-Ab nanomicelles.

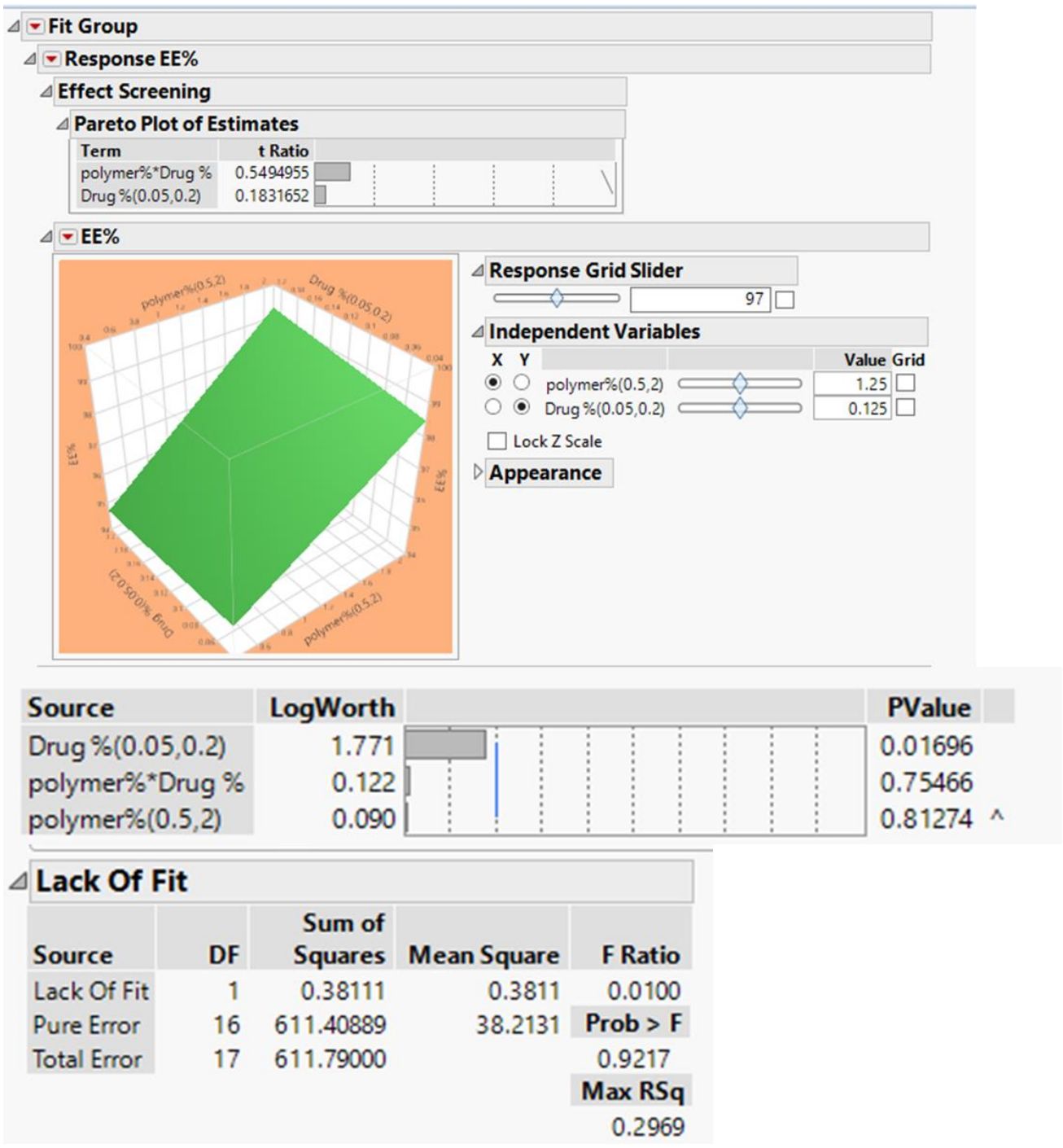

Figure 4. 16. Prediction profiler and parameter estimates showing the effect of drug%, and PB copolymer percentages on nanomicellar %EE and the desirability of the PTX-PBNM-Ab nanomicelles.

Cell Proliferation Assay of PTX-PBNM-Ab

Cytotoxicity of paclitaxel-loaded pentablock Nanomicelles conjugated with PSMA antibody was evaluated in PC-3 and T47D cell lines using a CyquantTM cell proliferation assay, which emits fluorescence due to interactions between DNA and a special dye in the assay. Percentage of cell growth inhibition was measured by fluorescence caused by DNA of surviving cells after 48 h incubation. Paclitaxel concentration in the formulations was adjusted to the same as that of free drug based on the IC_{50} exhibited by paclitaxel(124).

PTX-PBNM-Ab formulation showed significant cytotoxic effect in PC-3 cells after 48h incubation ($p < 0.05$) as shown in Fig. 4.16. It is worth noting that at 48 hours, the drug is not completely released from the nanomicelles (only 30%-40% released) as earlier depicted by the release profile.

PTX-PBNM-Ab nanomicelle formulation showed a significant difference in reduction of cell proliferation in PC-3 cells ($p < 0.05$). There was no effect on the T47D cells, this is because there was no overexpression of Prostatic specific membrane antigen (PSMA) on the surface of the T47D cells as earlier indicated by the uptake studies. Large amount of PTX within the PTX-PBNM-Ab was delivered into PC-3 cells by endocytosis, causing cytotoxic effect (123).

Direct impact of efflux mechanism on paclitaxel inside the cells may have been reduced by loading drug into the core of the PTX-PBNM-Ab. Nanomicelles showed no cytotoxicity in T47D cells. These results demonstrate that PSMA antibody aided the delivery of the Nanomicelles selectively to the prostate cancer (PC-3) cells. Furthermore, lodging of PTX drug into the core of pentablock nanomicelles strongly

enhanced the cytotoxic effect probably due to more drug molecules being ferried into the cells by nanomicelles. Sustained drug release within the cell and reduction of efflux may have played a great role on effectiveness of the delivery system. The lowest PTX concentration was calculated based on the IC_{50} which is 3.3±1.2 nM (124).

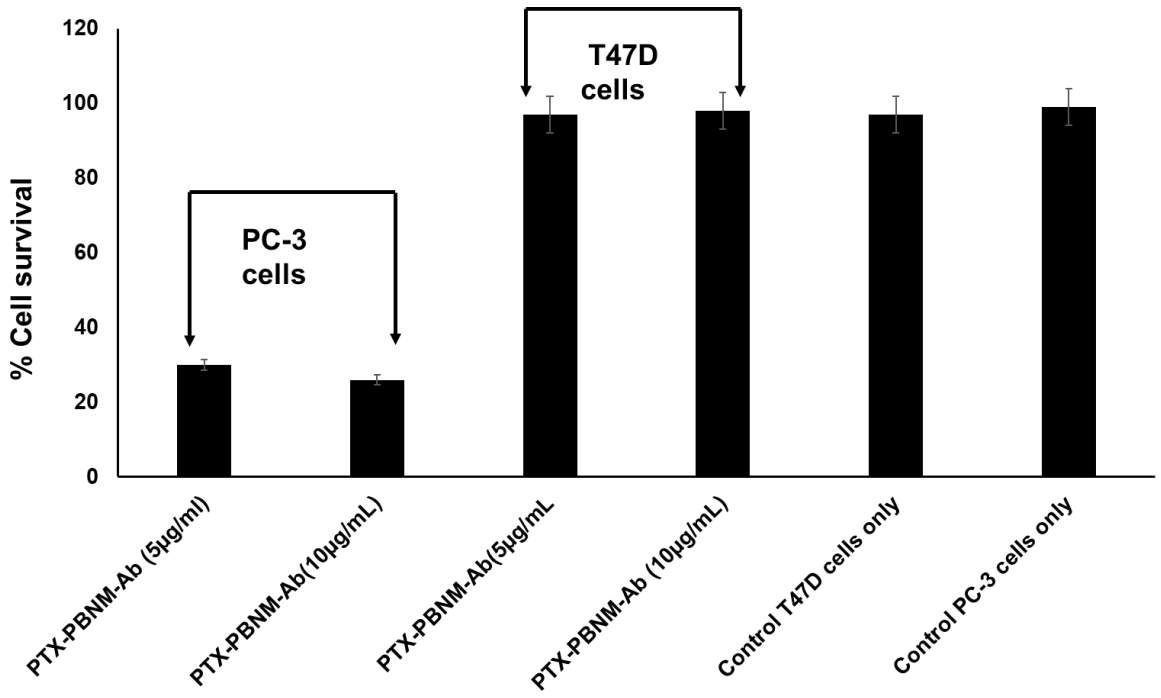

Figure 4. 17 Cell proliferation assay showing % Cell survival involving: PTX-PBNM-Ab at 5µg/mL & 10 µg/mL in both PC-3 and T47 cells compared to Controls (PC-3 and T47D cells only)

Conclusions

From the results obtained in this study, it is sensible to conclude that the synthesized pentablock copolymers proved to be safe for the cells tested. The Pentablock copolymers were able to compose drug-loaded nanomicelles of adequate sizes (45nm±2.5nm). The viscosity of the formulation was close to that of water, hence its suitability for application through IV route.

The cell uptake analysis showed a good uptake profile showing that the nanomicelles facilitated the entry of a great amount of drug(coumarin 6) into the cells. The release studies showed long time release, which can be significant in cancer chemotherapy. The cell proliferation assay showed a great effectiveness of the drug delivery system. The PSMA antibody conjugation onto the surface of the paclitaxel loaded pentablock nanomicelle selectively delivered the drug to prostate cancer cells.

Furthermore, the pentablock supported a high temperature above 200^{o} C showing significant stability to thermal degradation. This technique has proven ideal for delivering drugs into the specific cells when conjugated with a targeting moiety. In general, this method can be used for delivery of hydrophobic anticancer drugs like paclitaxel during cancer therapy to reduce side effects, frequency and dosage of the drug as administered to the patients currently.

CHAPTER 5

PREPARATION OF DOXORUBICIN-RETINOIC ACID HIP COMPLEX NANOMICELLAR FORMULATION

Rationale

Doxorubicin (DOX), available in the market as Adriamycin or Rubex, is a drug used in treatment of various cancers. Doxorubicin is a member of anthocyanin family and is grouped under anthracycline with both antitumor and antibiotic activities. It works by interfering with DNA function causing intercalation and alkylation of DNA, causing disruption to both RNA and DNA polymerase, inhibition of topoisomerase II which consequently kills the tumor cells (21, 22).

DOX is applied mostly in the treatment of breast and bladder cancers. It is also used in cases of sarcomas, lymphomas, and acute lymphatic leukemia. It is normally used as combination with other drugs by intra-venous application. However, there are many serious side effects associated with doxorubicin(23). These side effects include but not limited to allergic reactions which may cause tissue injuries damage at the site of injection. Another most notorious side effect is the accumulation of doxorubicin in the cardiac and respiratory tissues (24). This irreversible dose-dependent, side effect may cause toxicity to cardiac and respiratory tissues, resulting in cardiomyopathy, dyspnea and intolerance to exercise due to the production of mitochondrial reactive oxygen species (ROS)(25)

Other common collateral effects are: loss of hair, suppression of bone marrow, skin eruptions, vomiting, and mouth inflammation. Patients often experience red coloration of the urine for a few days during treatment with DOX.

Doxorubicin is a widely used drug in clinical setting. However, less entry and low distribution of doxorubicin in tumor tissue are the principal factors for its therapeutic backlash (23). Due to low pH in the tumor interstitial environment, weak base drugs like doxorubicin, are likely to ionized before entering leading to reduced cell uptake(26). In addition, serious cytotoxic effects may be caused to healthy cells due to non-targeted delivery. These may result in: dose-dependent cardiac damage, multidrug resistance, and myelosuppression thus, restricting its therapeutic application (27). It is important to develop new delivery systems that capable of ferrying sufficient amount of drug to the tumor cells, thereby avoiding the multidrug resistance and frequent dose administrations of chemotherapeutics.

One of the attempts to elevate the drug bioavailability in tumor tissue is the application of site-specific delivery systems that may release the encapsulated drugs within tumor cells. Another way is to attain higher accumulation of drug by specific tumor cell targeting. However, this may be difficult to achieve without using a ligand that is unique to the target on the cell surface. This lack of proper ligand may end up delivering the drug to the undesired site (28).

Some intrinsic variations in the tumor microenvironment such as enzymes, pH and oxidative stress, and the extrinsic factors i.e., light, temperature and magnetic fields, are known to cause site-specific drug release within the tumor cells and tissues (29). pH triggered drug release from a nanocarrier is the most acceptable way of drug release directly inside the cell cytoplasm(29). This strategy of using the acidic tumor microenvironment to trigger drug release has shown some short falls due to the fact that the lowest pH a tumors is located far from tumor blood vessels(30).

Since the interstitial region of a tumor has a pH lower than 6.5, the ability of nanocarrier might be restricted. For instance, some carriers such as liposomes become unstable and are altered before arriving at their intended targets. Another promising type of nanoformulation for delivery of hydrophobic drugs is nanomicelles.

Nanomicelles display higher efficiency compared to other carriers like liposomes. They also possess many advantages, which include: high bioavailability, improved stability of the encapsulated drug, better encapsulation and loading efficiencies and better delayed release profile (33). Furthermore, most of the materials utilized in its production are biologically safe for all forms of administration. The application of these nanomicelles is with respect to ability to improve drug entry into the tumor tissue, while reducing dosage and enhancing drug efficacy by limiting non-selective cytotoxicity(34-37). To cause pH-triggered intracellular release of doxorubicin (DOX), retinoic acid (RA), a lipophilic molecule, was utilized to form an ion paired complex (DOX-RA). The formed ion pair shows instability in an acidic microenvironment i.e. pH < 7.0, which is compatible with tumor tissue.

The complex attains stability in an environment with pH 7.4 , for instance, blood (148). This would help in increasing the drug levels in the cells of tumor tissue, sparing normal tissues cells. In addition, hydrophobicity caused by ion pairing can retain doxorubicin in the hydrophobic core of nanomicelles and raise the encapsulated amount of DOX in the nanomicelles. Furthermore, studies have revealed that RA may improve effectiveness of a drug by interfering with the permeability and fluidity of membrane of tumor cells (149).

Materials and Methods

Materials

Retinoic acid was purchased from Aeser, MA, USA. Pentablock copolymer containing Poly-ethylene glycol (PEG), L-lactide and ε-caprolactone monomers, was obtained from our laboratory, already synthesized from previous project. Cyquant™ cell proliferation assay kit was obtained from Invitrogen Life Technologies Inc. and distributed by Thermos-Fisher Scientific. Doxorubicin drug was obtained from ADOOQ Bioscience, Irvin, CA, USA. All other reagents utilized in this study were of analytical grade.

Methods

Preparation of DOX-RA Complex

In this study, a hydrophobic complex of doxorubicin and retinoic acid (DOX-RA) was prepared by co-precipitation technique(150). Briefly, doxorubicin aqueous solution (10 mg/mL), was prepared in an Eppendorf tube, 100mg/mL sodium bicarbonate solution was added to the tube while stirring. An ethanolic solution of retinoic acid (10 mg/mL), was added to the DOX solution while stirring continuously. After stirring the combined solutions for 1 h, the final solution was centrifuged at 6000 rpm for 20 min. Finally,

an orange to brick-red colored precipitate of DOX-RA (Fig.5.1) settled at the bottom of the tube. The precipitated complex was washed 3 times with deionized water, followed by drying at 40 °C before being stored at 4 °C. The DOX-RA complex was then used to prepare nanomicelles with pentablock copolymer previously prepared in our lab (151).

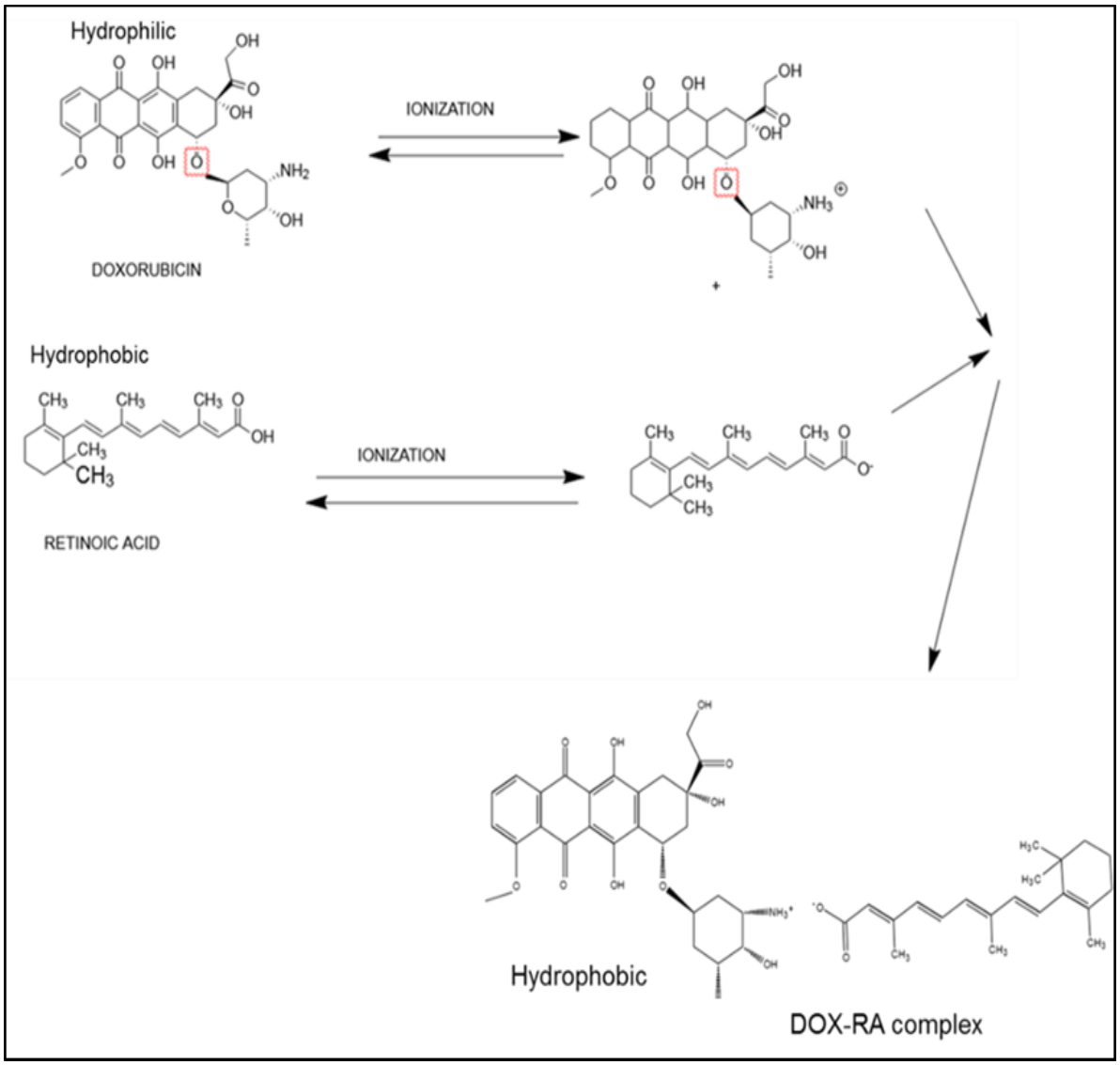

Figure 5. 1:. The schematic illustration of the reaction and the structures of DOX, RA and DOX-RA complex.

Determination of Hydrophobicity DOX-RA Complex

Hydrophobicity of DOX-RA complex was analyzed by studying its solubilities in octanol. DOX-RA was dissolved in octanol, while agitating for 48 h at room temperature (25 °C). The sample was then submitted to centrifugation for 20min at 6000 rpm. After centrifugation, the supernatant was collected and dissolved in isopropanol, homogenized and then analyzed using UV-vis spectrophotometer (Shimadzu, Kyoto, Japan) 495nm wavelength.

FTIR Analysis of DOX-RA Complex

To determine structural characteristic of the formed, DOX-RA complex, and the success of the complex formation. Samples of synthesized DOX-RA complex, RA and DOX were subjected to FT-IR, Thermo-Scientific Nicolet iZ10, with an ATR diamond and DTGS detector. Where samples of DOX-RA complex, DOX and RA were analyzed at scanning range of 650–4000 cm^{-1}.

Mass Spectrometry Analysis for DOX-RA complex

The DOX-RA complex was submitted to mass spectrometry (Thermo LCQ deca mass spectrometer). The analysis with LC-MS/MS involved a positive ion mode with electrospray ionization (ESI) as the main ion source (152). The source was set at 5 kV, the rates of both sheath gas and auxiliary gas flow were set at 80 and 20 units, respectively while capillary temperature was adjusted to 250 °C. C-18 column of 2.0mm × 50mm, and particle size limit 3 µm was used for Liquid Chromatography

separation applying using water with 0.1% formic acid as the mobile phase A and acetonitrile as the mobile phase B. The flow rate of LC was adjusted to 0.20 ml/min. The gradient of mobile phase B increased from 30% to 100%.

Preparation of DOX-RA Nanomicelles

Nanomicelles (NM) were prepared using hydration-dehydration method (16). Briefly, a specific amount (0.1%w/v) of DOX-RA complex was dissolved in 1ml of ethanol in an Eppendorf tube. On the other hand, 2%w/v of pentablock copolymer was dissolve in 1 mL ethanol in a separate tube. The two solutions were then mixed together, homogenized and evaporated in a speed vacuum for 24h until the formation of a thin film.

Resultant thin film was suspended in deionized (DI) water followed by vortexing until a complete dissolution was achieved (103). The solution was filtered using 0.22µm filter membrane to acquire uniform nanomicelle sizes and eliminate the polymer residues. The nanomicelle suspension was further freeze-dried using LABCONCO freeze-dryer, USA, with trehalose as cryoprotectants (22).

Determination of Nanomicelle Size and Zeta Potential for DOX-RA/PBNM

The sizes, zeta potentials and polydispersity indices (PDI) of DOX-RA-PBNM were obtained using dynamic laser scattering (DLS) with the help of Zetasizer HS 3000 (Malvern Instruments, UK), at a detection angle of 90 degrees at 25^{o}C. The samples were dissolved in deionized water, homogenized and filtered using 0.22µL before being transferred into a transparent cuvette for analysis. Average values of three measurements were obtained for all samples and the peaks for zeta sizes, PDI and zeta potentials were obtained and recorded accordingly(109).

Determination of Drug Encapsulation and Loading Efficiencies

The amount of doxorubicin encapsulated in the nanomicelles was measured by UV-vis. briefly, a portion of the nanomicellar formulation was freeze-dried. Then 2mg of the dry formulation was dissolved in 1mL dichloromethane (DCM) to break the nanomicelle structure followed by centrifugation at 10,000rpm for 5min and then eventual evaporation to remove DCM. Subsequently, dry content was collected and dissolved in ethanol.

The resultant ethanolic solution was then filtered through 0.22-mm nylon syringe filter. The filtrate was analyzed with UV-spectrophotometry at 495nm (Beckman, DU® 530, UV-vis spectrophotometer, Life science, CA, USA), for the determination of doxorubicin concentration. This process was performed in triplicate and a calibration curve with pure doxorubicin dissolved in ethanol at different concentrations produced an equation Y=42.024+0.031 and R^2 =0.9884 (110). Percentage encapsulation efficiency (%EE) and drug loading were calculated according to the equations below.

$$\text{Encapsulation efficiency (\%)} = \text{Total } \frac{\text{drug (mg)} - \text{Free drug (mg)}}{\text{Total drug (mg)}} \times 100$$

$$\text{Drug loading (\%)} = \frac{\text{Mass of PTX in nanomicelles}}{\text{Mass of PTX used + Mass of PB used}} \times 100$$

H^1-NMR Analysis for DOX-RA-PBNM

DOX-RA-PBNM were analyzed using deuterated dimethyl sulfoxide (DMSO) as solvent then subjected to H^1-NMR analysis. An adequate amount of both pure doxorubicin and retinoic acid were dissolved in DMSO before analysis. The spectra were obtained at room temperature upon submission to a Varian Inova 400 MHz spectrometer (Varian, Palo Alto, CA, USA). Chemical shifts values were reported in parts per million (ppm)(102). ^{1}H-NMR spectra were recorded from 0 to 12 ppm using a delay time of 4 seconds.

Transmission Electron Microscopy Analysis

Nanomicelles morphology was determined by transmission electron microscopy (TEM; Philips CM12 STEM, Hillsboro, OR.). Briefly; a small amount of freeze-dried DOX-RA-loaded pentablock nanomicellar formulations were dissolved in DI water to form aqueous solution. The samples were then stained with 1% uranium salt. The resultant solution containing nanomicelles was then placed on a carbon-coated copper grid, and excess liquid was removed using a piece of dry filter paper then submitted to transmission electron microscope.

In Vitro Release Study for DOX-RA Nanomicelles

The release of doxorubicin from DOX-RA/PBNM was conducted in various media of different pH conditions (pH 4.0, pH5.5 and pH 7.4) for 108 h in a dark room(153). Briefly, 2mL of (2%w/v), DOX-RA/PBNM aqueous solution was transferred into a dialysis membrane bag (MW 10kDa) (111). The dialysis bags were dipped into 15 mL tubes of release media and placed in a shaking water bath at 37 °C. The media

were completely replaced at different time intervals i.e. 3 h, 6 h, 12 h, 24 h, 36 h,48 h, 60 h, 72 h,84 h,96 h and 108 h respectively (112). The doxorubicin amount released from DOX-RA-PBNM was obtained with a UV spectrophotometer using 495nm wavelength(154).

Cell Uptake Analysis of DOX-RA-PBNM

During the uptake studies, confocal laser scan microscopy was applied to determine the intracellular distribution of both DOX-RA/PBNM in PC-3 cells. PC-3 cells were cultured until confluence in two different 4 chamber slides using appropriate growth media. A solution of DOX-RA-PBNM 20 µg/mL was made with culture medium. The solution was transferred into each 4 chamber slides containing PC-3 cells and incubated for different time intervals i.e., one was incubated for 12 h and the other for 24 h.

The slides were treated with 4%paraformaldehyde, washed 3 times with PBS, and then kept in mounting medium overnight. The slides were then observed using confocal scanning microscopy (Leica microsystems, wezler, Germany) at 340nm and 540 excitation and emission wavelengths respectively (102, 108).

In vitro Growth Inhibition Assay for DOX-RA-PBNM

Cell growth inhibition analysis was conducted using a DNA based Assay Kit called CyquantTM® Cell Proliferation (C7026) that contains fluorescent dye called CyquantTM® GR dye (113). Briefly; PC-3 cells were cultured in a 96 well plate with Dulbecco's F-12 medium as per protocol. Cells were incubated in 96 well plate at 37 ^{O}C and 5%CO_2 until confluence. The medium was then removed followed by addition

of different medium solutions made of pure doxorubicin (20µg/mL) and DOX-RA/PBNM (20µg/mL) in specific rows of the plate.

The plate was then incubated under humidified atmosphere at 37°C and 5% CO_2 for 24 h and 48 h. In each case, Cyquant reagent solution was prepared and added in each well after washing 3 times with PBS. The plate was kept at 4^o C before being submitted to fluorescent plate reader. The readings were recorded at wavelengths of 570 and 630 nm. All the measurements were done in triplicates and reported as mean plus or minus standard deviation.

Results and Discussions

Hydrophobicity Analysis for DOX-RA Complex

Hydrophobicity of DOX-RA complex was analyzed before the preparation of DOX-RA nanomicelles. The lipid solubility of saturated DOX-RA was measured in octanol in order to assess the impact of ion pairing on lipophilicity of doxorubicin (155). The solubility of doxorubicin in hydrophobic media improved significantly after the formation of ion pair with RA, which is a clear indicator of a high hydrophobicity caused by a successful complexing of DOX with RA. The enhanced lipophilicity of doxorubicin with retinoic acid ameliorate drug loading and encapsulation of DOX inside PBNM.

Mass Spectrometry Analysis for DOX-RA Complex

Mass spectrometry was conducted to confirm the constitution of the DOX-RA complex with the above-mentioned MS/MS conditions. The ion peaks were observed for both DOX and RA at different m/z. In positive ion mode MS/MS analysis, major

fragment peaks of both RA and DOX ($[M+H]^+$) were observed at m/z 301.3 and 544.3 respectively, while molecular ion peaks at m/z 844.6 were observed for the DOX-RA complex(Fig 2), this being the sum of both RA and DOX molecular weights(DOX=544g and RA=300g). The result shows evidence that DOX-RA complex was constituted of both doxorubicin (Mw 544) and Retinoic acid (Mw 300g).

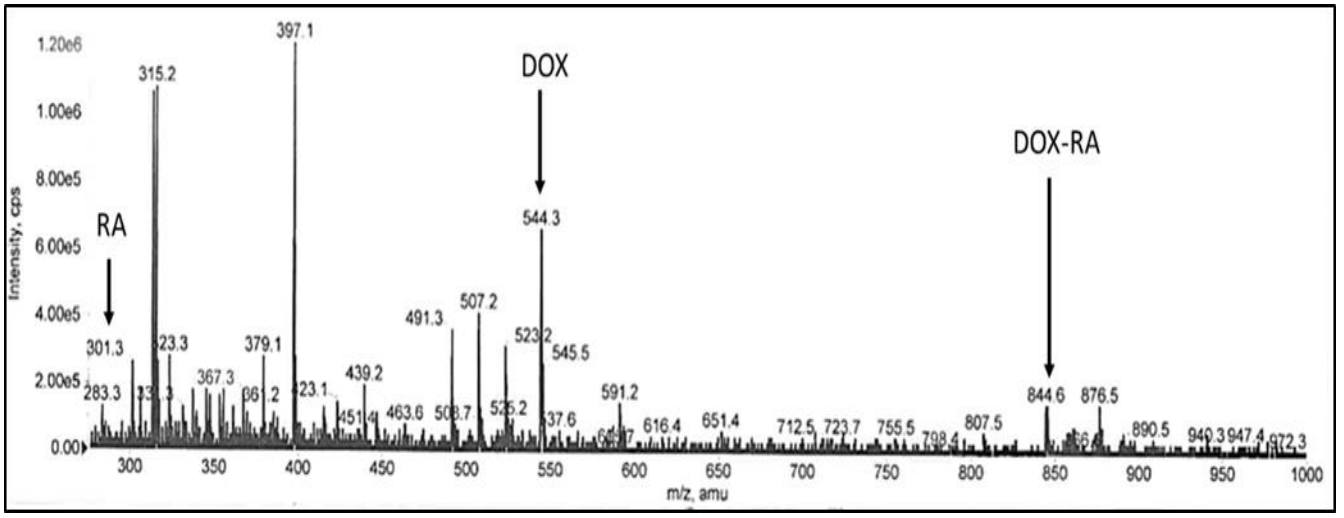

Figure 5. 2: The mass spectrometry spectra showing the Mz peak for RA, DOX and DOX-RA complex in a positive ion mode.

FTIR Analysis of DOX-RA Complex

FTIR spectra were obtained for dry samples of DOX-RA as well as pure doxorubicin drug and Retinoic acid samples. The results showed increase in absorption band at 1700 cm−1 and multiple bands that range from 1000–1500 cm−1 depicting the presence of increase in all the significant stretching's bands in DOX-RA as a result of complex formation.

This is in comparison to the individual molecules of DOX and RA. As shown in Figure 5.3, C=O bands at 1050 cm−1 and O-H band stretching at 3300 cm−1 are for DOX and RA. C-H stretching bands at 2940 and 2900 cm−1 indicate the presence of both DOX and RA. Bands manifested in the region around 3000cm $^{-1}$ can be assigned to aromatic C-H stretching of both DOX and RA in the DOX-RA complex. There is an increase in C-C ring stretching peak in DOX-RA complex compared to the individual molecules of both DOX and RA in the region around 1750cm-1. However, primary aliphatic amines in DOX is constant in the region 3450-3250cm-1.

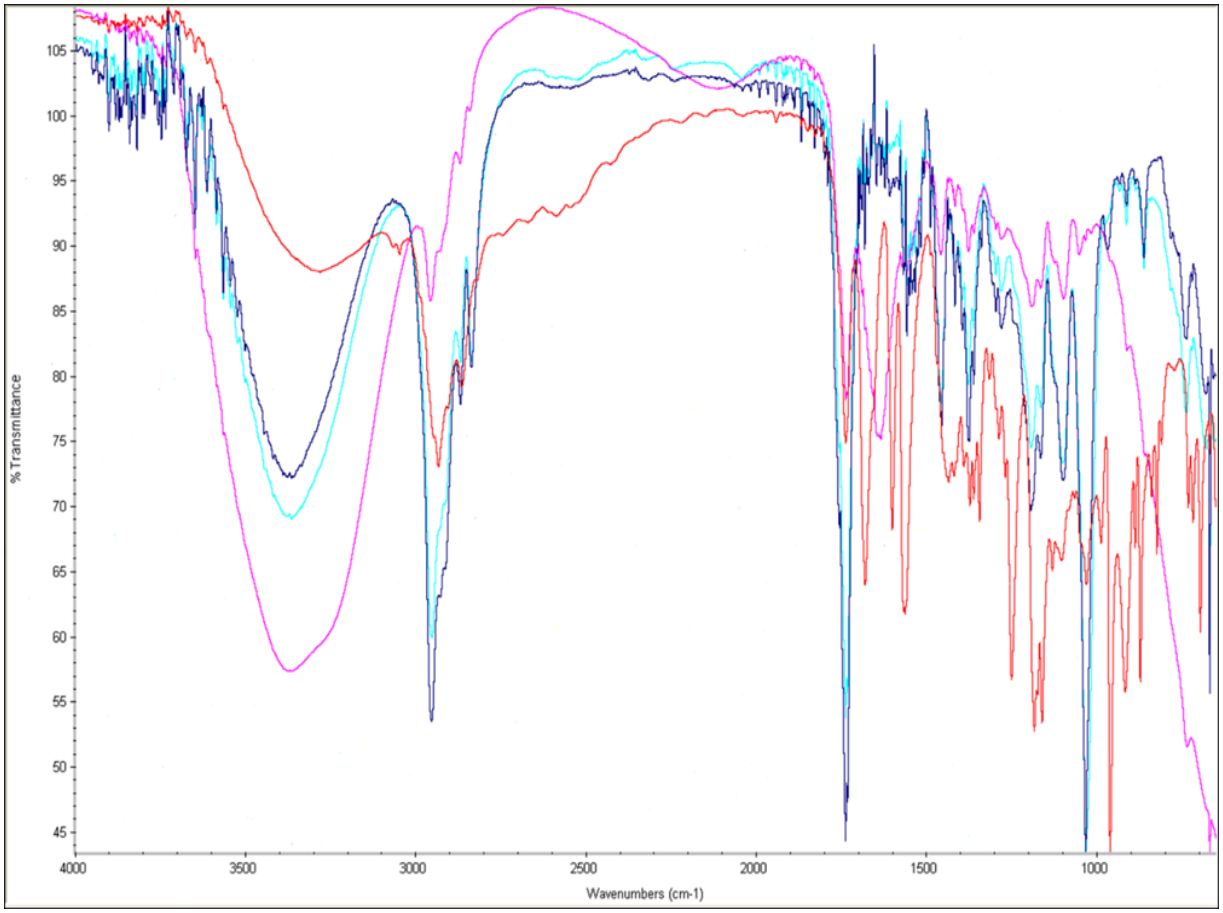

Figure 5. 3: The FTIR spectra of DOX (light blue), RA (red) and DOX-RA complex (blue)

^{1}H-NMR Analysis for DOX-RA Complex

H-NMR analysis was conducted in order to understand the structure of the newly formed DOX-RA. DMSO was used as solvent to analyze the samples. DOX-RA/PBNM, free DOX and Free RA were dissolved in DMSO. Although DOX is hydrophilic, DMSO was used for all the samples due to its ability to dissolve both hydrophobic and hydrophilic substances.

Samples containing DOX-RA complex in DMSO showed sharp peaks representing various protons of DOX and RA. Interestingly, a sample containing DOX-RA/PBNM in DMSO was devoid of any signal of signal of the substances suggesting that DOX-RA is inside the nanomicellar core. In the nanomicelle sample, broad peaks observed at 3.75 δ ppm and 2.30 δ ppm were attributed to the protons of DOX (-CH2-CH_2-) and (-CH_3) of RA, respectively (Fig.5.4). Proton peaks for the DOX and RA in the complex were very eminent. These results suggest that DOX-RA complex was successfully formed.

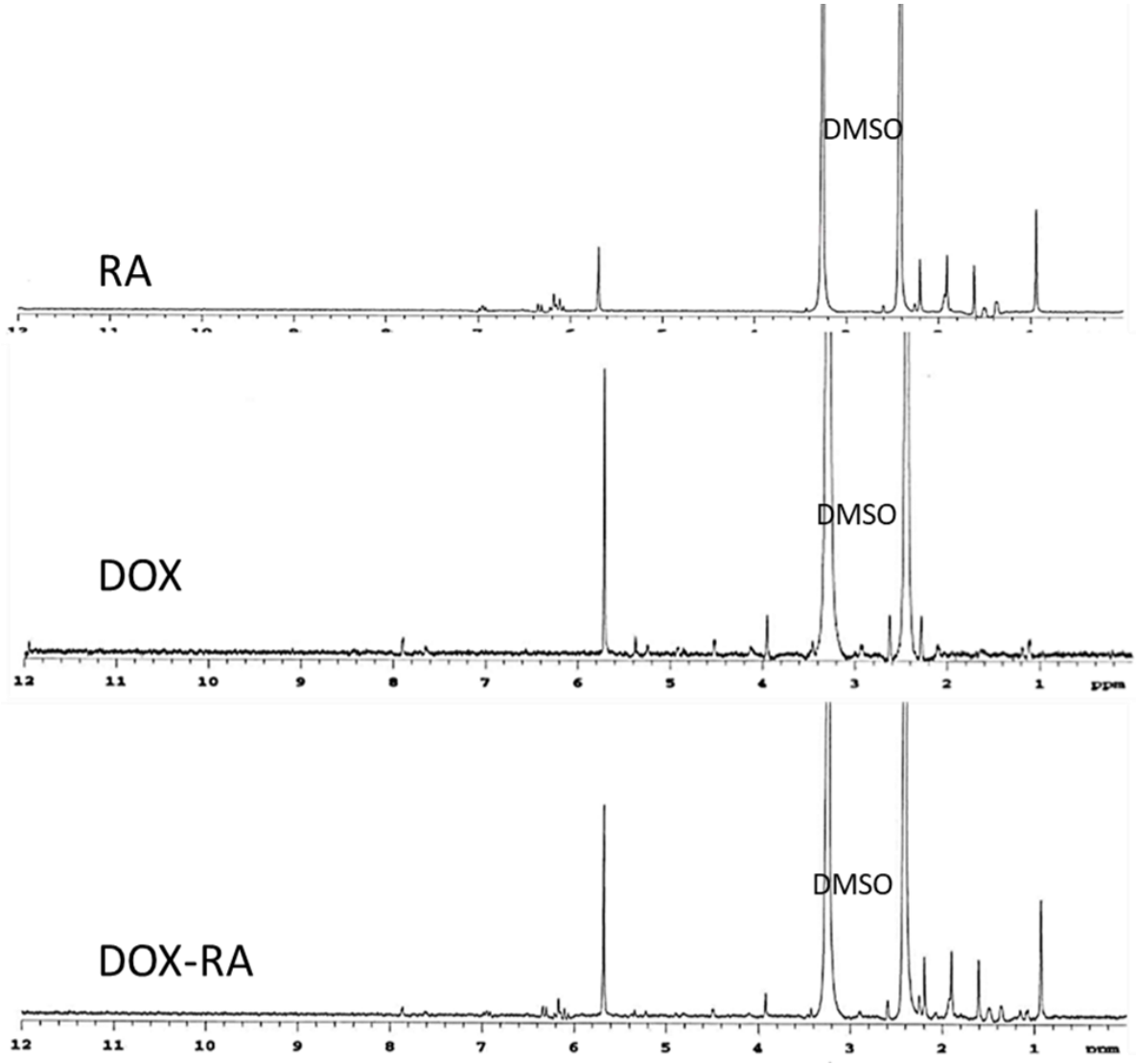

Figure 5. 4: Proton NMR spectra showing the peaks for RA, DOX and DOX-RA in DMSO

Size Distribution and Zeta Potential for DOX-RA Loaded Nanomicelles.

Solvent evaporation method was applied for the preparation of DOX-RA/PBNM. The PBNM formulations were analyzed to determine the size, polydispersity index (PDI), and zeta-potential. Average mean diameters for the nanomicelles (DOX-RA/PBNM) was 25.5±5.00nm (Fig 5.5). Small negligible peaks appeared at regions beyond 1000nm for DOX-RA/PBNM, perhaps due to a small aggregation in the sample, but still the majority peak (around 98%) was 25.5±5.00nm (fig.5 A).

The average PDI for DOX-RA/PBNM 0.037±0.005. PDI values suggest that the nanomicelles exhibit uniform particle size distribution with less aggregation. The drug-loaded nanomicelles display neutral zeta potential (around 0±2.5 mV) as shown in Figure 5.5 B. This makes it possible for the DOX-RA nanomicelles to be an excellent candidate for intravenous application since it is unlikely to produce interactions with blood components due to neutrality as neutral charge on particle surface prevent agglomeration with negatively charged blood tissue (156).

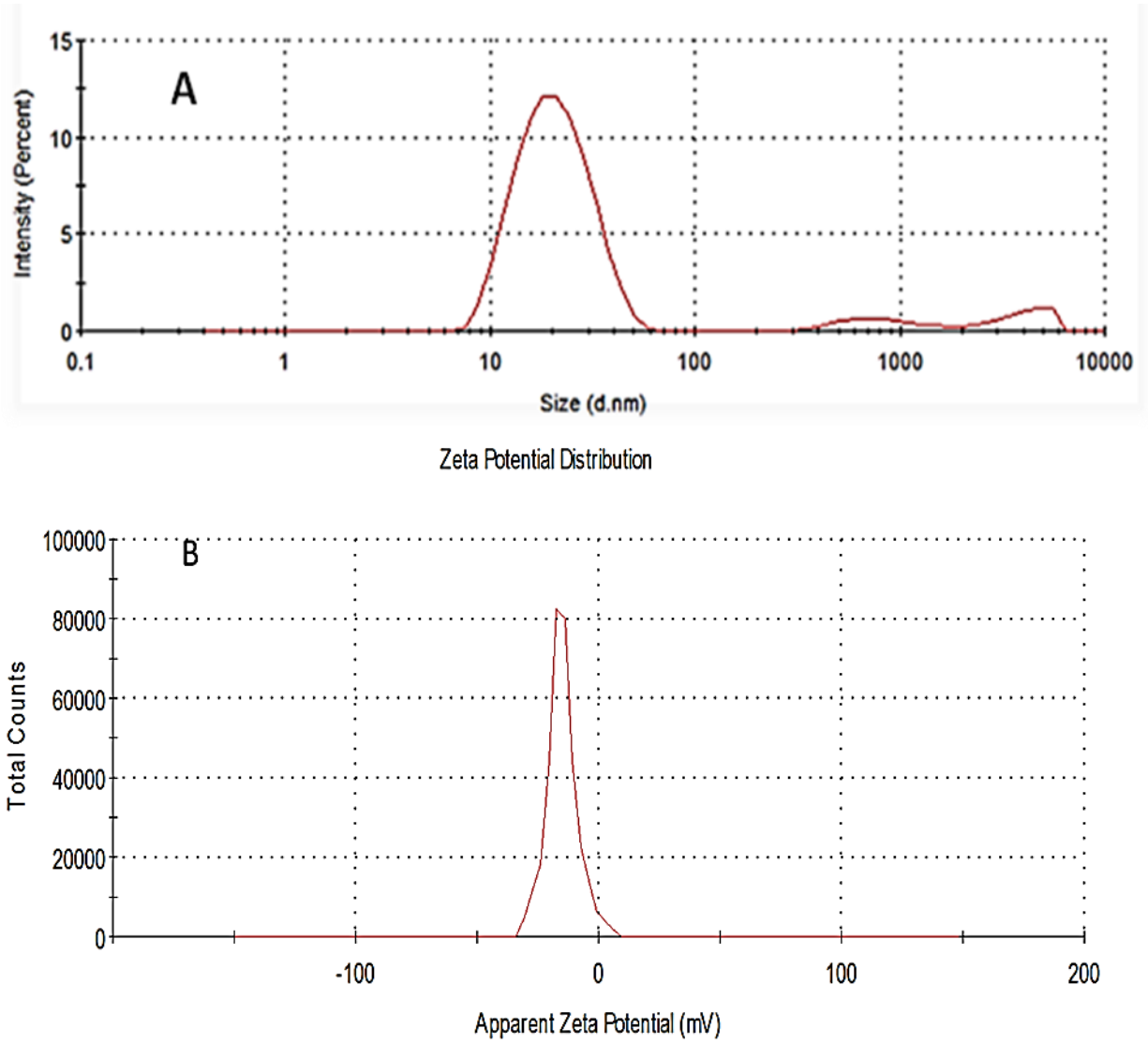

Figure 5. 5: The DLS peaks showing A) size and B) zeta potential of DOX-RA/PBNM in aqueous solution.

Entrapment Efficiency and Drug Loading of DOX-RA Nanomicelles

Percentage of drug encapsulation efficiency (EE) is a crucial factor for drug delivery carriers. The percentage EE of doxorubicin loaded in DOX-RA nanomicelles was calculated to be 97.5% while the drug loading was found to be approximately 12%. These results demonstrate that DOX-RA pentablock nanomicelles achieved high doxorubicin entrapment efficiency and adequate drug loading which might be attributed to the hydrophobicity caused to DOX by complexing it through ion pairing with retinoic acid, thereby creating its efficient lodging in the hydrophobic core formed by hydrophobic PCL and PLA of the pentablock nanomicelle.

This technique allows for efficient entrapment of doxorubicin drug in the nanomicellar core, which would have been hard to achieve due to hydrophilicity of doxorubicin. The encapsulation efficiency of the formed DOX-RA/PBNM was 98.5%, which is almost 100% of doxorubicin encapsulation. Furthermore, the percentage drug loading was 12%. This might be attributed to lipophilicity caused by ion pairing of DOX with RA. In addition, the lodging of high concentration of DOX-RA inside the hydrophobic core of PBNM shows the success in the complex formation and increased hydrophobicity of doxorubicin.

Analysis by Transmission Electron Microscopy (TEM).

The morphology of pentablock nanomicelles containing DOX-RA complex was investigated by transmission electron microscopy (TEM). This analysis showed that the nanomicelles were spherical, homogenous, and did not contain aggregates (Fig.5.6). Regarding size, pentablock nanomicelles had an average of 30±2.5nm. There was an apparent uniform morphology in DOX-RA/PBNM, with uniform

appearance. The particle sizes visualized in the TEM images corroborate with the sizes obtained by DLS which already depicts the DOX-RA/PBNM and the empty PBNM sizes as 30nm ±5.00nm.

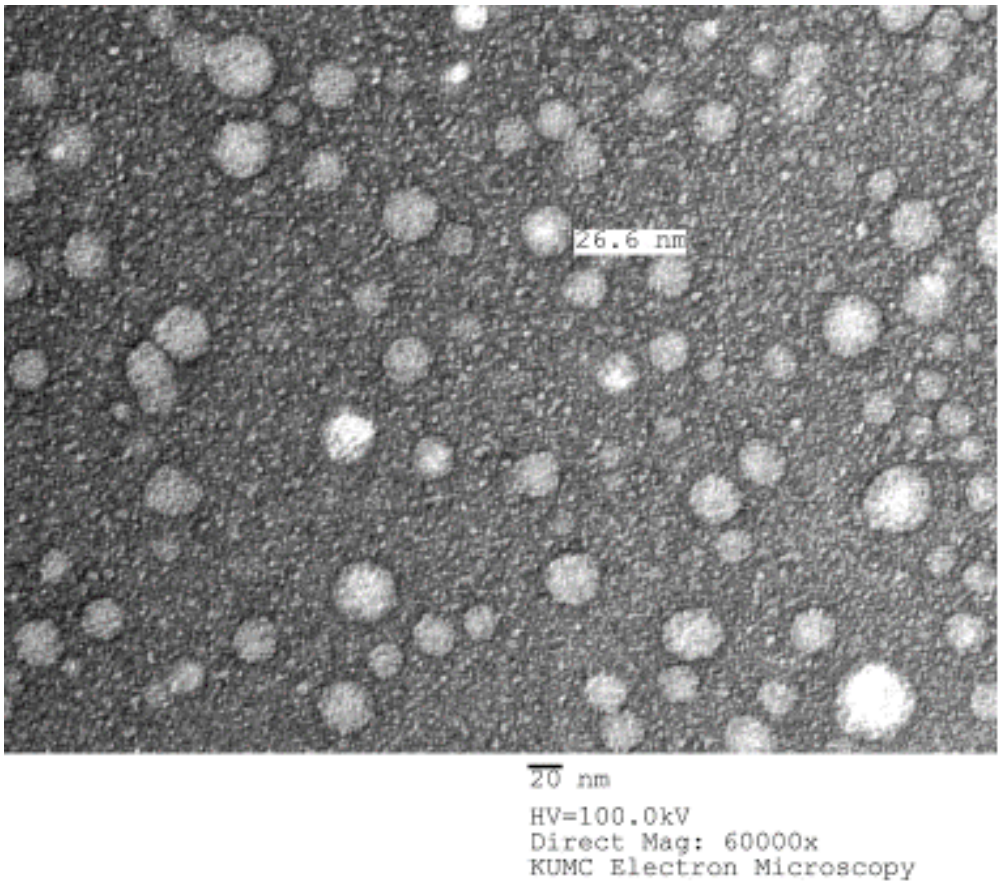

Figure 5. 6: The TEM image showing the DOX-RA-PBNM after freeze-drying using trehalose as cryoprotectant

In Vitro Release Study for DOX-RA-PBNM

The drug release profile of doxorubicin from DOX-RA/PBNM was analyzed for 108 h at 37 °C under different conditions i.e., pH 7.4 and pH 5.5 and pH4.0 phosphate buffer solutions. The acidic (pH 4.0) medium was applied to simulate the acidic microenvironment of cancer cells. The cumulative percentage release of DOX from DOX-RA/PBNM is shown in Fig. 5.7, where pH-dependent doxorubicin release from DOX-RA Nanomicelles was observed. The DOX release at pH 7.4 occurred slowly in a sustained manner, with approximately 40% of DOX being released within 108 h. This indicates that if administered through IV, DOX-RA/PBNM could keep the drug in blood circulation for a long time.

Studies have revealed that the amount of drug released from the a carrier like nanomicelle is suppressed while in systemic circulation(157). However, in this study, the release profile in low pH media (pH 5.5 and pH 4.0) occurred relatively faster with time compared to that in pH 7.4. There was high doxorubicin release (60% and 80%) after 108 h in media conditions of pH 5.5 and pH 4.0, respectively. This may be due to the formation of cations of doxorubicin at acidic pH, which increased its hydrophilicity thus returning it to its original form (26).

These results indicate that DOX-RA complex can keep a large amount of DOX within the core of nanomicelles for a long time in the blood stream upon intravenous administration. The drug release in the PC-3 cells may have been enhanced by the low pH within the lysosomes of tumor cells or due to the acidic microenvironment inside the cellular endosomes while the cell uptake of nanomicelles occurred by endocytosis

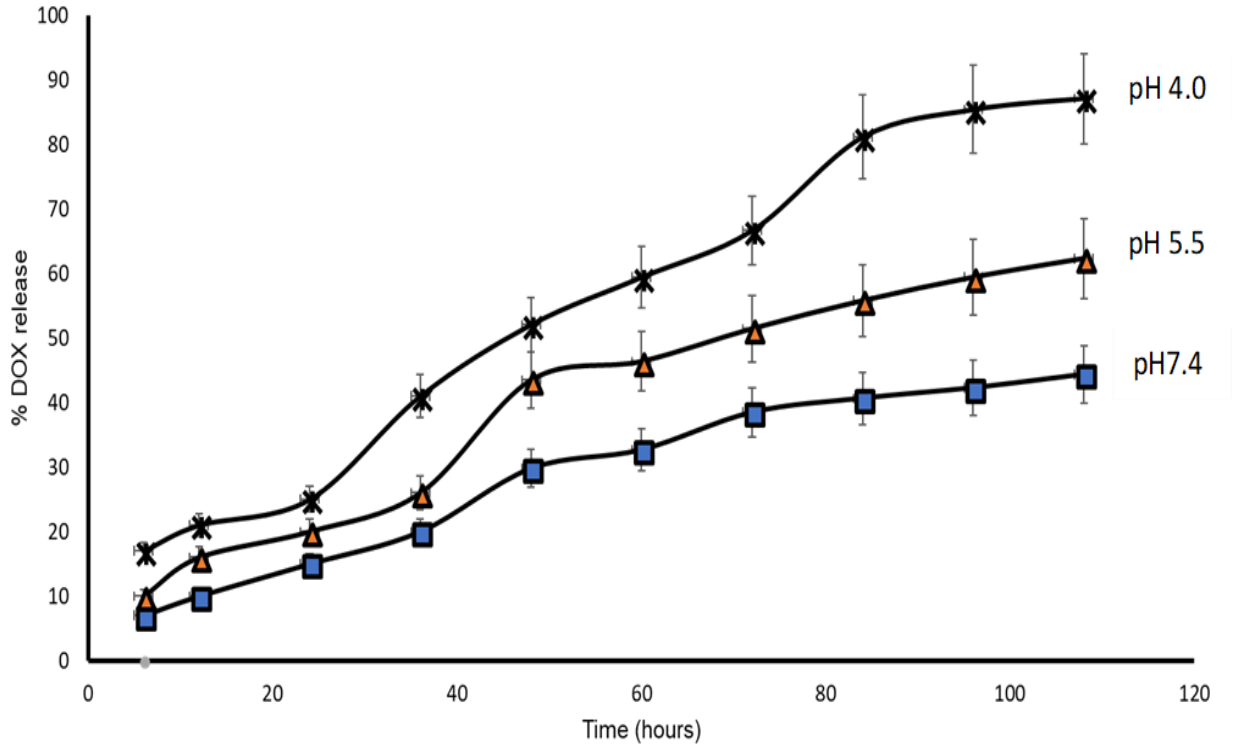

Figure 5. 7: In vitro release profiles of DOX from DOX-RA/PBNM in pH 7.4, pH 5.5 and pH 4.0 media at 37 ± 0.5 °C recorded as the mean ± SD (n = 3).

In Vitro Cell Uptake Studies of DOX-RA/PBNM

Cell uptake study was conducted to ascertain the presence of DOX inside the cells after exposure to the Nanomicelles. DOX-RA loaded pentablock nanomicellar formulation was incubated with Prostate cancer PC-3 cells for 12 h and 24 h under conducive conditions of 5% carbon dioxide, 37 ^{o}C (142). An appropriate media for the growth of the cells was used (142-144).

Cells were incubated in chamber slides with pentablock nanomicelles bearing DOX-RA complex (140, 141). The results of this study showed that there was a significant uptake of the nanomicelles into prostate cancer (PC-3) cells, with higher amount of drug entering the cells after 24 h compared to 12 h as shown in Fig.8 (145-147). In figure 8 B, brick-red DOX was observed with high intensity all over the cytoplasmic region including the nucleus. Therefore, it can be concluded that fluorescent DOX molecules are inside the cells. This indicates that nanomicelles were internalized by PC-3 cells.

This is an evidence that a large amount DOX was taken inside the cells with DOX-RA-PBNM and the release was maximum after 24 h (Fig.5. 8 B). The intensity of fluorescence is therefore directly proportional to the amount of DOX that enter the cells. Fig.5. 8 shows a confocal image of PC-3 cells observed after incubation with DOX-RA/PBNM for 12 h and 24 h. The fluorescence intensity within cells treated with DOX-RA/PBNM for 24 h was higher than that of cells treated for 12 h.

Fluorescence is very explicitly visible all over the cytoplasmic region after 24 h incubation. The cell uptake amount of DOX-RA/PBNM increased with time in PC-3 cells. After cell uptake, the nanomicelles could be degraded by lysosomal enzymes

and other related factors within the cells, resulting in their structural disruption and subsequent release of doxorubicin DOX inside the cytoplasm. There was a significant amount of DOX-RA- loaded nanomicelles inside the cytoplasm ($p < 0.05$). This observation suggests that high uptake of the drug loaded DOX-RA-PBNM nanomicelles may have been due to endocytosis.

The uptake and distribution of DOX-RA/PBNM by PC-3 cells that was observed by confocal microscopy could be related to the anti-tumor efficacy of DOX. Since DOX itself is fluorescent, it could be applied to directly measure cell uptake without applying any fluorescent marker.

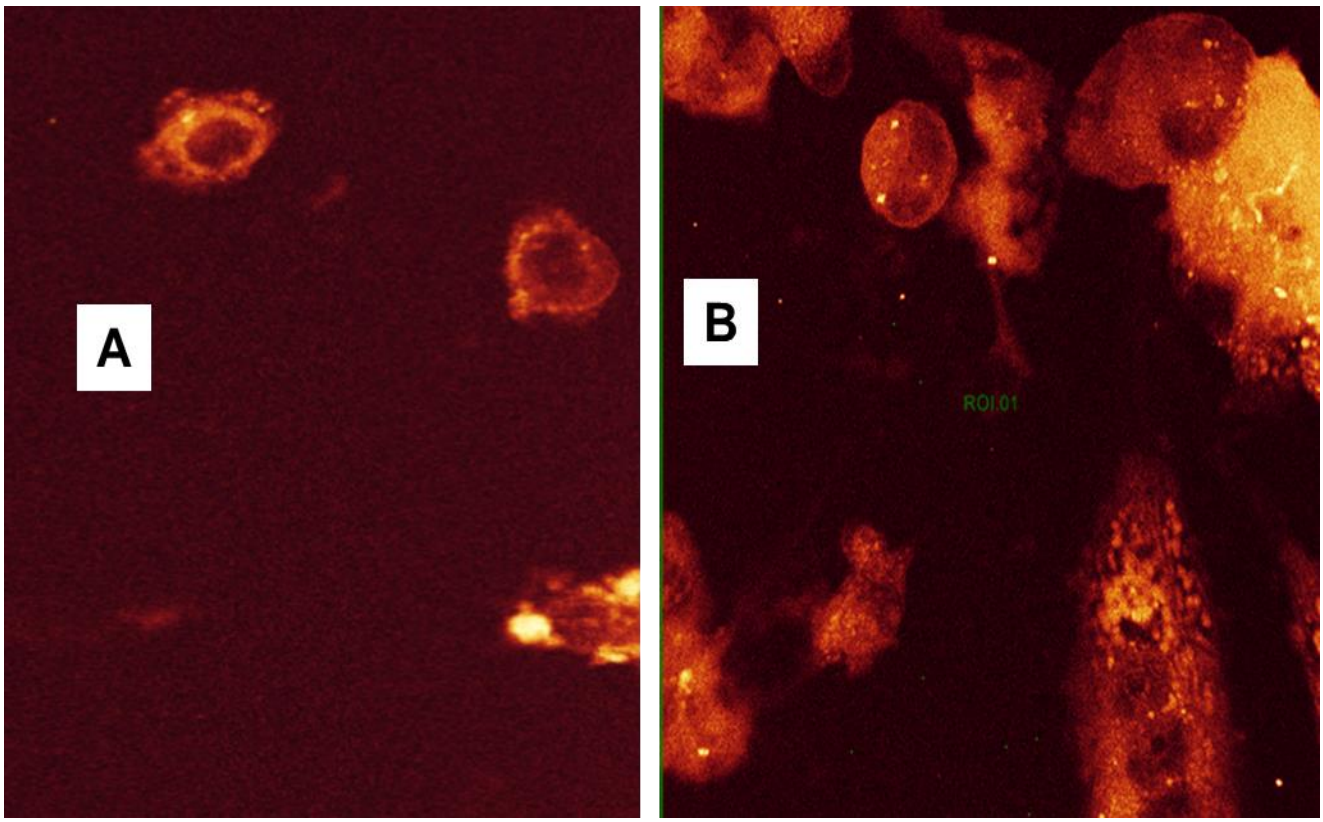

Figure 5. 8: Confocal images featuring the time dependent (A) 12 h and (B) 24 h) intracellular uptake of DOX-RA/PBNM by PC-3 cells.

In vitro Growth Inhibition Assay for DOX-RA-PBNM

Cytotoxicity of DOX-RA-PBNM was evaluated in PC-3 cells using a CyquantTM cell proliferation assay kit, which emits fluorescence due to interactions between DNA and a special dye in the assay. Percentage of cell growth inhibition was measured by fluorescence caused by DNA of surviving cells after 48 h incubation. Doxorubicin concentration in the DOX-RA-PBNM formulation was adjusted to the same as that of free drug. DOX-RA-PBNM formulation showed significant cytotoxic effect in PC-3 cells after 48 h incubation ($p < 0.05$).

It is worth noting that at 48 hours, the drug is not completely released from the nanomicelles (only 25%-40% released) as earlier depicted by the release profile. DOX-RA-PBNM nanomicelle formulation showed a significant difference in reduction of cell proliferation in PC-3 cells ($p < 0.05$).

Large amount of DOX from the DOX-RA-PBNM was delivered into PC-3 cells by endocytosis, causing high cytotoxic effect (123). Direct impact of efflux mechanism on doxorubicin inside the cells may have been reduced by loading drug into the core of the DOX-RA-PBNM. Furthermore, lodging of DOX-RA-PBNM into the core of pentablock nanomicelles strongly enhanced the cytotoxic effect probably due to more drug molecules being ferried into the cells. Sustained drug release within the cell and reduction of efflux may have played a great role on effectiveness of the delivery system. The survival of PC-3 cells after incubation with DOX-RA/PBNM for 24 h and 48 h. The DOX/RA-PBNM amounts were calculated based on the IC_{50} of doxorubicin which is 478±13nM (124)

The vulnerability of cancer cells to the treatment regimen is related to the doxorubicin concentration. After 48 h, it was observed the cell survival decreased with the increase in drug concentration. The cytotoxicity of DOX was almost the same as that of DOX-RA/PBNM at 24 h time point. However, depending on the increase in concentration of DOX-RA/PBNM, cytotoxicity continuously increased to a level much greater than that of pure doxorubicin, perhaps as a result of the delayed release of doxorubicin from pentablock nanomicelles (Fig 5.9).

In general terms, long-term treatment with a drug where concentration gradually increases is much safer than an abrupt supply of high drug level (158). This study demonstrates that delivery systems such as DOX-RA/PBNM may lower cytotoxicity or side effects caused by chemotherapy involving doxorubicin (28, 158).

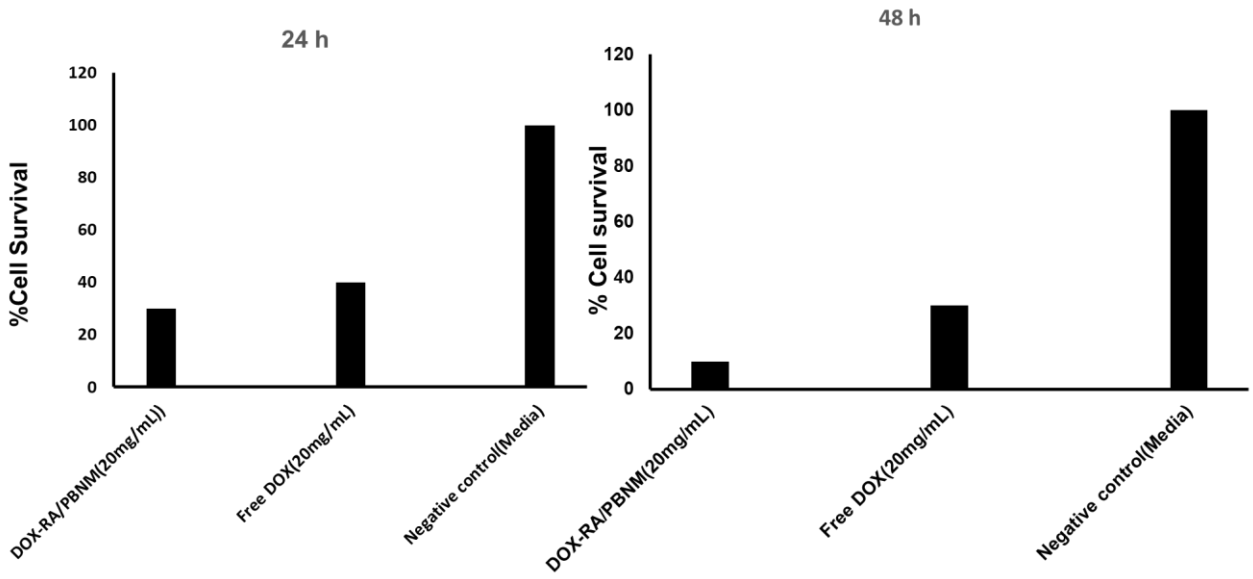

Figure 5. 9: The cell proliferation assay graphs showing %Cell survival after treatment of PC-3 cells for 24 h and 48 h.

Conclusion

Stable DOX-RA/PBNM with mean diameters of 30nm ±5.0 nm were obtained. The release of doxorubicin from nanomicelles at pH 7.4 occurred slower, with approximately 40% of the total drug content being released within 108 h. This proved an adequate stability of doxorubicin in DOX-RA/PBNM at this pH, making it suitable for a long circulation period in an intravenous administration. DOX released much faster in acidic environments (pH 4.0) similar to that of tumors, allowing tumor specific drug release.

FTIR and mass spectrometry analysis indicated that DOX and RA were present in the DOX-RA complex, which further confirmed the successful complex formation. The complex was perfectly lodged inside the nanomicelle core, which further reiterates that ion pairing of DOX with RA significantly raised the hydrophobicity of DOX. *In vitro* cell proliferation assay study showed that DOX-RA/PBNM had more toxicity compared with pure doxorubicin after 24 h as more drug molecules managed to enter the cells via the nanomicelles.

The results of the release profile indicated that DOX-RA/PBNM had a sustained release from the nanomicelles hence the retention of high concentration of DOX which maximized the anticancer effect. The cytoplasmic distribution clearly indicate that DOX-RA/PBNM was taken up all over the cytoplasm and that the uptaken amount of DOX-RA/PBNM increased with time (time-dependent). This technique can reduce the systemic cytotoxicity and side effects caused by DOX therapy.

CHAPTER 6

OVERALL SUMMARY

Development of formulation for long-term or sustained release of drugs used in the treatment of cancer, is a very difficult task for the pharmaceutical scientists. The ideal formulation for intravenous delivery is expected to possess the following characteristics, (a) high drug loading (b) provide constant release (zero-order release) throughout the release period without any burst effect, (c) easy to administer such as injectables (d) ensure stability of encapsulated drugs including protein/peptide, (e) biodegradable and biocompatible, and (f) easy biodegration process of the polymer upon complete drug release.

In order to achieve this goal, we have synthesized novel biodegradable and biocompatible PB copolymers. our PB copolymers are composed of various FDA approved polymeric blocks such as PEG, PCL, and PLA. Each block plays an important role such as presence of PEG helps to improve stability of nanomicelles by reducing aggregation, and also helps to promote solubility in aqueous environment resulting in homogenous clear aqueous solution.

PCL is a slow degrading semi-crystalline hydrophobic polymer which improves hydrophobic drug lodging in nanomicellar core and also sustains drug release for longer period of time.

It is important for formulation scientists to understand both polymer degradation profiles and the drug release profiles in order to prevent accumulation of drug and or formulation in body systems.

Covalent bonding of PLA to PCL chains can significantly reduce crystallinity resulting in faster degradation of the block coplymers after reaching the intended tissue or cells. PB copolymers were utilized to prepare nanomicelles which were then loaded with paclitaxel or doxorubicin in form of a hydrophobic complex.

The synthesized pentablock copolymers proved to be safe for cellular delivery as confirmed by cytotoxicity analysis and Tukey post Hoc test. The Pentablock copolymers drug-loaded nanomicelles were ideal for delivering drugs into cells in large quantity due to adequate sizes (20.98±5.00nm).

Cell analysis displayed an excellent uptake profile demonstrating that the nanomicelles facilitated the entry of more drug (coumarin 6) molecules into the cells. Release studies showed long term release profile, which can be significant in cancer chemotherapy. Cell proliferation assay showed a high effectiveness of this drug delivery system.

We further prepared PSMA conjugated pentablock nanomicelles and we were able to achieve drug-loaded nanomicelles of adequate sizes (45nm±2.5nm). The viscosity of the formulation was close to that of water, hence its suitability for application through IV route.

The cell uptake analysis conducted with the pentablock nanomicelles showed a significant uptake profile showing that the nanomicelles facilitated the entry of a great amount of drug (coumarin 6) into the cells. The release studies showed long time release, which can be significant in cancer chemotherapy. The cell proliferation assay showed a great effectiveness of the drug delivery system. The PSMA antibody

conjugation onto the surface of the paclitaxel loaded pentablock nanomicelle selectively delivered the drug to prostate cancer cells.

Furthermore, the pentablock supported a high temperature above 200^{o} C showing significant stability to thermal degradation.

In general, this method can be used for delivery of hydrophobic anticancer drugs like paclitaxel during cancer therapy to reduce side effects, frequency and dosage of the drug as administered to the patients currently.

We proceeded to produce pentablock nanomicelles using a hydrophobic HIP complex of doxorubicin, where stable DOX-RA/PBNM with mean diameters of 30nm ±5.0 nm were obtained. FTIR and mass spectrometry analysis indicated that DOX and RA were present in the DOX-RA complex, which further confirmed the successful complex formation. The release of doxorubicin from nanomicelles at pH 7.4 occurred slower, with approximately 40% of the total drug content being released within 108 h. This proved an adequate stability of doxorubicin in DOX-RA/PBNM in blood pH, making it suitable for a long circulation period in an intravenous administration. DOX released much faster in acidic environments (pH 4.0) similar to that of tumors, allowing tumor specific drug release. .

The complex was perfectly lodged inside the nanomicellar core, which further reiterates that ion pairing of DOX with RA significantly raised the hydrophobicity of DOX. *In vitro* cell proliferation assay study showed that DOX-RA/PBNM had more toxicity compared with pure doxorubicin after 24 h as more drug molecules managed to enter the cells via the nanomicelles.

The release profile indicated that DOX-RA/PBNM had a sustained release from the nanomicelles hence the retention of high concentration of DOX which maximized the anticancer effect. The cytoplasmic distribution clearly indicates that DOX-RA/PBNM was taken up all over the cytoplasm and that the uptaken amount of DOX-RA/PBNM increased with time (time-dependent).

This technique can reduce the systemic cytotoxicity and side effects caused by DOX therapy. In general, this method can be directed to delivery of hydrophobic anticancer drugs during in cancer therapy. This strategy may reduce side effects, diminish frequency and drug dosage. Additionally, these strategies are valuable for application in delivery of therapeutic drugs for treatment of various diseases apart from cancer therapy.

References

1. society Ac. prostate cancer prevalence. https://wwwcancerorg/cancer/prostate-cancer/about/key-statisticshtml. 2018.
2. Odedina FT, Akinremi TO, Chinegwundoh F, Roberts R, Yu D, Reams RR, et al. Prostate cancer disparities in Black men of African descent: a comparative literature review of prostate cancer burden among Black men in the United States, Caribbean, United Kingdom, and West Africa. Infect Agent Cancer. 2009;4 Suppl 1:S2.
3. Ward-Smith P. Brachytherapy for prostate cancer: the patient's perspective. Urol Nurs. 2003;23(3):213-7.
4. Chung PH, Gayed BA, Thoreson GR, Raj GV. Emerging drugs for prostate cancer. Expert Opin Emerg Drugs. 2013;18(4):533-50.
5. Akhtar MJ, Ahamed M, Alhadlaq HA, Alrokayan SA, Kumar S. Targeted anticancer therapy: overexpressed receptors and nanotechnology. Clinica chimica acta; international journal of clinical chemistry. 2014;436:78-92.
6. NIH. Prostate problems. https://wwwnianihgov/health/prostate-problems. 2016.
7. Lam HT, Le-Vinh B, Phan TNQ, Bernkop-Schnurch A. Self-emulsifying drug delivery systems and cationic surfactants: do they potentiate each other in cytotoxicity? J Pharm Pharmacol. 2018.
8. Rizvi SA, Shamsi SA. Polymeric alkenoxy amino acid surfactants: I. Highly selective class of molecular micelles for chiral separation of beta-blockers. Electrophoresis. 2003;24(15):2514-26.
9. Garcia Daza FA, Mackie AD. Low Critical Micelle Concentration Discrepancy between Theory and Experiment. The journal of physical chemistry letters. 2014;5(11):2027-32.
10. Schiff PB, Fant J, Horwitz SB. Promotion of microtubule assembly in vitro by taxol. Nature. 1979;277:665.
11. Singla AK, Garg A, Aggarwal D. Paclitaxel and its formulations. Int J Pharm. 2002;235(1-2):179-92.
12. Zhou J, Zhao WY, Ma X, Ju RJ, Li XY, Li N, et al. The anticancer efficacy of paclitaxel liposomes modified with mitochondrial targeting conjugate in resistant lung cancer. Biomaterials. 2013;34(14):3626-38.
13. He Y, Liang S, Long M, Xu H. Mesoporous silica nanoparticles as potential carriers for enhanced drug solubility of paclitaxel. Mater Sci Eng C Mater Biol Appl. 2017;78:12-7.
14. Zhou Y, Wen H, Gu L, Fu J, Guo J, Du L, et al. Aminoglucose-functionalized, redox-responsive polymer nanomicelles for overcoming chemoresistance in lung cancer cells. J Nanobiotechnology. 2017;15(1):87.
15. Creel CJ, Lovich MA, Edelman ER. Arterial paclitaxel distribution and deposition. Circ Res. 2000;86(8):879-84.
16. Vadlapudi AD, Cholkar K, Vadlapatla RK, Mitra AK. Aqueous nanomicellar formulation for topical delivery of biotinylated lipid prodrug of acyclovir: formulation development and ocular biocompatibility. Journal of ocular pharmacology and therapeutics : the official journal of the Association for Ocular Pharmacology and Therapeutics. 2014;30(1):49-58.
17. Vaishya RD, Khurana V, Patel S, Mitra AK. Controlled ocular drug delivery with nanomicelles. Wiley interdisciplinary reviews Nanomedicine and nanobiotechnology. 2014;6(5):422-37.
18. Yang X, Trinh HM, Agrahari V, Sheng Y, Pal D, Mitra AK. Nanoparticle-Based Topical Ophthalmic Gel Formulation for Sustained Release of Hydrocortisone Butyrate. AAPS PharmSciTech. 2016;17(2):294-306.
19. H.B. Bohidar a b MBb. Characterization of reverse micelles by dynamic light scattering Colloids and Surfaces

2001; (178):313–23.
20. Chatzidaki MD, Papavasileiou KD, Papadopoulos MG, Xenakis A. Reverse Micelles As Antioxidant Carriers: An Experimental and Molecular Dynamics Study. Langmuir. 2017;33(20):5077-85.
21. Patel KJ, Tredan O, Tannock IF. Distribution of the anticancer drugs doxorubicin, mitoxantrone and topotecan in tumors and normal tissues. Cancer Chemother Pharmacol. 2013;72(1):127-38.
22. Luo JW, Zhang ZR, Gong T, Fu Y. One-step self-assembled nanomicelles for improving the oral bioavailability of nimodipine. Int J Nanomedicine. 2016;11:1051-65.
23. Primeau AJ, Rendon A, Hedley D, Lilge L, Tannock IF. The distribution of the anticancer drug Doxorubicin in relation to blood vessels in solid tumors. Clin Cancer Res. 2005;11(24 Pt 1):8782-8.
24. van Asperen J, van Tellingen O, Tijssen F, Schinkel AH, Beijnen JH. Increased accumulation of doxorubicin and doxorubicinol in cardiac tissue of mice lacking mdr1a P-glycoprotein. Br J Cancer. 1999;79(1):108-13.
25. Min K, Kwon OS, Smuder AJ, Wiggs MP, Sollanek KJ, Christou DD, et al. Increased mitochondrial emission of reactive oxygen species and calpain activation are required for doxorubicin-induced cardiac and skeletal muscle myopathy. J Physiol. 2015;593(8):2017-36.
26. Zhao S, Minh LV, Li N, Garamus VM, Handge UA, Liu J, et al. Doxorubicin hydrochloride-oleic acid conjugate loaded nanostructured lipid carriers for tumor specific drug release. Colloids Surf B Biointerfaces. 2016;145:95-103.
27. Wei WH, Dong XM, Liu CG. In vitro investigation of self-assembled nanoparticles based on hyaluronic acid-deoxycholic acid conjugates for controlled release doxorubicin: effect of degree of substitution of deoxycholic acid. Int J Mol Sci. 2015;16(4):7195-209.
28. Luk BT, Fang RH, Zhang L. Lipid- and polymer-based nanostructures for cancer theranostics. Theranostics. 2012;2(12):1117-26.
29. Andresen TL, Jensen SS, Jorgensen K. Advanced strategies in liposomal cancer therapy: problems and prospects of active and tumor specific drug release. Prog Lipid Res. 2005;44(1):68-97.
30. Yatvin MB, Kreutz W, Horwitz BA, Shinitzky M. pH-sensitive liposomes: possible clinical implications. Science. 1980;210(4475):1253-5.
31. Cholkar K, Gunda S, Earla R, Pal D, Mitra AK. Nanomicellar Topical Aqueous Drop Formulation of Rapamycin for Back-of-the-Eye Delivery. AAPS PharmSciTech. 2015;16(3):610-22.
32. Cholkar K, Hariharan S, Gunda S, Mitra AK. Optimization of dexamethasone mixed nanomicellar formulation. AAPS PharmSciTech. 2014;15(6):1454-67.
33. Mehnert W, Mader K. Solid lipid nanoparticles: production, characterization and applications. Adv Drug Deliv Rev. 2001;47(2-3):165-96.
34. Maia CS, Mehnert W, Schafer-Korting M. Solid lipid nanoparticles as drug carriers for topical glucocorticoids. Int J Pharm. 2000;196(2):165-7.
35. zur Muhlen A, Schwarz C, Mehnert W. Solid lipid nanoparticles (SLN) for controlled drug delivery--drug release and release mechanism. Eur J Pharm Biopharm. 1998;45(2):149-55.
36. Schwarz C, Mehnert W. Solid lipid nanoparticles (SLN) for controlled drug delivery. II. Drug incorporation and physicochemical characterization. J Microencapsul. 1999;16(2):205-13.
37. Jores K, Haberland A, Wartewig S, Mader K, Mehnert W. Solid lipid nanoparticles (SLN) and oil-loaded SLN studied by spectrofluorometry and Raman spectroscopy. Pharm Res. 2005;22(11):1887-97.
38. Society AC. Prostate Cancer updates. https://wwwcancerorg/cancer/prostate-cancer/about/what-is-prostate-cancerhtml. 2016.
39. Gucalp A, Iyengar NM, Zhou XK, Giri DD, Falcone DJ, Wang H, et al. Periprostatic adipose inflammation is associated with high-grade prostate cancer. Prostate cancer and prostatic diseases. 2017;20(4):418-23.

40. Singapore Urological Association Male Lower Urinary Tract Symptoms/Benign Prostatic Hyperplasia Guidelines C. Singapore Urological Association Clinical Guidelines for Male Lower Urinary Tract Symptoms/Benign Prostatic Hyperplasia. Singapore Med J. 2017;58(8):473-80.
41. Tonon L, Fromont G, Boyault S, Thomas E, Ferrari A, Sertier AS, et al. Mutational Profile of Aggressive, Localised Prostate Cancer from African Caribbean Men Versus European Ancestry Men. Eur Urol. 2018.
42. Emeville E, Giusti A, Coumoul X, Thome JP, Blanchet P, Multigner L. Associations of plasma concentrations of dichlorodiphenyldichloroethylene and polychlorinated biphenyls with prostate cancer: a case-control study in Guadeloupe (French West Indies). Environ Health Perspect. 2015;123(4):317-23.
43. Mohler JL, Kantoff PW, Armstrong AJ, Bahnson RR, Cohen M, D'Amico AV, et al. Prostate cancer, version 2.2014. Journal of the National Comprehensive Cancer Network : JNCCN. 2014;12(5):686-718.
44. Li H, Jin H, Wan W, Wu C, Wei L. Cancer nanomedicine: mechanisms, obstacles and strategies. Nanomedicine. 2018:1639-56.
45. Luo Z, Tian H, Liu L, Chen Z, Liang R, Chen Z, et al. Tumor-targeted hybrid protein oxygen carrier to simultaneously enhance hypoxia-dampened chemotherapy and photodynamic therapy at a single dose. Theranostics. 2018;8(13):3584-96.
46. Oroojalian F, Babaei M, Taghdisi SM, Abnous K, Ramezani M, Alibolandi M. Encapsulation of Thermo-responsive Gel in pH-sensitive Polymersomes as Dual-Responsive Smart carriers for Controlled Release of Doxorubicin. Journal of controlled release : official journal of the Controlled Release Society. 2018.
47. Parks SK, Chiche J, Pouyssegur J. pH control mechanisms of tumor survival and growth. J Cell Physiol. 2011;226(2):299-308.
48. Gerweck LE, Vijayappa S, Kurimasa A, Ogawa K, Chen DJ. Tumor cell radiosensitivity is a major determinant of tumor response to radiation. Cancer research. 2006;66(17):8352-5.
49. Sercombe L, Veerati T, Moheimani F, Wu SY, Sood AK, Hua S. Advances and Challenges of Liposome Assisted Drug Delivery. Frontiers in pharmacology. 2015;6:286.
50. Akbarzadeh A, Rezaei-Sadabady R, Davaran S, Joo SW, Zarghami N, Hanifehpour Y, et al. Liposome: classification, preparation, and applications. Nanoscale research letters. 2013;8(1):102.
51. Salvati E, Re F, Sesana S, Cambianica I, Sancini G, Masserini M, et al. Liposomes functionalized to overcome the blood-brain barrier and to target amyloid-beta peptide: the chemical design affects the permeability across an in vitro model. Int J Nanomedicine. 2013;8:1749-58.
52. Hatzifoti C, Bacon A, Marriott H, Laing P, Heath AW. Liposomal co-entrapment of CD40mAb induces enhanced IgG responses against bacterial polysaccharide and protein. PLoS One. 2008;3(6):e2368.
53. Mitra AK, Agrahari V, Mandal A, Cholkar K, Natarajan C, Shah S, et al. Novel delivery approaches for cancer therapeutics. Journal of controlled release : official journal of the Controlled Release Society. 2015;219:248-68.
54. Mitra R, Pezron I, Chu WA, Mitra AK. Lipid emulsions as vehicles for enhanced nasal delivery of insulin. Int J Pharm. 2000;205(1-2):127-34.
55. Zhang X, Sun X, Li J, Zhang X, Gong T, Zhang Z. Lipid nanoemulsions loaded with doxorubicin-oleic acid ionic complex: characterization, in vitro and in vivo studies. Die Pharmazie. 2011;66(7):496-505.
56. Cholkar K, Patel A, Vadlapudi AD, Mitra AK. Novel Nanomicellar Formulation Approaches for Anterior and Posterior Segment Ocular Drug Delivery. Recent patents on nanomedicine. 2012;2(2):82-95.

57. Cholkar K, Patel SP, Vadlapudi AD, Mitra AK. Novel strategies for anterior segment ocular drug delivery. Journal of ocular pharmacology and therapeutics : the official journal of the Association for Ocular Pharmacology and Therapeutics. 2013;29(2):106-23.
58. Macha S, Mitra AK. Ocular disposition of ganciclovir and its monoester prodrugs following intravitreal administration using microdialysis. Drug metabolism and disposition: the biological fate of chemicals. 2002;30(6):670-5.
59. Macha S, Duvvuri S, Mitra AK. Ocular disposition of novel lipophilic diester prodrugs of ganciclovir following intravitreal administration using microdialysis. Current eye research. 2004;28(2):77-84.
60. Gaudana R, Ananthula HK, Parenky A, Mitra AK. Ocular drug delivery. The AAPS journal. 2010;12(3):348-60.
61. Patel A, Cholkar K, Agrahari V, Mitra AK. Ocular drug delivery systems: An overview. World journal of pharmacology. 2013;2(2):47-64.
62. Boddu SH, Gunda S, Earla R, Mitra AK. Ocular microdialysis: a continuous sampling technique to study pharmacokinetics and pharmacodynamics in the eye. Bioanalysis. 2010;2(3):487-507.
63. Katragadda S, Gunda S, Hariharan S, Mitra AK. Ocular pharmacokinetics of acyclovir amino acid ester prodrugs in the anterior chamber: evaluation of their utility in treating ocular HSV infections. Int J Pharm. 2008;359(1-2):15-24.
64. Swain S, Sahu PK, Beg S, Babu SM. Nanoparticles for Cancer Targeting: Current and Future Directions. Curr Drug Deliv. 2016;13(8):1290-302.
65. Yang X, Shah SJ, Wang Z, Agrahari V, Pal D, Mitra AK. Nanoparticle-based topical ophthalmic formulation for sustained release of stereoisomeric dipeptide prodrugs of ganciclovir. Drug delivery. 2016;23(7):2399-409.
66. Pignatello R, Ricupero N, Bucolo C, Maugeri F, Maltese A, Puglisi G. Preparation and characterization of Eudragit Retard nanosuspensions for the ocular delivery of cloricromene. AAPS PharmSciTech. 2006;7(1):E192-E8.
67. Pignatello R, Ricupero N, Bucolo C, Maugeri F, Maltese A, Puglisi G. Preparation and characterization of eudragit retard nanosuspensions for the ocular delivery of cloricromene. AAPS PharmSciTech. 2006;7(1):E27.
68. Jang CH, Park H, Cho YB, Choi CH, Park IY. The use of piperacillin-tazobactam coated tympanostomy tubes against ciprofloxacin-resistant Pseudomonas biofilm formation: an in vitro study. Int J Pediatr Otorhinolaryngol. 2009;73(2):295-9.
69. Marella S, Tollamadugu N. Nanotechnological approaches for the development of herbal drugs in treatment of diabetes mellitus - a critical review. IET Nanobiotechnol. 2018;12(5):549-56.
70. Field LD, Nag OK, Sangtani A, Burns KE, Delehanty JB. The role of nanoparticles in the improvement of systemic anticancer drug delivery. Ther Deliv. 2018;9(7):527-45.
71. Rao NV, Ko H, Lee J, Park JH. Recent Progress and Advances in Stimuli-Responsive Polymers for Cancer Therapy. Front Bioeng Biotechnol. 2018;6:110.
72. Maxa J, Dittrich M. [Use of synthetic biodegradable polymers in medicine]. Ceska Slov Farm. 2001;50(1):28-34.
73. Taghizadeh B, Taranejoo S, Monemian SA, Salehi Moghaddam Z, Daliri K, Derakhshankhah H, et al. Classification of stimuli-responsive polymers as anticancer drug delivery systems. Drug delivery. 2015;22(2):145-55.
74. Wischke C, Schneider C, Neffe AT, Lendlein A. Polyalkylcyanoacrylates as in situ formed diffusion barriers in multimaterial drug carriers. Journal of controlled release : official journal of the Controlled Release Society. 2013;169(3):321-8.

75. Fox A, Rogers JC, Gilbart J, Morgan S, Davis CH, Knight S, et al. Muramic acid is not detectable in Chlamydia psittaci or Chlamydia trachomatis by gas chromatography-mass spectrometry. Infect Immun. 1990;58(3):835-7.
76. Lucio D, Martinez-Oharriz MC, Gonzalez-Navarro CJ, Navarro-Herrera D, Gonzalez-Gaitano G, Radulescu A, et al. Coencapsulation of cyclodextrins into poly(anhydride) nanoparticles to improve the oral administration of glibenclamide. A screening on C. elegans. Colloids Surf B Biointerfaces. 2018;163:64-72.
77. Chmielowski RA, Abdelhamid DS, Faig JJ, Petersen LK, Gardner CR, Uhrich KE, et al. Athero-inflammatory nanotherapeutics: Ferulic acid-based poly(anhydride-ester) nanoparticles attenuate foam cell formation by regulating macrophage lipogenesis and reactive oxygen species generation. Acta Biomater. 2017;57:85-94.
78. Brenza TM, Ghaisas S, Ramirez JEV, Harischandra D, Anantharam V, Kalyanaraman B, et al. Neuronal protection against oxidative insult by polyanhydride nanoparticle-based mitochondria-targeted antioxidant therapy. Nanomedicine. 2017;13(3):809-20.
79. Gunatillake P, Mayadunne R, Adhikari R. Recent developments in biodegradable synthetic polymers. Biotechnol Annu Rev. 2006;12:301-47.
80. Mhlanga N, Sinha Ray S, Lemmer Y, Wesley-Smith J. Polylactide-based Magnetic Spheres as Efficient Carriers for Anticancer Drug Delivery. ACS applied materials & interfaces. 2015;7(40):22692-701.
81. Patel SP, Vaishya R, Pal D, Mitra AK. Novel pentablock copolymer-based nanoparticulate systems for sustained protein delivery. AAPS PharmSciTech. 2015;16(2):327-43.
82. Horakova J, Mikes P, Saman A, Jencova V, Klapstova A, Svarcova T, et al. The effect of ethylene oxide sterilization on electrospun vascular grafts made from biodegradable polyesters. Mater Sci Eng C Mater Biol Appl. 2018;92:132-42.
83. Brannigan RP, Dove AP. Synthesis, properties and biomedical applications of hydrolytically degradable materials based on aliphatic polyesters and polycarbonates. Biomater Sci. 2016;5(1):9-21.
84. Patel SP, Vaishya R, Patel A, Agrahari V, Pal D, Mitra AK. Optimization of novel pentablock copolymer based composite formulation for sustained delivery of peptide/protein in the treatment of ocular diseases. J Microencapsul. 2016;33(2):103-13.
85. Patel SP, Vaishya R, Yang X, Pal D, Mitra AK. Novel thermosensitive pentablock copolymers for sustained delivery of proteins in the treatment of posterior segment diseases. Protein and peptide letters. 2014;21(11):1185-200.
86. Patel SP, Vaishya R, Mishra GP, Tamboli V, Pal D, Mitra AK. Tailor-made pentablock copolymer based formulation for sustained ocular delivery of protein therapeutics. Journal of drug delivery. 2014;2014:401747.
87. Schnoor B, Elhendawy A, Joseph S, Putman M, Chacon-Cerdas R, Flores-Mora D, et al. Engineering Atrazine Loaded Poly (lactic- co-glycolic Acid) Nanoparticles to Ameliorate Environmental Challenges. J Agric Food Chem. 2018;66(30):7889-98.
88. Fatkhudinov T, Tsedik L, Arutyunyan I, Lokhonina A, Makarov A, Korshunov A, et al. Evaluation of resorbable polydioxanone and polyglycolic acid meshes in a rat model of ventral hernia repair. J Biomed Mater Res B Appl Biomater. 2018.
89. Kang Y, Lee E, Lee JW, Kim SR, Kang MJ, Choi YW, et al. Effect of Poly(Lactide-Co-Glycolide) Nanoparticles on Local Retention of Fluorescent Material: An Experimental Study in Mice. Korean J Radiol. 2018;19(5):950-6.
90. Pesoa JI, Rico MJ, Rozados VR, Scharovsky OG, Luna JA, Mengatto LN. Paclitaxel delivery system based on poly(lactide-co-glycolide) microparticles and chitosan thermo-sensitive gel for mammary adenocarcinoma treatment. J Pharm Pharmacol. 2018.

91. Yuan Z, Qu X, Wang Y, Zhang DY, Luo JC, Jia N, et al. Retraction notice to "Enhanced Antitumor Efficacy of 5-Fluorouracil loaded Methoxy Poly(ethylene glycol)- Poly(lactide) Nanoparticles for Efficient Therapy against Breast cancer" Colloids and Surfaces B: Biointerfaces 128 (2015) 489-497. Colloids Surf B Biointerfaces. 2018;170:737.
92. Martinez-Perez B, Quintanar-Guerrero D, Tapia-Tapia M, Cisneros-Tamayo R, Zambrano-Zaragoza ML, Alcala-Alcala S, et al. Controlled-release biodegradable nanoparticles: From preparation to vaginal applications. Eur J Pharm Sci. 2018;115:185-95.
93. Mura S, Hillaireau H, Nicolas J, Le Droumaguet B, Gueutin C, Zanna S, et al. Influence of surface charge on the potential toxicity of PLGA nanoparticles towards Calu-3 cells. Int J Nanomedicine. 2011;6:2591-605.
94. Tang R, Palumbo RN, Ji W, Wang C. Poly(ortho ester amides): acid-labile temperature-responsive copolymers for potential biomedical applications. Biomacromolecules. 2009;10(4):722-7.
95. Heller J, Barr J, Ng SY, Abdellauoi KS, Gurny R. Poly(ortho esters): synthesis, characterization, properties and uses. Adv Drug Deliv Rev. 2002;54(7):1015-39.
96. Pool R, Bolhuis PG. Accurate free energies of micelle formation. J Phys Chem B. 2005;109(14):6650-7.
97. Tamboli V, Mishra GP, Mitra AK. Novel pentablock copolymer (PLA-PCL-PEG-PCL-PLA) based nanoparticles for controlled drug delivery: Effect of copolymer compositions on the crystallinity of copolymers and in vitro drug release profile from nanoparticles. Colloid and polymer science. 2013;291(5):1235-45.
98. Agrahari V, Agrahari V, Mandal A, Pal D, Mitra AK. How are we improving the delivery to back of the eye? Advances and challenges of novel therapeutic approaches. Expert opinion on drug delivery. 2017;14(10):1145-62.
99. Kabanov AV, Batrakova EV, Alakhov VY. Pluronic block copolymers as novel polymer therapeutics for drug and gene delivery. Journal of controlled release : official journal of the Controlled Release Society. 2002;82(2-3):189-212.
100. Bobbala S, Tamboli V, McDowell A, Mitra AK, Hook S. Novel Injectable Pentablock Copolymer Based Thermoresponsive Hydrogels for Sustained Release Vaccines. The AAPS journal. 2016;18(1):261-9.
101. Vaishya RD, Gokulgandhi M, Patel S, Minocha M, Mitra AK. Novel dexamethasone-loaded nanomicelles for the intermediate and posterior segment uveitis. AAPS PharmSciTech. 2014;15(5):1238-51.
102. Youm I, Agrahari V, Murowchick JB, Youan BB. Uptake and cytotoxicity of docetaxel-loaded hyaluronic acid-grafted oily core nanocapsules in MDA-MB 231 cancer cells. Pharm Res. 2014;31(9):2439-52.
103. Wei Z, Hao J, Yuan S, Li Y, Juan W, Sha X, et al. Paclitaxel-loaded Pluronic P123/F127 mixed polymeric micelles: formulation, optimization and in vitro characterization. Int J Pharm. 2009;376(1-2):176-85.
104. Xia D, Lai DV, Wu W, Webb ZD, Yang Q, Zhao L, et al. Transition from androgenic to neurosteroidal action of 5alpha-androstane-3alpha, 17beta-diol through the type A gamma-aminobutyric acid receptor in prostate cancer progression. J Steroid Biochem Mol Biol. 2017.
105. Abdelwahed W, Degobert G, Stainmesse S, Fessi H. Freeze-drying of nanoparticles: formulation, process and storage considerations. Adv Drug Deliv Rev. 2006;58(15):1688-713.
106. Youm I, Yang XY, Murowchick JB, Youan BB. Encapsulation of docetaxel in oily core polyester nanocapsules intended for breast cancer therapy. Nanoscale research letters. 2011;6(1):630.
107. Youm I, Murowchick JB, Youan BB. Entrapment and release kinetics of furosemide from pegylated nanocarriers. Colloids Surf B Biointerfaces. 2012;94:133-42.

108. Youm I, Youan BB. Uptake mechanism of furosemide-loaded pegylated nanoparticles by cochlear cell lines. Hear Res. 2013;304:7-19.
109. Agrahari V, Li G, Agrahari V, Navarro I, Perkumas K, Mandal A, et al. Pentablock copolymer dexamethasone nanoformulations elevate MYOC: in vitro liberation, activity and safety in human trabecular meshwork cells. Nanomedicine. 2017;12(16):1911-26.
110. Agrahari V, Agrahari V, Mitra AK. Nanocarrier fabrication and macromolecule drug delivery: challenges and opportunities. Ther Deliv. 2016;7(4):257-78.
111. Sawdon AJ, Peng CA. Polymeric micelles for acyclovir drug delivery. Colloids Surf B Biointerfaces. 2014;122:738-45.
112. Lian H, He Z, Meng Z. Rational design of hybrid nanomicelles integrating mucosal penetration and P-glycoprotein inhibition for efficient oral delivery of paclitaxel. Colloids Surf B Biointerfaces. 2017;155:429-39.
113. Jones LJ, Gray M, Yue ST, Haugland RP, Singer VL. Sensitive determination of cell number using the CyQUANT (R) cell proliferation assay. J Immunol Methods. 2001;254(1-2):85-98.
114. Hoque ME, Hutmacher DW, Feng W, Li S, Huang MH, Vert M, et al. Fabrication using a rapid prototyping system and in vitro characterization of PEG-PCL-PLA scaffolds for tissue engineering. Journal of biomaterials science Polymer edition. 2005;16(12):1595-610.
115. Bosca S, Barresi AA, Fissore D. Fast freeze-drying cycle design and optimization using a PAT based on the measurement of product temperature. Eur J Pharm Biopharm. 2013;85(2):253-62.
116. Abdelwahed W, Degobert G, Fessi H. Investigation of nanocapsules stabilization by amorphous excipients during freeze-drying and storage. Eur J Pharm Biopharm. 2006;63(2):87-94.
117. Abdelwahed W, Degobert G, Fessi H. A pilot study of freeze drying of poly(epsilon-caprolactone) nanocapsules stabilized by poly(vinyl alcohol): formulation and process optimization. Int J Pharm. 2006;309(1-2):178-88.
118. Kataoka K, Matsumoto T, Yokoyama M, Okano T, Sakurai Y, Fukushima S, et al. Doxorubicin-loaded poly(ethylene glycol)-poly(beta-benzyl-L-aspartate) copolymer micelles: their pharmaceutical characteristics and biological significance. Journal of controlled release : official journal of the Controlled Release Society. 2000;64(1-3):143-53.
119. Qiu LY, Bae YH. Self-assembled polyethylenimine-graft-poly(epsilon-caprolactone) micelles as potential dual carriers of genes and anticancer drugs. Biomaterials. 2007;28(28):4132-42.
120. Fernandes HP, Cesar CL, Barjas-Castro Mde L. Electrical properties of the red blood cell membrane and immunohematological investigation. Rev Bras Hematol Hemoter. 2011;33(4):297-301.
121. Yashwant Pathak DT. Drug Delivery Nanoparticles Formulation and Characterization. In: Yashwant p DT, editor. 1912009. p. 80-3.
122. Katragadda S, Budda B, Anand BS, Mitra AK. Role of efflux pumps and metabolising enzymes in drug delivery. Expert opinion on drug delivery. 2005;2(4):683-705.
123. Yoo HS, Park TG. Biodegradable polymeric micelles composed of doxorubicin conjugated PLGA-PEG block copolymer. Journal of controlled release : official journal of the Controlled Release Society. 2001;70(1-2):63-70.
124. Vadlapatla RK PD, Vadlapudi AD Mitra AK Ritonavir: A Powerful Boosting Agent for Overcoming Drug Resistance in Cancer Chemotherapy. J Cancer Sci Ther. 2014; 6:446-54.
125. Zheng L, Chen S, Cao Y, Zhao L, Gao Y, Ding X, et al. Combination of comprehensive two-dimensional prostate cancer cell membrane chromatographic system and network pharmacology for characterizing membrane binding active components from Radix et Rhizoma Rhei and their targets. J Chromatogr A. 2018.
126. Trivedi R, Kompella UB. Nanomicellar formulations for sustained drug delivery: strategies and underlying principles. Nanomedicine. 2010;5(3):485-505.

127. Chen Y, Su N, Zhang K, Zhu S, Zhao L, Fang F, et al. In-Depth Analysis of the Structure and Properties of Two Varieties of Natural Luffa Sponge Fibers. Materials. 2017;10(5).
128. Reddy KO, Maheswari CU, Dhlamini MS, Mothudi BM, Kommula VP, Zhang J, et al. Extraction and characterization of cellulose single fibers from native african napier grass. Carbohydrate polymers. 2018;188:85-91.
129. Ogieglo W, Tempelman K, Napolitano S, Benes NE. Evidence of a Transition Layer between the Free Surface and the Bulk. The journal of physical chemistry letters. 2018;9(6):1195-9.
130. Jia C, Li Y, Zhang S, Fei T, Pang S. Thermogravimetric analysis, kinetic study, and pyrolysis-GC/MS analysis of 1,1'-azobis-1,2,3-triazole and 4,4'-azobis-1,2,4-triazole. Chemistry Central journal. 2018;12(1):22.
131. Laidler P, Dulinska J, Lekka M, Lekki J. Expression of prostate specific membrane antigen in androgen-independent prostate cancer cell line PC-3. Arch Biochem Biophys. 2005;435(1):1-14.
132. Pienta KJ, Isaacs WB, Vindivich D, Coffey DS. The effects of basic fibroblast growth factor and suramin on cell motility and growth of rat prostate cancer cells. The Journal of urology. 1991;145(1):199-202.
133. Sherwood ER, Fong CJ, Lee C, Kozlowski JM. Basic fibroblast growth factor: a potential mediator of stromal growth in the human prostate. Endocrinology. 1992;130(5):2955-63.
134. Ihms EC, Brinkman DW. Thermogravimetric analysis as a polymer identification technique in forensic applications. Journal of forensic sciences. 2004;49(3):505-10.
135. Basu S, Harfouche R, Soni S, Chimote G, Mashelkar RA, Sengupta S. Nanoparticle-mediated targeting of MAPK signaling predisposes tumor to chemotherapy. Proceedings of the National Academy of Sciences of the United States of America. 2009;106(19):7957-61.
136. Zhang JX, Qiu LY, Jin Y, Zhu KJ. Thermally responsive polymeric micelles self-assembled by amphiphilic polyphosphazene with poly(N-isopropylacrylamide) and ethyl glycinate as side groups: polymer synthesis, characterization, and in vitro drug release study. Journal of biomedical materials research Part A. 2006;76(4):773-80.
137. Kasten BB, Liu T, Nedrow-Byers JR, Benny PD, Berkman CE. Targeting prostate cancer cells with PSMA inhibitor-guided gold nanoparticles. Bioorg Med Chem Lett. 2013;23(2):565-8.
138. Murphy GP, Snow P, Simmons SJ, Tjoa BA, Rogers MK, Brandt J, et al. Use of artificial neural networks in evaluating prognostic factors determining the response to dendritic cells pulsed with PSMA peptides in prostate cancer patients. Prostate. 2000;42(1):67-72.
139. Zuccolotto G, Fracasso G, Merlo A, Montagner IM, Rondina M, Bobisse S, et al. PSMA-specific CAR-engineered T cells eradicate disseminated prostate cancer in preclinical models. PLoS One. 2014;9(10):e109427.
140. Jin J, Sui B, Gou J, Liu J, Tang X, Xu H, et al. PSMA ligand conjugated PCL-PEG polymeric micelles targeted to prostate cancer cells. PLoS One. 2014;9(11):e112200.
141. Patil Y, Shmeeda H, Amitay Y, Ohana P, Kumar S, Gabizon A. Targeting of folate-conjugated liposomes with co-entrapped drugs to prostate cancer cells via prostate-specific membrane antigen (PSMA). Nanomedicine. 2018.
142. Zhao Y, Duan S, Zeng X, Liu C, Davies NM, Li B, et al. Prodrug strategy for PSMA-targeted delivery of TGX-221 to prostate cancer cells. Molecular pharmaceutics. 2012;9(6):1705-16.
143. Pearce AK, Simpson JD, Fletcher NL, Houston ZH, Fuchs AV, Russell PJ, et al. Localised delivery of doxorubicin to prostate cancer cells through a PSMA-targeted hyperbranched polymer theranostic. Biomaterials. 2017;141:330-9.
144. Ben Jemaa A, Sallami S, Ceraline J, Oueslati R. A novel regulation of PSMA and PSA expression by Q640X AR in 22Rv1 and LNCaP prostate cancer cells. Cell Biol Int. 2013;37(5):464-70.

145. Wolf P, Gierschner D, Buhler P, Wetterauer U, Elsasser-Beile U. A recombinant PSMA-specific single-chain immunotoxin has potent and selective toxicity against prostate cancer cells. Cancer Immunol Immunother. 2006;55(11):1367-73.
146. Salgaller ML, Lodge PA, McLean JG, Tjoa BA, Loftus DJ, Ragde H, et al. Report of immune monitoring of prostate cancer patients undergoing T-cell therapy using dendritic cells pulsed with HLA-A2-specific peptides from prostate-specific membrane antigen (PSMA). Prostate. 1998;35(2):144-51.
147. Feldmann A, Arndt C, Bergmann R, Loff S, Cartellieri M, Bachmann D, et al. Retargeting of T lymphocytes to PSCA- or PSMA positive prostate cancer cells using the novel modular chimeric antigen receptor platform technology "UniCAR". Oncotarget. 2017;8(19):31368-85.
148. Wong HL, Bendayan R, Rauth AM, Wu XY. Development of solid lipid nanoparticles containing ionically complexed chemotherapeutic drugs and chemosensitizers. Journal of pharmaceutical sciences. 2004;93(8):1993-2008.
149. Ma P, Dong X, Swadley CL, Gupte A, Leggas M, Ledebur HC, et al. Development of idarubicin and doxorubicin solid lipid nanoparticles to overcome Pgp-mediated multiple drug resistance in leukemia. J Biomed Nanotechnol. 2009;5(2):151-61.
150. Munnier E, Tewes F, Cohen-Jonathan S, Linassier C, Douziech-Eyrolles L, Marchais H, et al. On the interaction of doxorubicin with oleate ions: fluorescence spectroscopy and liquid-liquid extraction study. Chemical & pharmaceutical bulletin. 2007;55(7):1006-10.
151. Zhang J, Chen XG, Li YY, Liu CS. Self-assembled nanoparticles based on hydrophobically modified chitosan as carriers for doxorubicin. Nanomedicine. 2007;3(4):258-65.
152. Verkerk UH, Kebarle P. Ion-ion and ion-molecule reactions at the surface of proteins produced by nanospray. Information on the number of acidic residues and control of the number of ionized acidic and basic residues. J Am Soc Mass Spectrom. 2005;16(8):1325-41.
153. Xu J, Zhao Q, Jin Y, Qiu L. High loading of hydrophilic/hydrophobic doxorubicin into polyphosphazene polymersome for breast cancer therapy. Nanomedicine. 2014;10(2):349-58.
154. Christophersen OA. Radiation protection following nuclear power accidents: a survey of putative mechanisms involved in the radioprotective actions of taurine during and after radiation exposure. Microb Ecol Health Dis. 2012;23.
155. Gou M, Gong C, Zhang J, Wang X, Wang X, Gu Y, et al. Polymeric matrix for drug delivery: honokiol-loaded PCL-PEG-PCL nanoparticles in PEG-PCL-PEG thermosensitive hydrogel. Journal of biomedical materials research Part A. 2010;93(1):219-26.
156. Schuster BS, Ensign LM, Allan DB, Suk JS, Hanes J. Particle tracking in drug and gene delivery research: State-of-the-art applications and methods. Adv Drug Deliv Rev. 2015;91:70-91.
157. Ding H, Wu F. Image guided biodistribution of drugs and drug delivery. Theranostics. 2012;2(11):1037-9.
158. Bruge F, Damiani E, Puglia C, Offerta A, Armeni T, Littarru GP, et al. Nanostructured lipid carriers loaded with CoQ10: effect on human dermal fibroblasts under normal and UVA-mediated oxidative conditions. Int J Pharm. 2013;455(1-2):348-56.

APPENDIX

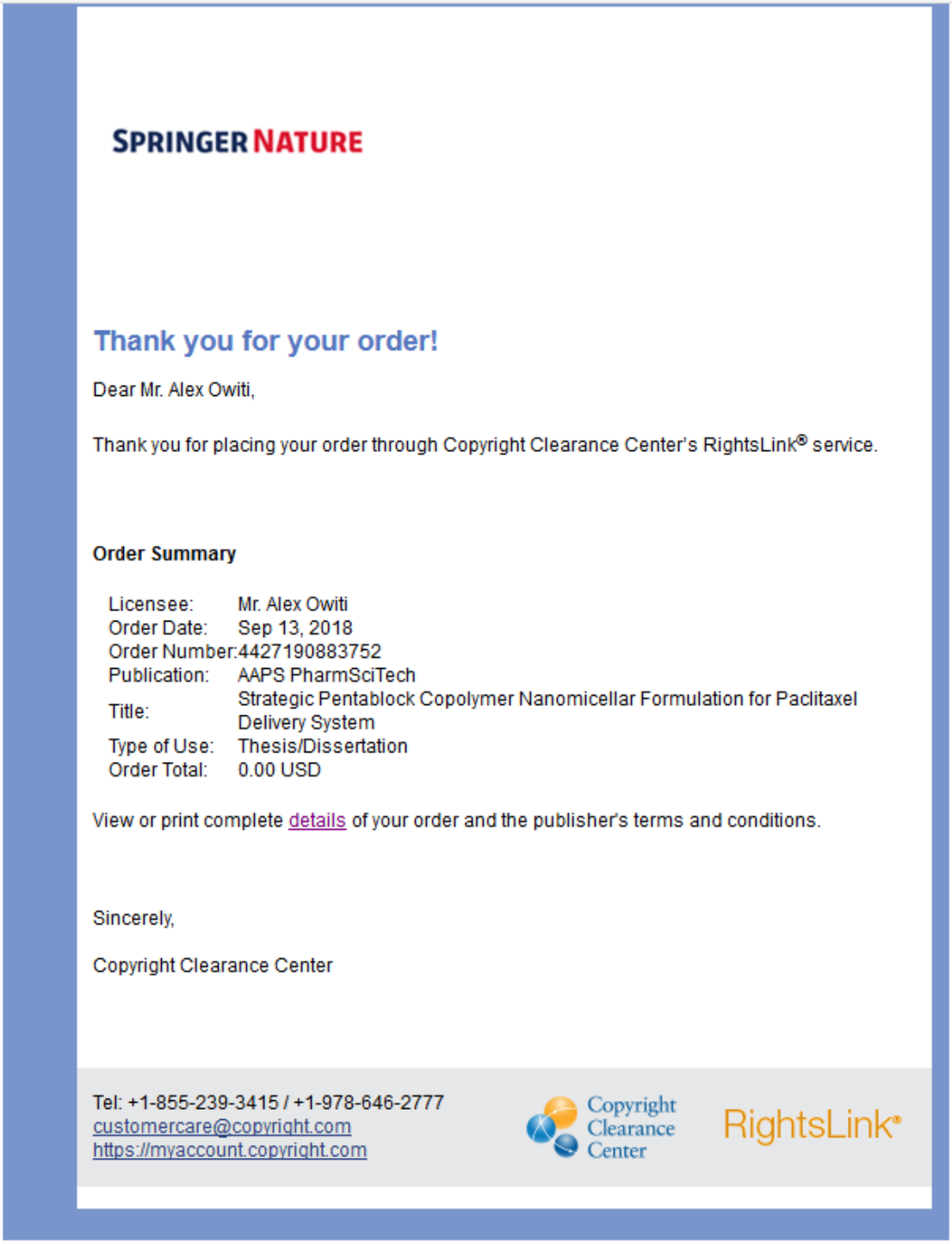

SPRINGER NATURE

Thank you for your order!

Dear Mr. Alex Owiti,

Thank you for placing your order through Copyright Clearance Center's RightsLink® service.

Order Summary

Licensee:	Mr. Alex Owiti
Order Date:	Sep 13, 2018
Order Number:	4427190883752
Publication:	AAPS PharmSciTech
Title:	Strategic Pentablock Copolymer Nanomicellar Formulation for Paclitaxel Delivery System
Type of Use:	Thesis/Dissertation
Order Total:	0.00 USD

View or print complete details of your order and the publisher's terms and conditions.

Sincerely,

Copyright Clearance Center

Tel: +1-855-239-3415 / +1-978-646-2777
customercare@copyright.com
https://myaccount.copyright.com

Copyright Clearance Center RightsLink®

SPRINGER NATURE LICENSE
TERMS AND CONDITIONS

Sep 18, 2018

This Agreement between Mr. Alex Owiti ("You") and Springer Nature ("Springer Nature") consists of your license details and the terms and conditions provided by Springer Nature and Copyright Clearance Center.

License Number	4427190883752
License date	Sep 13, 2018
Licensed Content Publisher	Springer Nature
Licensed Content Publication	AAPS PharmSciTech
Licensed Content Title	Strategic Pentablock Copolymer Nanomicellar Formulation for Paclitaxel Delivery System
Licensed Content Author	Alex Oselu Owiti, Ashim Mitra, Mary Joseph et al
Licensed Content Date	Jan 1, 2018
Type of Use	Thesis/Dissertation
Requestor type	academic/university or research institute
Format	print and electronic
Portion	full article/chapter
Will you be translating?	no
Circulation/distribution	<501
Author of this Springer Nature content	yes
Title	Research assistant
Instructor name	Ashim K Mitra
Institution name	University Of Missouri Kansas City
Expected presentation date	Sep 2018
Requestor Location	Mr. Alex Owiti 2464 Charlotte Street Kansas City KANSAS CITY, MO 64108 United States Attn: Mr. Alex Owiti
Billing Type	Invoice
Billing Address	Mr. Alex Owiti 2464 Charlotte Street Kansas City KANSAS CITY, MO 64108 United States Attn: Mr. Alex Owiti
Total	0.00 USD
Terms and Conditions	

Springer Nature Terms and Conditions for RightsLink Permissions

SPRINGER NATURE

Thank you for your order!

Dear Mr. Alex Owiti,

Thank you for placing your order through Copyright Clearance Center's RightsLink® service.

Order Summary

Licensee:	Mr. Alex Owiti
Order Date:	Sep 13, 2018
Order Number:	4427190560061
Publication:	AAPS PharmSciTech
Title:	PSMA Antibody-Conjugated Pentablock Copolymer Nanomicellar Formulation for Targeted Delivery to Prostate Cancer
Type of Use:	Thesis/Dissertation
Order Total:	0.00 USD

View or print complete details of your order and the publisher's terms and conditions.

Sincerely,

Copyright Clearance Center

Tel: +1-855-239-3415 / +1-978-646-2777
customercare@copyright.com
https://myaccount.copyright.com

Copyright Clearance Center RightsLink®

SPRINGER NATURE LICENSE
TERMS AND CONDITIONS

Sep 18, 2018

This Agreement between Mr. Alex Owiti ("You") and Springer Nature ("Springer Nature") consists of your license details and the terms and conditions provided by Springer Nature and Copyright Clearance Center.

License Number	4427190560061
License date	Sep 13, 2018
Licensed Content Publisher	Springer Nature
Licensed Content Publication	AAPS PharmSciTech
Licensed Content Title	PSMA Antibody-Conjugated Pentablock Copolymer Nanomicellar Formulation for Targeted Delivery to Prostate Cancer
Licensed Content Author	Alex Oselu Owiti, Dhananjay Pal, Ashim Mitra
Licensed Content Date	Jan 1, 2018
Type of Use	Thesis/Dissertation
Requestor type	academic/university or research institute
Format	print and electronic
Portion	full article/chapter
Will you be translating?	no
Circulation/distribution	<501
Author of this Springer Nature content	yes
Title	Research assistant
Instructor name	Ashim K Mitra
Institution name	University Of Missouri Kansas City
Expected presentation date	Sep 2018
Requestor Location	Mr. Alex Owiti 2464 Charlotte Street Kansas City KANSAS CITY, MO 64108 United States Attn: Mr. Alex Owiti
Billing Type	Invoice
Billing Address	Mr. Alex Owiti 2464 Charlotte Street Kansas City KANSAS CITY, MO 64108 United States Attn: Mr. Alex Owiti
Total	0.00 USD
Terms and Conditions	

Springer Nature Terms and Conditions for RightsLink Permissions

Springer Nature Customer Service Centre GmbH (the Licensor) hereby grants you a non-exclusive, world-wide licence to reproduce the material and for the purpose and requirements specified in the attached copy of your order form, and for no other use, subject to the conditions below:

1. The Licensor warrants that it has, to the best of its knowledge, the rights to license reuse of this material. However, you should ensure that the material you are requesting is original to the Licensor and does not carry the copyright of another entity (as credited in the published version).

   If the credit line on any part of the material you have requested indicates that it was

VITA

Alex Oselu Owiti was born on 9th January 1979, in Kisumu, Kenya. He completed his Bachelor of Pharmacy from Federal University of Para, Belem, Brazil in 2007 and received his Master of Pharmaceutical Science degree in 2011 from the same University. Alex Owiti worked as a regional director of Food and Drug Administration-ANVISA/FDA in Brazil (2012-2013), and as Pharmacist in various Brazilian pharmacies, drug stores hospitals and pharmaceutical industries(2006-2012). To pursue a Ph.D. degree, Alex Owiti initiated Doctoral study in the Interdisciplinary Ph.D. program in the school of Pharmacy at the University of Missouri-Kansas City(UMKC),USA in August 2013. During his PhD studies, Alex Owiti worked on drug delivery, focusing on drug delivery systems for human anticancer therapy especially prostate cancer. Alex completed his doctoral studies in July, 2018 under the guidance of Dr. Ashim K. Mitra. He has authored/co-authored various peer reviewed publications and book chapters and has also presented his work in several annual local and national conferences in USA and abroad.